

12-2012

Trim24-Regulated Estrogen Response Is Dependent On Specific Histone Modifications In Breast Cancer Cells

Teresa T. Yiu

Follow this and additional works at: https://digitalcommons.library.tmc.edu/utgsbs_dissertations



Part of the [Biochemistry Commons](#), [Cancer Biology Commons](#), [Medicine and Health Sciences Commons](#), and the [Molecular Biology Commons](#)

Recommended Citation

Yiu, Teresa T., "Trim24-Regulated Estrogen Response Is Dependent On Specific Histone Modifications In Breast Cancer Cells" (2012). *Dissertations and Theses (Open Access)*. 313.
https://digitalcommons.library.tmc.edu/utgsbs_dissertations/313

This Dissertation (PhD) is brought to you for free and open access by the MD Anderson UTHealth Houston Graduate School at DigitalCommons@TMC. It has been accepted for inclusion in Dissertations and Theses (Open Access) by an authorized administrator of DigitalCommons@TMC. For more information, please contact digcommons@library.tmc.edu.

**TRIM24-REGULATED ESTROGEN RESPONSE IS DEPENDENT ON
SPECIFIC HISTONE MODIFICATIONS IN BREAST CANCER CELLS**

By

Teresa Tingting Yiu, B.S.

APPROVED:

Michelle Barton, Ph.D., Supervisory Professor

Gary Gallick, Ph.D.

Pierre McCrea, Ph.D.

Xiaobing Shi, Ph.D.

Jessica Tyler, Ph.D.

APPROVED:

Dean, The University of Texas
Graduate School of Biomedical Sciences at Houston

**TRIM24-REGULATED ESTROGEN RESPONSE IS DEPENDENT ON
SPECIFIC HISTONE MODIFICATIONS IN BREAST CANCER CELLS**

A DISSERTATION

Presented to the Faculty of
The University of Texas
Health Science Center at Houston
and
The University of Texas
M.D. Anderson Cancer Center
Graduate School of Biomedical Sciences
in Partial Fulfillment
of the Requirements
for the Degree of

DOCTOR OF PHILOSOPHY

By
Teresa Tingting Yiu, B.S.
Houston, Texas

December, 2012

DEDICATION

This thesis is dedicated to my beloved father, in memory of the sacrifice of his life to cancer in 2008, to whom I promised to persevere at the pursuance of this degree and dedicate my career to cancer research.

I thank the Creator for giving me the burden to help the unfortunate ones and the opportunity to take flight and solve this complicated human disease at M.D. Anderson Cancer Center, a world-renowned cancer institute.

Because of the unconditional love, endless support and encouragement from my family, friends, advisor, committees, and lab-mates, I have sustained till this point, and am ready to start a whole new chapter of my life, to be filled with exciting research discoveries in making this deadly disease history.

ACKNOWLEDGEMENT

First I would like to acknowledge the Center for Cancer Epigenetics at M.D. Anderson Cancer Center, especially Director Dr. Sharon Dent, for funding my first year's education. I am also thankful for the generous contribution from NIH T32 Training Grant and the American Legion Auxiliary Fellowship.

I am extremely thankful for my advisor, Dr. Michelle Barton, for the opportunity to learn and mature in experimental knowledge, critical thinking and communication. She has opened up many opportunities in my research, inspired and assisted me tremendously in the past three years. I am thankful for her patience, encouragement, and the freedom to pursue my research interest in her laboratory. Most importantly, because of her support, I am able to have a balanced life between work and family.

I would like to acknowledge members of my present and past committees, for their patience, guidance, scientific discussion, intuitive comments and time commitment: Drs. Sharon Dent, Gary Gallick, Guillermina Lozano, Pierre McCrea, Gary Gallick, Xiaobing Shi, Jessica Tyler, Shinoko Takata, and Bin Wang. I especially thank Dr. Gary Gallick for his encouragement and inspiration, which greatly helped me to persist in pursuing science; Drs. Pierre McCrea and Bin Wang for their guidance in fulfilling my candidacy exam requirements; Dr. Xiaobing Shi for sharing his ideas and experimental skills when I was exploring the field of epigenetics. I would also like to thank present and past members of Barton laboratory, who have assisted in my experiments, inspired my research, and encouraged me, especially when my goals seem impossible to accomplish.

TRIM24-REGULATED ESTROGEN RESPONSE IS DEPENDENT ON SPECIFIC HISTONE MODIFICATIONS IN BREAST CANCER CELLS

Publication No. _____

Teresa Tingting Yiu, B.S.

Supervisory Professor: Michelle Barton, Ph.D.

In this dissertation, I discovered that function of TRIM24 as a co-activator of ER α -mediated transcriptional activation is dependent on specific histone modifications in tumorigenic human breast cancer-derived MCF7 cells. In the first part, I proved that TRIM24-PHD finger domain, which recognizes unmethylated histone H3 lysine K4 (H3K4me0), is critical for ER α -regulated transcription. Therefore, when LSD1-mediated demethylation of H3K4 is inhibited, activation of TRIM24-regulated ER α target genes is greatly impaired. Importantly, I demonstrated that TRIM24 and LSD1 are cyclically recruited to estrogen responsive elements (EREs) in a time-dependent manner upon estrogen induction, and depletion of their expression exert corresponding time-dependent effect on target gene activation. I also identified that phosphorylation of histone H3 threonine T6 disrupts TRIM24 from binding to the chromatin and from activating ER α -regulated targets. In the second part, I revealed that TRIM24 depletion has additive effect to LSD1 inhibitor- and Tamoxifen-mediated reduction in survival and proliferation in breast cancer cells.

TABLE OF CONTENTS

DEDICATION	iii
ACKNOWLEDGEMENT	iv
TABLE OF CONTENTS	vi
LIST OF FIGURES	xi
LIST OF ABBREVIATIONS	xv
CHAPTER 1: GENERAL INTRODUCTION	1
1.1.1. Epigenetics control literally all DNA-templated processes in the cell	1
1.1.2. Histone acetylation opens up chromatin for transcriptional activation ...	3
1.1.3. Histone methylation and transcription activation/repression	4
1.1.4. Histone phosphorylation cooperates with nearby PTMs	6
1.1.5. The histone code hypothesis	6
1.1.6. Histone binding modules decode the histone language	7
1.1.7. The RBCC protein family member TRIM24	11
1.1.8. TRIM24 regulates nuclear receptor-mediated signaling pathways	13
1.1.9. TRIM24 associates with chromatin and remodeling proteins	14
1.1.10. Histone demethylase 1 (LSD1) specifically demethylates H3K4me1/2	15
1.1.11. LSD1 mediates transcription repression	18
1.1.12. LSD1 plays important roles during development and differentiation...	18
1.2. AIMS OF THIS WORK	20
CHAPTER 2: ACTIVATION OF TRIM24-REGULATED ERα TARGET GENES IS DEPENDENT ON LSD1-MEDIATED H3K4ME2 DEMETHYLATION	22
2.1. INTRODUCTION	22
2.1.1. Estrogen receptor-alpha (ER α) is the master transcriptional regulator..	22
2.1.2. ER α and the transcriptional machinery	23

2.1.3. Histone modifying enzymes as ER α co-regulators	25
2.1.4. Chromatin remodeling and estrogen response	26
2.1.5. Potential involvement of histone chaperones in ER α regulation	29
2.1.6. Timely cyclical recruitment of ER α and its co-factors	29
2.1.7. TRIM24 functions as an ER α co-activator through chromatin recognition	31
2.1.8. TRIM24 simultaneously recognizes two histone signatures on H3.....	34
2.1.9. TRIM24 preferentially binds to regions depleted of H3K4me2	35
2.1.10. LSD1 as a transcription co-activator in androgen and estrogen receptors-mediated signaling	37
2.1.11. H3T6ph inhibits H3K4 demethylation mediated by LSD1 and chromatin binding by H3K4me0 reader proteins	38
2.1.12. <i>Hypothesis</i> : Function of TRIM24 is dependent on LSD1-mediated H3K4 demethylation	39
2.2. MATERIALS AND METHODS	41
2.2.1. Cell culture	41
2.2.2. Mutagenesis	41
2.2.3. Transient DNA plasmid transfection	41
2.2.4. Transient knockdown by siRNAs	42
2.2.5. RNA extraction, cDNA, and real-time-RT-PCR	42
2.2.6. Chromatin immunoprecipitation (ChIP)	43
2.2.7. GST-tagged protein expression and purification	46
2.2.8. Biotinylated peptide pulldown assay	47
2.3. RESULTS	48
2.3.1. Estrogen triggers immediate dynamic histone modifications	48

2.3.2. TRIM24 expression is essential for timely estrogen response	55
2.3.3. Recruitment of LSD1 and TRIM24 and changes of H3K4 methylation at <i>GREB1</i> ERE upon estrogen induction	64
2.3.4. Recruitment of LSD1 and TRIM24 and changes of H3K4 methylation at <i>PR</i> ERE upon estrogen induction	68
2.3.5. Recruitment of LSD1 and TRIM24 and changes of H3K4 methylation at <i>pS2</i> ERE upon estrogen induction	71
2.3.6. LSD1 enzymatic activity is critical for ER α -mediated transcription	75
2.3.7. Chromatin-binding ability of TRIM24 is dependent on the enzymatic activity of LSD1	89
2.3.8. H3T6ph disrupts TRIM24 from binding to histone peptide	107
2.3.9. H3T6ph and its potential role in ER α target gene activation	111
2.4. FUTURE DIRECTIONS AND PRELIMINARY RESULTS	119
2.4.1. Does depletion of LSD1 also exert time-specific effect?	119
2.4.2. Does TRIM24 and LSD1 physically interact and when?	119
2.4.3. Role of H3T6 phosphorylation in regulating estrogen response	120
2.5. DISCUSSIONS	121
2.5.1. Immediate E ₂ -induced changes of chromatin structure at enhancers	121
2.5.2. Cyclical recruitment of LSD1 and concurrent changes in H3K4me ₂ ..	122
2.5.3. TRIM24 binding not always concurrent with H3K4me ₂ demethylation	123
2.5.4. Inhibition of LSD1 does not affect H3K4me ₃ or H3K9me ₂	124
2.5.5. Establishment of the role of H3T6ph in ER α -regulated transcription	124

CHAPTER 3: BIOLOGICAL SIGNIFICANCE OF TRIM24- AND LSD1-MEDIATED ER-ALPHA CO-ACTIVATION IN BREAST CANCER CELLS	126
3.1. INTRODUCTION	126
3.1.1. Epigenetics and cancers	126
3.1.2. Implication of histone methylation in oncogenesis	127
3.1.3. Aberrant expression of TRIM24 is correlated with tumorigenesis	130
3.1.4. Possible roles of TRIM24 in breast cancer transformation and cell cycle regulation	131
3.1.5. Roles of LSD1 in tumorigenesis	132
3.1.6. <i>Hypothesis</i> : Functions of TRIM24 for the survival and proliferation of breast cancer cells in dependent on the enzymatic activity of LSD1	138
3.2. MATERIAL AND METHODS	140
3.2.1. Clonogenic assay	140
3.2.2. Statistical analysis	140
3.3. RESULTS	141
3.3.1. Activated ER α is required for the survival and proliferation of MCF7	143
3.3.2. Depletion of TRIM24 affects survival and proliferation of MCF7	144
3.3.3. Inhibition of LSD1 by TCP affects survival and proliferation of MCF7	144
3.3.4. Knockdown of TRIM24 is highly additive to TCP- and 4-OHT-induced inhibition in colony formation	149
3.4. DISCUSSIONS AND FUTURE DIRECTIONS	154
3.4.1. TRIM24 affects breast cancer cell survival and proliferation	154

3.4.2. Correlation of TCP effectiveness and TRIM24 expression?	154
3.4.3. HDAC inhibitors and TRIM24 knockdown?	155
3.4.5. Biological functions of LSD1 and TRIM24 <i>in vivo</i> ?	156
CHAPTER 4: CONCLUSION	157
REFERENCES	160
VITA	190

LIST OF FIGURES

Figure 1-1: Overview of epigenetic regulator mechanisms	2
Figure 1-2: Covalent histone modifications mediated by epigenetic enzymes	5
Figure 1-3: Readers of histone modifications	9
Figure 1-4: TRIM24 protein domains	12
Figure 1-5: LSD1 protein domains	16
Figure 1-6: Postulated chemical reactions for LSD1-catalyzed demethylation of H3K4me2	17
Figure 2-1: Protein complexes involved in estrogen-induced activation of pS2 gene	24
Figure 2-2: Coactivators of estrogen receptor-alpha	28
Figure 2-3: ER α and TRIM24 are recruited together to EREs upon estrogen induction	32
Figure 2-4: Depletion of TRIM24 decreases ER α binding to ERE and estrogen-activated gene induction	33
Figure 2-5: TRIM24 binds to regions depleted of H3K4me2	36
Figure 2-6: Total H3 decreases immediately upon estrogen treatment	49
Figure 2-7: Changes of H3K23ac levels upon estrogen treatment	50
Figure 2-8: Changes of H3K27ac levels upon estrogen treatment	51
Figure 2-9: Recruitment of ER α upon estrogen treatment	52
Figure 2-10: Changes of H3K4me2 levels upon estrogen treatment	53
Figure 2-11: Changes of H3K4me3 levels upon estrogen treatment	54
Figure 2-12: Ectopic expression of TRIM24 in MCF7 depleted of endogenous TRIM24	56
Figure 2-13: TRIM24 expression allows estrogen response at lower levels of hormone	57
Figure 2-14: Western blot analysis revealed decreased TRIM24 protein level mediated by siRNA in MCF7 cells	58

Figure 2-15: Knockdown of LSD1 by siRNAs	59
Figure 2-16: Effects of siTRIM24 or siLSD1 on ER α target gene activation	60
Figure 2-17: Effects of siTRIM24 or siLSD1 on ER α target gene activation	62
Figure 2-18: Effects of siTRIM24 or siLSD1 on non-E ₂ response gene <i>BCAS4</i>	63
Figure 2-19: Cyclical recruitments of LSD1 and TRIM24 to <i>GREB1</i> distal ERE site	65
Figure 2-20: Dynamic changes in H3K4 methylation levels at <i>GREB1</i> distal ERE site	67
Figure 2-21: Cyclical recruitments of LSD1 and TRIM24 to <i>PR</i> ERE site.....	70
Figure 2-22: Dynamic changes in H3K4 methylation levels at <i>PR</i> ERE site.....	71
Figure 2-23: Cyclical recruitments of LSD1 and TRIM24 to <i>pS2</i> ERE site.....	72
Figure 2-24: Dynamic changes in H3K4 methylation levels at <i>pS2</i> ERE site.....	74
Figure 2-25: Effects of LSD1 inhibitor TCP on ER α target gene activation	75
Figure 2-26: Pilot study of LSD1 inhibitors and their effects on ER α target gene activation	81
Figure 2-27: Effects of potent LSD1 inhibitors on LSD1 protein expression in MCF7 cells	83
Figure 2-28: Effects of potent LSD1 inhibitors on global H3K4me2 in MCF7 cells	84
Figure 2-29: Effects of potent LSD1 inhibitor AH124 on ER α target gene activation	85
Figure 2-30: Effects of potent LSD1 inhibitors Chem778 and Chem779 on ER α target gene activation	87
Figure 2-31: LSD1 inhibitor Tranylcypromine (TCP) leads to changes in H3K4 methylation	91
Figure 2-32: LSD1 inhibitor Tranylcypromine (TCP) impairs recruitment of TRIM24 and ER α	93

Figure 2-33: LSD1 inhibitor Tranylcypromine (TCP) does not affect H3K9 methylation	95
Figure 2-34: LSD1 inhibitor Tranylcypromine (TCP) leads to changes in H3K4 methylation	96
Figure 2-35: LSD1 inhibitor Tranylcypromine (TCP) impairs recruitment of TRIM24 and ER α	98
Figure 2-36: LSD1 inhibitor Tranylcypromine (TCP) leads to re-methylation of H3K4	100
Figure 2-37: LSD1 inhibitor Tranylcypromine (TCP) impairs TRIM24 recruitment	102
Figure 2-38: LSD1 inhibitor Tranylcypromine (TCP) impairs ER α recruitment..	104
Figure 2-39: Summary of changes in histone modifications and recruitment of TRIM24 and ER α in the presence of Tranylcypromine (TCP)	106
Figure 2-40: Purification of GST-only and GST-tagged TRIM24 recombinant proteins	108
Figure 2-41: H3T6 phosphorylation and/or H3K4 methylation hinder TRIM24 from binding to H3	110
Figure 2-42: Specificity of H3T6ph antibody	112
Figure 2-43: Changes of H3T6 phosphorylation upon estrogen treatment	113
Figure 2-44: Inhibition of H3T6-specific protein kinase C (PKC) by BisI Leads to dephosphorylation of H3T6 at <i>GREB1</i> , <i>PR</i> , <i>pS2</i> and <i>IGFBP4</i> EREs	115
Figure 2-45: Effects of Bis I on ER α target gene induction	117
Figure 3-1: H3K4 methylation is tightly associated with cancer development ..	129
Figure 3-2: Global TRIM24 target genes upon E ₂ treatment	134

Figure 3-3: TRIM24 expression is highly enriched in E ₂ -treated cells during G2/M transition	135
Figure 3-4: TRIM24 binding to ER α target genes during cell cycle	136
Figure 3-5: 4-hydroxy-tamoxifen (4-OHT)-induced reduction of colony Formation in MCF7 but not MDA-MB-231 cells	142
Figure 3-6: Depletion of TRIM24 has additive effect in Tamoxifen-inhibited ER α target gene activation	145
Figure 3-7: Representative images of Tet-treated colonies in the presence Of the indicated treatment	146
Figure 3-8: Depletion of TRIM24 expression leads inhibit the survival of MCF7 breast cancer cells, and is highly addictive to 4-hydroxy-tamoxifen (4-OHT)-induced survival inhibition	147
Figure 3-9: Decreased TRIM24 expression sensitizes MCF7 cells lower dosage of TCP-mediated reduction in colonies	150
Figure 3-10: Knockdown of TRIM24 is highly additive to TCP- and 4-OHT- Induced inhibition in colony formation	152

LIST OF ABBREVIATIONS

4-OHT	4-hydroxy-Tamoxifen
AML	Acute myeloid leukemia
AR	Androgen receptor
Bromo	Bromodomain
CBP	CREB-binding protein
ChIP	Chromatin immunoprecipitation
ChIP-Seq	ChIP-sequencing
COREST	REST corepressor
CREB	cAMP response element-binding
CTD	C-terminal domain of RNAP II
DHT	Dihydrotestosterone
E ₂	17 β estradiol, estrogen
EMS	Myeloproliferative syndrome
EMT	Epithelial-mesenchymal transition
ER α	Estrogen receptor alpha
ER β	Estrogen receptor beta
ERE	Estrogen-responsive DNA elements
FAD	Flavin adenine dinucleotide
GRIP1	Glucocorticoid receptor-interacting protein 1
H3K23ac	Acetylated H3K23
H3K27ac	Acetylated H3K27
H3K4me0	Unmethylated H3K4
H3K4me1	Mono-methylated H3K4
H3K4me2	Di-methylated H3K4
H3K4me3	Tri-methylated H3K4

H3K9me2	Di-methylated H3K9
H3T6ph	Phosphorylated H3T6
HAT	Histone acetyltransferase
hESCs	Human embryonic stem cells
HDAC	Histone deacetylase
HMEC	Human mammary epithelial cells
HMT	Histone methyltransferase
HDM	Histone demethylase
HP1 α	Heterochromatin protein 1 alpha
ING2	Inhibitor of growth 2
ISWI	Imitation switch chromatin remodeling complex
ITC	Isothermal titration calorimetry
K _D	Dissociation constant
KDM5B	Lysine-specific demethylase 5B
KDM5C	Lysine-specific demethylase 5C
LSD1	Lysine demethylase 1
MLL	Mixed-lineage leukemia
MYC	Myelocytomatosis viral oncogene homolog
NR	Nuclear receptor
NUP98	Nucleoporin 98
OGG1	8-oxoguanine-DNA glycosylase 1
PHD	Plant homeo domain
PIC	Pre-initiation complex
PKC	Protein kinase C
PTM	Post-translational modification
RBP2	Retinol-binding protein 2
REST	Repressor element 1-silencing transcription factor

RAR	Retinoic acid receptor alpha
RNAP II	RNA polymerase II
RXR	Retinoid X receptor
RING	Really interesting new gene
siRNA	Small interfering RNA
SIRT1	Sirtuin 1
SWIRM	SWI13p, Rsc8p and Moira
SWI/SNF	Switch/sucrose non-fermenting chromatin remodeling complex
TAM	Tamoxifen
TBP	TATA-box containing protein
TCP	Tranylcyromine, a LSD1 inhibitor
TET	Tetracyclin
TF	Transcription factors
TRIM24	Tripartite motif containing 24
TSA	Trichostatin A
VDR	Vitamin D3 receptor

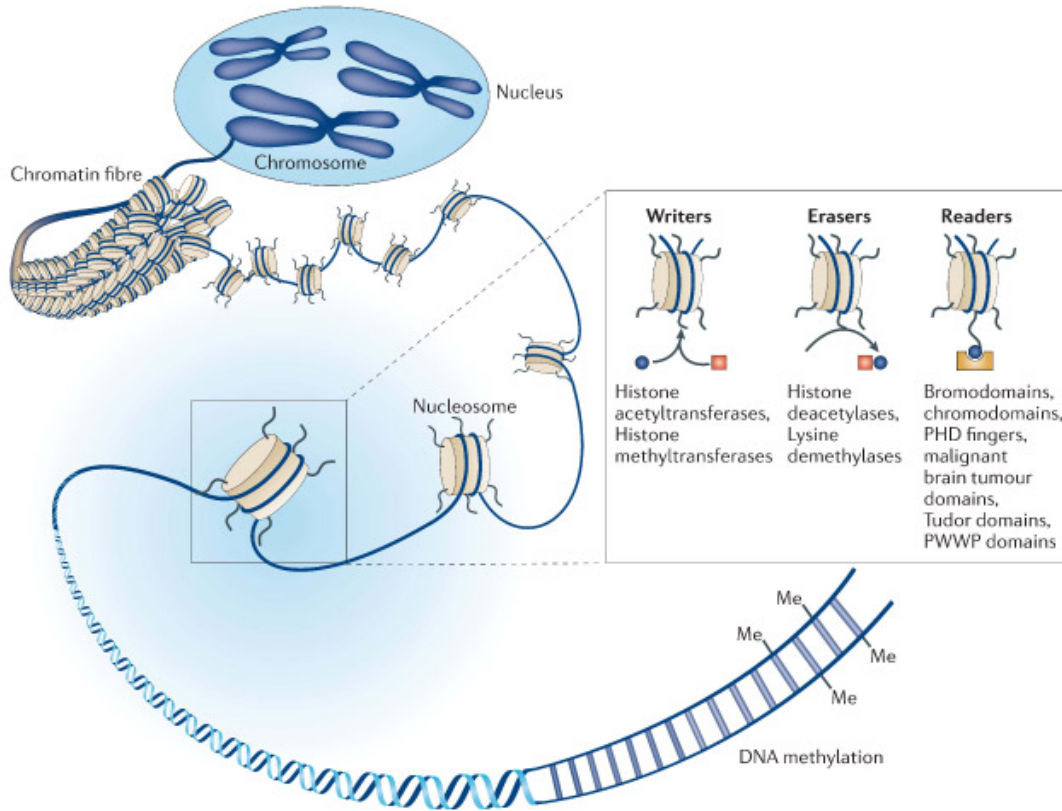
CHAPTER 1: GENERAL INTRODUCTION

1.1.1. Epigenetics control literally all DNA-templated processes in the cell

Eukaryotic DNA is packaged by an octamer of highly conserved histone proteins (two H2A/H2B dimers and one H3/H4 tetramer) into the basic unit called the nucleosome [1]. Repeating unit of nucleosomes are connected by the linker histone (H1) to generate nucleosomal arrays, and then further organized into higher-order chromatin structure (illustrated in Figure 1-1). These structures are highly plastic and governs the accessibility of DNA through epigenetic processes such as ATP-catalyzed remodeling and repositioning of the nucleosomes [2,3], covalent modifications of residues on the tail or globular domains of histone proteins [4], as well as methylation of 5' position of the cytosine ring in CpG dinucleotides. Orchestration of these epigenetic regulatory mechanisms controls literally all DNA-templated cellular processes, such as transcription, DNA replication, DNA repair, recombination and others [5].

This thesis focuses on the post-translational modifications (PTMs) decorating the N-terminal tails of the core histone H3 and their effects on gene transcription such as H3K4 methylation, H3 acetylation, and H3T6 phosphorylation. Essentially, specific residues on histone tails are targeted by a wide array of histone-modifying enzymes, which either add or remove PTMs from different histone residues. To date, numerous PTMs have been identified, such as methylation, acetylation, phosphorylation, ubiquitination and others [6,7], which result in either an open (euchromatin) or closed chromatin structure (heterochromatin), leading to gene activation or repression, respectively.

Figure 1-1: Overview of epigenetic regulatory mechanisms. Reprinted by permission from Macmillan Publishers Ltd: *Nature Reviews Drug Discovery* **11**: 384-400, copyright (2012) [8].



1.1.2. Histone acetylation opens up chromatin for transcriptional activation

Histone acetylation is probably the most studied of the PTMs, and the functions in transcriptional activation are widely appreciated [9]. Earlier observation suggested that acetylated chromatin regions are associated with active gene transcription [10]. In fact, hyper-acetylation creates an accessible chromatin conformation and thus enhances the exposure of DNA to restriction enzymes and transcription factors to allow transcription [11,12,13]. Removal of the positive charge on the acetylated histone tails disrupts the stability between histones and the negatively charged DNA, as well as the inter-nucleosomal interactions [14]. Another hypothesis is that histone acetylation may be part of the combinatorial modifications that lead to downstream events via binding of other epigenetic regulatory proteins [15]. In fact, adjacent phosphorylation and methylation can also regulate histone acetyltransferase (HAT) activity [16,17]. The enzymes involved (histone acetyltransferases, HATs; histone deacetylases, HDACs) are not only responsible for the steady-state balance of histone acetylation, but are also present in different regulatory complexes and have distinct biological functions [18].

1.1.3. Histone methylation and transcription activation/repression

In contrast to acetylation, histone methylation is associated with both transcriptional activation and repression, in a context-specific manner [19]. Histone methylation occurs on both lysine (K) and arginine (R) residues [19,20,21]. Particularly, lysine methylation on different sites (H3K4, H3K9, H3K27, H3K79, and H4K20), and to different degrees (mono-, di-, or tri-methylation) [22], contributes to the complexity of transcription in regulation. Histone lysine methylation is dynamically mediated through histone methyltransferases (HMTs), and the opposing enzymes, histone demethylases (HDMs). SET-domain containing HMTs [23,24], especially in H3K4 methylation, include MLL1-5, SET1/7/9, ASH1, and SMYD3 (summarized in Figure 1-2) [25]. Histone lysine demethylase 1 (LSD1) was the first HDM identified and is specific for the demethylation of monomethylated and dimethylated H3K4 (H3K4me_{1/2}) [4,16]. LSD1 plays critical roles in several cellular processes such as regulation of transcription, development and differentiation (to be further discussed below).

In addition to LSD1, more HDMs have been identified from members of the Jimonji-containing protein family. H3K4-specific HDMs also include retinol-binding protein 2 (RBP2/JARID1A/KDM5A), which demethylates H3K4me_{2/3} and lysine-specific demethylase 5B (KDM5B/PLU-1/JARID1B) and lysine-specific demethylase 5C (KDM5C/SMCX/JARID1C), both of which enzymatically target H3K4me₃ (summarized in Figure 1-2) [25].

1.1.4. Histone phosphorylation cooperates with nearby PTMs

Phosphorylation of histones is especially important in cell cycle regulation [26,27]. However, emerging evidence also suggests its functions in transcriptional regulation [28]. For example, phosphorylation on Histone H3 threonine T3 (H3T3ph) interrupts the recognition of H3K4 by other chromatin binding modules due to the close proximity of T3 and K4 on H3 [29]. Notably, H3T3ph and H3K4me1 often associate with regions of repressed transcription [30]. Therefore, it is possible that H3T3 phosphorylation creates electrostatic interference for H3K4 recognition, leading to silent chromatin. Another example is H3T6ph, which also antagonizes the binding of H3K4-specific reader module and demethylation mediated by LSD1 and JARID1B [31]. On the other hand, H3T11ph enhances JMJD2C-mediated demethylation of H3K9me3 [32]. Taken together, histone phosphorylation underlies a complex language of histone modifications, yet its effects on combinatorial modifications await further investigations.

1.1.5. The histone code hypothesis

The histone code hypothesis proposes that combinatorial or sequential histone PTMs can be decoded by different reader proteins or protein modules to amplify a cascade of downstream responses [5,15]. The hypothesis is appealing because it may explain how distinct patterns of histone marks achieve context-specific diversity on transcriptional regulation. For example, tri-methylation on H3K4 (H3K4me3) recruits chromatin-remodeling complexes, and is considered

an active mark for transcription. Although methylated H3K4 is generally associated with euchromatin and transcriptional activation [8,25,33,34], further studies support the concept that cellular context determines the outcome of histone methylation. In response to DNA damage, robust recognition of H3K4me3 by the PHD domain of ING2 (inhibitor of growth 2, a tumor suppressor protein) mediates gene repression by serving as a bridging module with mSin3a–HDAC1 complex at the promoters [35]. Therefore, specific effector proteins, acting as a reader module for specific histone modifications, determine the outcome of dynamic and highly contextual gene regulation. In fact, a recent study investigated how chromatin reader modules interact with histone H3 decorated by combinatorial modifications on different residues in close proximity. This finding showed that combinatorial PTMs on the same histone tail affect the binding affinity for effector proteins, leading to divergent downstream “readouts” [29].

1.1.6. Histone binding modules decode the histone language

The histone code hypothesis postulates the importance of effector (or chromatin binding modules) in determining the biological outcomes of single or combinatorial histone PTMs [5,15], which, in the last decade, has led to extensive discoveries in their interaction with specifically modified histone peptides [36]. These reader/binding modules are highly evolved and are able to recognize distinct histone marks. For example, proteins with bromodomains recognize acetylated lysines, whereas (un)methylated lysines can be bound by proteins containing chromodomains, double chromo, double Tudor domains,

MBT (malignant brain tumor) 1 repeats, PHD (plant homeo domain) fingers, cysteine-rich ADD domain, WD40 repeats and others. Notably, relatively fewer readers for phosphorylated histone peptides have been identified, which include 14-3-3 and tandem BRCT (BRCA1 C terminus) -containing proteins [36,37].

For the recognition of methylation status on H3K4, unmethyl-H3K4 (H3K4me0) can be read by PHD-finger readers AIRE [38] and BHC80 [39], WD40-reader WDR5/9 [40,41] and ADD-reader DNMT3L/3A [42,43]; while methylated-H3K4 (H3K4me) by chromo-reader CHD1 [44,45], PHD readers RAG2 [46], ING2 [41], BPTF [47], TAF3 [48], PHF2 [49], ING4 [50], YNG1 [35,51] and PHF8 [52], Tudor-readers JMJD2A [53] and Sgf29 [54], Zf-CW reader ZCWPW1 [55] and others. Readers for other histone modifications are summarized in Figure 1-3. The majority of the epigenetic binding modules can recognize multiple histone marks and represent an active area of research. However, how the histone code is decoded also largely depends on the complicated network between epigenetic readers as well as modifying enzymes in response to combinatorial histone PTMs, in specific context and cell types [36,56].

Figure 1-3: Readers of histone modifications. Reprinted by permission from Macmillan Publishers Ltd: *Cell Research* 21:564-578, copyright (2011) [37].

PTMs	Position		Recognition Module(s)	Protein	Related Modifications		Functions	3D	
					Enhanced by	Inhibited by			
Lysine Methylation	H3	K4me0	PHD	BHC80			LSD1.com	Y	
				AIRE		H3R2me	Autoimmune regulator	Y	
			WD40	WDR5/ WDR9			HAT	Y	
		ADD	Dnmt3L		K4me	DNA methylation	Y		
		K4me	Chromo	CHD1				ATPase	Y
			PHD	RAG2				Recombination	
				ING2				HDAC	Y
				BPTF	H3K9Ac, H3K14Ac			ATPase	Y
			TAF3	H3K9Ac, H3K14Ac	H3R2me2		TFIID	Y	
			PHF2				H3K9 demethylation		
			ING4				HBO1.com, H3 acetylation		
			YNG1				NuA3, histone acetylation		
			PHF8	H3K9Ac, H3K14Ac			Histone demethylation		
			Tudor	JMJD2A				Histone demethylase	
				JMJD2C				Histone demethylase	
				Sgf29	H3K9Ac, H3K14Ac			Histone acetylation (SAGA)	
		MBT	PHF20L1				–		
		Zf-CW	ZCWPW1				Novel PTM reader	Y	
		K9	Chromo	HP1	SU(VAR) Protein	Y41Ph, S10Ph		Heterochromatin	Y
					CDY1				–
				CDY, CDYL, CDYL2		S10Ph		Repressor of REST	
			PHD	SMCX				Demethylation	
			Tudor	TDRD7				–	
				UHRF1				–	Y
			WD40	EED				PRC2 activity	Y
				LRWD1				DNA replication (ORC binding)	
			Ankyrin Repeats	G9a/GLP				Methyltransferase	Y
			K23	Chromo	MPP8				–
		K27	WD40	EED				PRC mediated repression	Y
				LRWD1		S28Ph		DNA replication (ORC binding)	
Chromo	PC					PRC1	Y		
	CDY, CDYL, CDYL2					–			
	CBX7					PRC mediated repression			
MPP8				–					
K36	Chromo	Eaf3				Histone deacetylation	Y		

Figure 1-3 (Continued): Readers of histone modifications. Reprinted by permission from Macmillan Publishers Ltd: *Cell Research* 21:564-578, copyright (2011) [37]

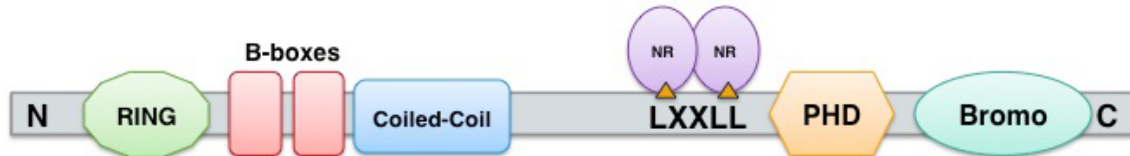
PTMs	Position		Recognition Module(s)	Protein	Related Modifications		Functions	3D	
					Enhanced by	Inhibited by			
			PWWP	MSL3			Dosage compensation		
				MRG15			Splicing		
				DNMT3A			Guide DNA methylation		
				BRPF1			Histone acetylation (MOZ)	Y	
				NSD1,2,3			Histone methylation		
				MSH-6			DNA mismatch recognition		
				N-PAC			Transcription elongation		
		K79	Tudor	53BP1			DSB response		
	H4	K20	Tudor	53BP1/Crb2			DNA damage repair	Y	
				PHF20			–		
			MBT	PHF20L1			–		
				L(3)MBTL1			Chromatin lock	Y	
				Sfmbt			Polycomb group repression	Y	
			PWWP	Pdp1			Localizes Set9, promotes K20me3		
WD40	LRWD1			DNA replication (ORC binding)					
H1	K26	MBT	L(3)MBTL1			Chromatin lock			
		WD40	EED			Inhibits PRC2 methyltransferase			
Arginine Methylation	H3	R2							
		R17	Tudor	TDRD3			Transcription activation		
		R26							
	H4	R3	Tudor	TDRD3			Transcription activation		
			?	PCAF or p300			H3 acetylation		
		ADD	Dnmt3a						
Phosphorylation	H3	S10	(Gen5)	Gen5			Histone acetylation	Y	
			2014-3-3	2014-3-3			Adaptor protein	Y	
				Bmh1, Bmh2		K14Ac	Adaptor protein		
		Y41	–			Exclude HP1 α binding			
	H2AX	S139		BRCT repeat		MDC1	Damage repair		
Ubiquitination	H2B	K120/123	?	Cps35			H3K4 methylation		
	H2A	K119	–						
Acetylation	H3	K14	Tandem PHD	DPF3b		K4me	Remodeling (BAF.com)	Y	
			Tandem Bromo	Rsc4			Remodeling	Y	
			Bromo 2	Polybromo			Remodeling (hPBAF.com)		
		K56		Snf5			Gene expression		
	H4	K5,8	Bromo	Brdt				Chromatin compaction	Y
		K16	Bromo	GCN5				Histone acetylation	Y

1.1.7. The RBCC protein family member TRIM24

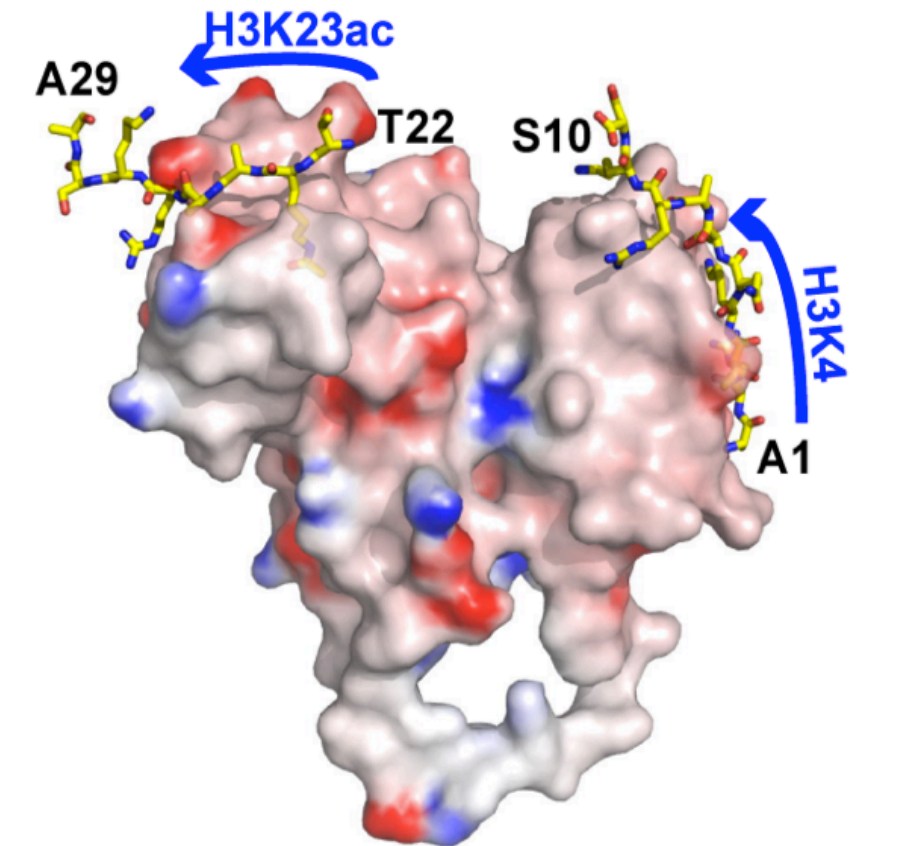
Our lab discovered new function of TRIM24 (Tripartite Motif containing 24) as an epigenetic reader, which simultaneously recognizes two histone marks, H3K4me0K23ac [57]. The TRIM/RBCC protein family is characterized by the presence of a conserved, N-terminal tripartite motif, containing a Really Interesting New Gene (RING) domain, two B-boxes, and a coiled-coil domain, while the carboxyl-terminal domains are variable [58,59]. TRIM24, also known as TIF1 α (Transcription Intermediary Factor 1 Alpha), belongs to the TIF1 sub-family, and contains a consensus LXXLL nuclear receptor interaction motif, a tandem Plant Homeo Domain (PHD) domain and a bromodomain (Bromo) at the C-terminus (Figure 1-4). TRIM24 is a multi-functional protein: through its N-terminal RING domain, TRIM24 functions as an E3 ligase of p53, and targets p53 protein for post-translational proteasomal degradation; upon ligand stimulation, TRIM24-LXXLL motif interacts with, and acts as a potent co-regulator of multiple nuclear receptors (NRs) [60], including RAR (retinoic acid receptor alpha), retinoid X receptor (RXR) [61], Vitamin D3 receptor (VDR), Androgen Receptor (AR), progesterone receptor (PR) and ER α (estrogen receptor alpha) [57,60,62,63,64], as well as NR co-activators coactivator-associated arginine methyltransferase 1 (CARM1) and glucocorticoid receptor-interacting protein 1 (GRIP1) [65]. TRIM24-Bromo also associates with the chromatins through bromodomain–DNA and bromodomain–nucleosome interactions [66].

Figure 1-4: TRIM24 protein domains. (A) Diagram of TRIM24 protein structure. NR: nuclear receptor. (B) Crystal structure of TRIM24 PHD-Bromo domain. Reprinted by permission from Macmillan Publishers Ltd: *Nature* **468**:927-932, copyright (2009) [57].

A



B



1.1.8. TRIM24 regulates nuclear receptor-mediated signaling pathways

TRIM24 promotes ligand-dependent transcriptional activation by RAR, RXR, and VDR *in vitro*, suggesting that TRIM24 may function as a nuclear receptor co-activator. However, in mice lacking Trim24, RAR α - and VDR-repressed genes are re-expressed [67,68,69,70], implicating that Trim24 acts as a co-repressor in RAR- and VDR-mediated signaling *in vivo*. In addition, Trim24 loss leads to overactivation of interferon (IFN)/STAT pathway. Notably, Trim24 and RAR bind to the retinoid acid (RA)-responsive element of the *Stat1* promoter and mediate ligand-dependent repression [71,72], indicating that Trim24 is a co-repressor of the IFN/STAT signaling pathway in mice. Moreover, the *Drosophila* homolog of TIF1 proteins, Bonus, interacts with nuclear receptor beta-FTZ-F1 and represses its target gene transcription *in vivo* [73,74].

However, *in vitro* evidence supports the co-activation function of TRIM24. In prostate cancer cells, TRIM24 promotes AR-mediated transactivation in response to dihydrotestosterone (DHT), through functional interaction and synergy with histone acetyltransferase TIP60, as well as bromodomain containing 7 (BRD7), a negative regulator for cell proliferation and growth [75,76]. TRIM24 also physically interacts with co-activators CARM1 and GRIP1, whereas TRIM24-depletion attenuates GRIP- and AR-mediated transactivation [57,65].

In addition, TRIM24 also play critical roles in the activation of ER α -mediated gene regulation in breast cancer cells. Our lab uses chromatin immunoprecipitation (ChIP)-sequencing (ChIP-seq) analysis and reveals that TRIM24 is recruited by ER α to hundreds of estrogen-response elements (EREs)

in response to estrogen (E₂) stimulation. TRIM24 and ER α physically interact with each other on the chromatin, in an estrogen-dependent manner. When TRIM24 is depleted by shRNA, binding of ER α to, and induction of, estrogen-responsive target genes is reduced.

1.1.9. TRIM24 associates with chromatin and remodeling proteins

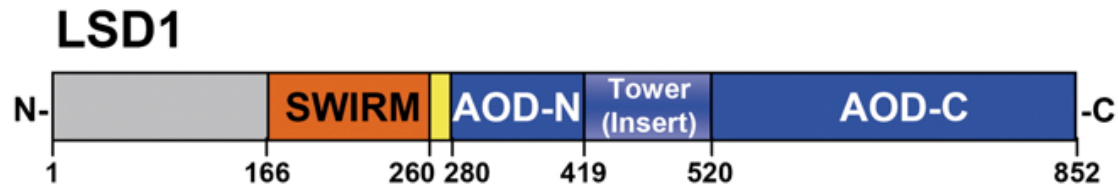
Earlier studies show that mouse heterochromatin protein 1 alpha (mHP1 α) physically interacts with Trim24 [1,60], which is dependent on the HP1-binding region and PHD-Bromo domain of Trim24. However, transcription repression mediated by *Drosophila* homolog of TIF1 proteins, Bonus, requires its RBCC motif, but is not dependent on HP1 binding [2,3,74]. In addition, Bonus is not physically associated with *Drosophila* HP1 proteins. Strikingly, in early mouse embryos Trim24 is highly expressed and co-localizes with the euchromatin of interphase nuclei [4,77]. In addition, Trim24 is involved in the regulation of gene expression during the first wave of transcription activation in mouse embryo development, where Trim24 is localized to the site of active transcription enriched with the mouse chromatin remodeling proteins BRG-1 and SNF2H [6,7,78]. Remarkably, Trim24 depletion leads to mis-regulation of gene expression in the zygote via SNF2H. Taken together, these observations indicate that Trim24 regulates gene activation during the first wave of mouse embryo development and cell differentiation.

1.1.10. Histone demethylase 1 (LSD1) specifically demethylates H3K4me1/2

Histone lysine methylation is dynamically mediated through histone methyltransferases (HMTs) and the opposing enzymes, histone demethylases (HDMs), in response to cellular signals. LSD1 is the first identified HDM, which functions as a transcriptional regulator by catalyzing the demethylation of H3K4me1/2 [9,70,72]. LSD1 possess a SWIRM (SWI3p, Rsc8p and Moira) domain, a FAD (flavin adenine dinucleotide)-binding motif, and a C-terminal amine oxidase domain (Figure 1-5); all of these are structurally indispensable for the demethylation of specific histone lysine substrates. In particular, SWIRM domain is commonly found in histone-interacting proteins. The SWIRM domain of LSD1 forms a structural interface with the amine oxidase domain to assist in substrate binding. Through its FAD-binding motif, LSD1 uses FAD as a cofactor to act on the methylated H3K4 side chain [10,79,80]. The flavin-dependent reaction results in unmodified lysines, and the reduction of FAD to FADH₂, which is re-oxidized by oxygen and forms hydrogen peroxide H₂O₂ as a by-product. The imine intermediate is then further demethylated via hydrolysis, together with the release of formaldehyde (Figure 1-6). However, LSD1 is unable to act on tri-methylated H3K4 due to electrostatic limitation.

Figure 1-5: LSD1 protein domains. (A) Diagram of LSD1 protein structure [33]. (B) Crystal structure of LSD1 protein. Republished with permission of *Annu Rev Biochem*, from Reversal of histone methylation: biochemical and molecular mechanisms of histone demethylases, N. Mosammaparast, Y. Shi, **79**, 155–179, 2010. [67].

A



B

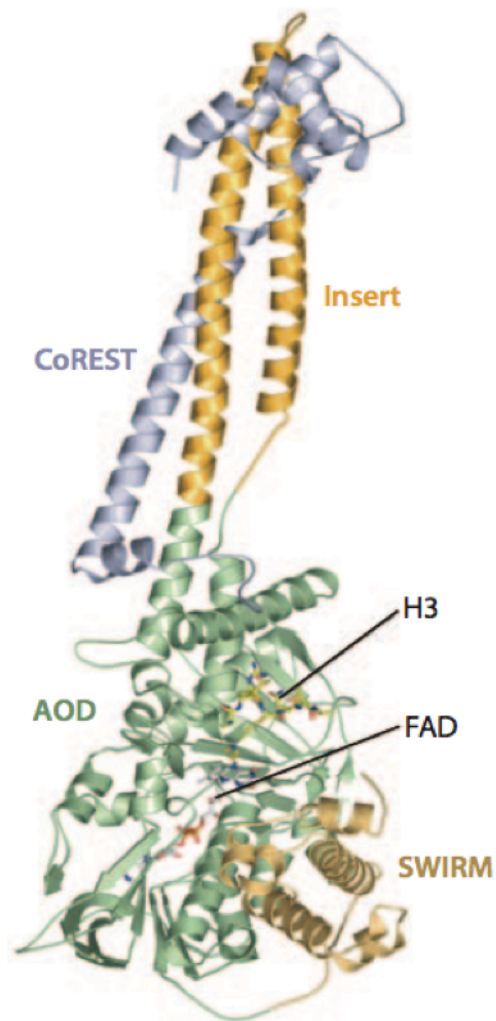
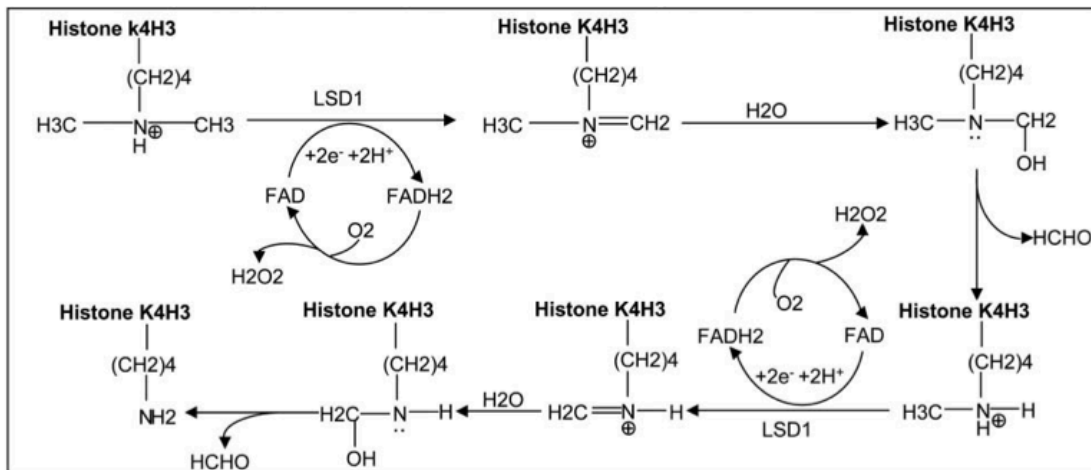


Figure 1-6: Postulated chemical reactions for LSD1-catalyzed demethylation of H3K4me2. Reprinted from *Cell*, **119**, Y. Shi, F. Lan, C. Matson, P. Mulligan, J.R. Whetstine, P.A. Cole, R.A. Casero, Histone demethylation mediated by the nuclear amine oxidase homolog LSD1, 941–953, Copyright (2004), with permission from Elsevier [72].



1.1.11. LSD1 mediates transcription repression

Recombinant LSD1 can demethylate H3K4me1/2 on histone peptides or free histone substrates *in vitro*, but not on nucleosomal substrates [11,12,13,81,82], suggesting that associated factors are required for LSD1-mediated demethylation. In fact, LSD1 is associated with repressor element 1-silencing transcription factor (REST) corepressor (CoREST), histone deacetylases HDAC1/2, and BHC80 (also known as PHD finger protein 21A, PHF21A, a PHD finger protein) for the repression of neuronal genes in non-neuronal cells [14,39]. BHC80 inhibits the enzymatic activity of LSD1, while CoREST functions in the opposite way by allowing LSD1 to demethylate nucleosomal substrates and protecting LSD1 from proteasomal degradation.

In addition, LSD1 also interacts with the orphan nuclear receptor TLX (homolog of the *Drosophila* *tailless* gene), which are both recruited to the *PTEN* gene at regions depleted of H3K4me2 and deacetylated of H3. Knockdown of LSD1 results in de-repression of endogenous *PTEN* expression and inhibition of cell proliferation [15,83]. Moreover, direct interaction between LSD1, additional sex comblike protein 1 (ASXL1), and HP1 α suggests that LSD1 cooperates with ASXL1 in RAR-mediated repression through HP1 α [16,17,84].

1.1.12. LSD1 plays important roles during development and differentiation

Several lines of evidence suggested that LSD1 is functionally critical in the processes of development. For example, temporal and spatial expression of

mouse LSD1 is tightly correlated with demethylation of H3K4 during male germ cell differentiation [17,85]. Notably, Lsd1 is required for pituitary terminal cell-type differentiation through previous regulation of transcriptional activation and repression of developmentally essential genes [5,15,86]. In addition, Lsd1 has been shown to be critical for gastrulation during mouse embryogenesis, possibly through demethylating and stabilizing DNA methyltransferase Dnmt1 protein, and thus maintaining global DNA methylation during embryogenesis [29,87]. Particularly, DNMT1 recruits LSD1 to target gene promoters and regulates DNMT1 target gene expression in human colon cancer cell line [88]. The LSD1-CoREST-HDAC corepressor core also physically interacts with Gfi-1/1b and regulates hematopoietic differentiation by demethylating H3K4 at the promoters of Gfi targets [89]. The association with the transcriptional repressor B lymphocyte-induced maturation protein-1 (Blimp-1) leads to the binding of Lsd1 to Blimp1 target sites and Blimp-1-mediated silencing of mature B-cell genes in plasma cell differentiation [90].

LSD1 is also involved in stem cell differentiation. Through its interaction with CoREST, LSD1 demethylates H3K4me1/2 at a subset of developmentally essential genes that contain bivalent domains of both H3K4me2/3 and H3K27me3 marks in human embryonic stem cells (hESCs) [91]. LSD1 regulates the pattern of H3K4 and H3K27 methylation, leading to the precise balance between self-renewal and differentiation in hESCs. In addition, the inhibition of LSD1 enzymatic activity prevents the proliferation of pluripotent cancer stem cells [92]. Interestingly, mouse Lsd1 is recruited to and is required for

decommissioning enhancers of the pluripotency genes during differentiation. Notably, depletion of LSD1 results in incomplete chromatin demethylation and failure of mESC differentiation in new cell states.

The function and structure of LSD1/CoREST corepressor complex is evolutionally conserved in vertebrates and invertebrates [93]. Particularly, sirtuin 1 (SIRT1) and LSD1 physically interact and cooperatively regulation gene repression by mediating H3K16 deacetylation and H3K4 demethylation respectively. Mutations in *dSirt1* and *dLsd1* (*Drosophila* Sirt1 and Lsd1) genetically interact with the Notch pathway in *Drosophila*. In particular, SIRT1-LSD1 expression is required for NOTCH target repression [94]. In addition, an inactivating mutation of *dLsd1* (*Drosophila* Lsd1) disrupts H3K4 methylation and expression of a subset of target genes, resulting in tissue-specific defects (sterility especially in females) and reduction of animal viability in a gender-specific manner during *Drosophila* development [94]. In addition, studies on *SPR-5*, the *C. elegans* ortholog of human LSD1, showed that LSD1 possibly controls the reprogramming of epigenetic memory in the germline. Notably, *spr-5* mutants exhibit defects in H3K4me2 demethylation in the primordial germ cells, resulting in transgenerational misregulation of spermatogenesis-associated gene expression and progressive sterility.

1.2. AIMS OF THIS WORK

The histone code hypothesis postulates that histone modifying enzymes “write” or “erase” histone marks, while histone binding modules “read”, decode

and execute these marks to effectively trigger downstream responses [5,15]. Here I focus my thesis on estrogen receptor-alpha ($ER\alpha$), the master transcriptional regulator in breast cancer [95], and determine the significance of erasure and recognition of H3K4 methylation on estrogen-responsive elements (EREs) over a time course of LSD1- and TRIM24-regulated estrogen response. Chapter 2 focuses on the co-activation of $ER\alpha$ -mediated transcription by LSD1 and TRIM24, the binding events and dynamics of histone modifications during the time course. I will also discuss how TRIM24 binding and estrogen response is influenced by H3T6 phosphorylation. Chapter 3 focuses the biological functions mediated by LSD1 and TRIM24 and how they affect survival and proliferation in breast cancer cells. The work presented in the dissertation provides a comprehensive analysis of the kinetics of demethylated histones through enzymatic activities and recognition by epigenetic reader proteins, and the molecular events leading to effective histone demethylation, a prerequisite for the chromatin association of TRIM24 and activated $ER\alpha$ -mediated transcription. The findings on the inhibitory effects mediated by depleting or inhibiting TRIM24 and LSD1 in the proliferation breast cancer cells may give insights to future development of combinatorial therapeutics in breast cancer.

Introduction of $ER\alpha$ -mediated signaling, $ER\alpha$ co-activators, involvement of TRIM24 and LSD1 in hormone receptor is presented in section 2.1; introduction of disease-related functions of TRIM24 and LSD1 is presented in section 3.1.

CHAPTER 2: ACTIVATION OF TRIM24-REGULATED ER α TARGET GENES IS DEPENDENT ON LSD1-MEDIATED H3K4ME2 DEMETHYLATION

(Part of this chapter is published: *Wen-Wei Tsai, *Zhanxin Wang, Teresa T Yiu, et. al and Barton MC. 2010. Nature 468, 927–932. *Equal contribution)

2.1. INTRODUCTION

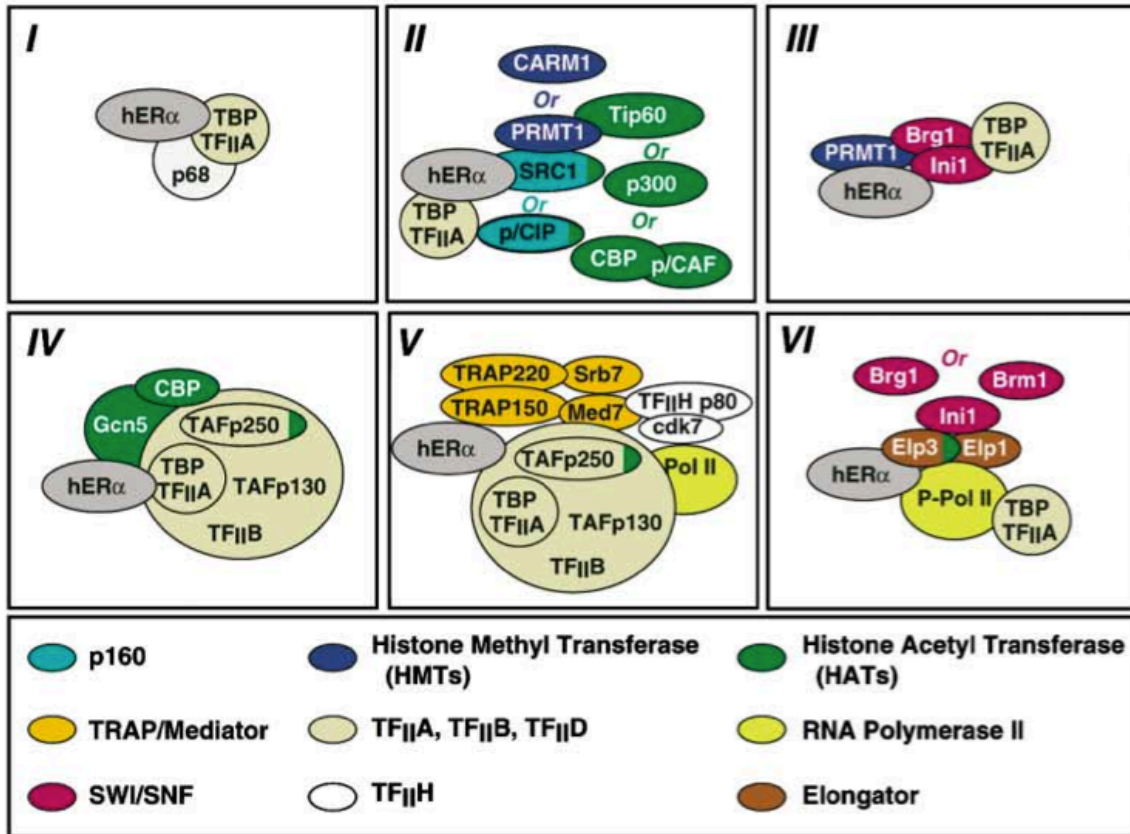
2.1.1. Estrogen receptor-alpha (ER α) is the master transcriptional regulator

Estrogen receptors (ER α and ER β) belong to the ligand-dependent nuclear receptors (NRs), activated by the binding of 17 β -estradiol (E₂), a predominantly naturally occurring estrogen in human. This dissertation focuses on the ER α subtype because it is the master transcriptional regulator that influences most of the physiological processes, such as the growth and maintenance of the reproductive tract, central nervous system and skeletons, and disruptions of ER α functions in the hormone-responsive tissues often lead to the pathological development of cancers, such as breast cancer [57,60,62,63,64,95,96,97]. Ligand-activated ER α immediately undergo conformational change [65,98] and directly binds to sequence-specific DNA elements (termed estrogen-responsive elements; EREs), upstream of target gene promoters, to mediate massive changes in the transcriptome [66,99,100,101]. This process requires the recruitment of transcription factors as well as a plethora of co-regulator proteins. In fact, hundreds of ER α co-regulators have been identified to date [102,103], most of them exist in multi-subunit complexes, and contribute to our understanding of the orchestral molecular events upon estrogen stimulation.

2.1.2. ER α and the transcriptional machinery

In eukaryotic cells, the transduction of cellular and environmental signals often lead to gene transcription, whose activation or repression is regulated through a series of temporal-specific recruitments of transcription factors (TFs) and co-regulators on EREs (Figure 2-1). The model of transcription initiation postulates that during the assembly of pre-initiation complex (PIC), TATA-box binding protein (TBP, a subunit of transcription factor TFIID) is first recruited to the TATA box and is stabilized by TFIIA [104]. TFIIB is then associated with PIC for the conformational remodeling of PIC and for the selection of transcription initiation sites, where RNA polymerase II (RNAP II) is loaded to activate transcription [105,106,107]. TRAP/mediator complex is recruited and structurally remodeled to co-activate the phosphorylation of C-terminal domain of RNAP II (CTD/Rbp1, the largest subunit of RNAP II) [108,109,110], and then exchanged by elongation complexes [111], for transcription to initiate. Components of the transcriptional machinery, such as TFIIB, TFIIIE, and TFIIIF, as well as TAFs and the TBP of TFIID, interact with ER α and are involved in ER α -mediated transcription activation [112,113]. A closer look at the kinetic profile of transcription machinery reveals that every cyclical engagement of TFIIB is aligned with ER α [73], suggesting that ER α recruitment associates with the structural remodeling of PIC by TFIIB. Importantly, ER α -driven cycles lead to the sequential and cyclical recruitment of TRAP/mediator (Med7 and TRAP220), cdk7 (essential component of the transcription factor TFIIH), followed by activated RNAP II and transcriptional elongators (Elp1 and Elp3) [73].

Figure 2-1. Protein complexes involved in estrogen-induced activation of *pS2* gene. Reprinted from *Cell*, **115**, R. Metivier, G. Penot, M.R. Hubner, G. Reid, H. Brand, M. Kos, F. Gannon, Estrogen receptor-alpha directs ordered, cyclical, and combinatorial recruitment of cofactors on a natural target promoter, p.751-763, Copyright (2003) [73].



In fact, DNA accessibility is largely dependent on the nucleosomal architecture, which determines subsequently whether transcription is to be initiated. Enhanced ER α binding is achieved by epigenetic machinery that modifies the histone-DNA interface of the surrounding chromatin architecture. Through covalent histone modifications, chromatin remodeling, and histone-octamer exchange by histone chaperones, recruitment or dismissal of specific regulatory proteins occur in a context- and temporal-dependent manner [25,114,115].

2.1.3. Histone modifying enzymes as ER α co-regulators

Recent works demonstrated the potential role of histone-modifying enzymes as ER α co-regulators [116,117]. Histone acetyltransferase p300/CBP is the first epigenetic regulator that links epigenetics to transcription co-regulation. p300/CBP relaxes the nucleosomal DNA to allow for TF binding and is always associated with transcription activation. HATs not only co-activate ER α , but also other classes of TFs, in order to enhance activated transcription [118]. For example, the cAMP response element-binding (CREB)-binding protein (CBP)/p300 and the GCN5 complex, TFTC/SAGA [TATA-binding protein (TBP)-free TBP associated factors (TAF)-containing complex/Spt-Ada-Gcn5 acetyltransferase] are both HATs that have been shown to co-activate ER α -mediated transactivation [119]. Certain HDACs are also associated with ER α , possibly for the termination of activated transcription [120,121].

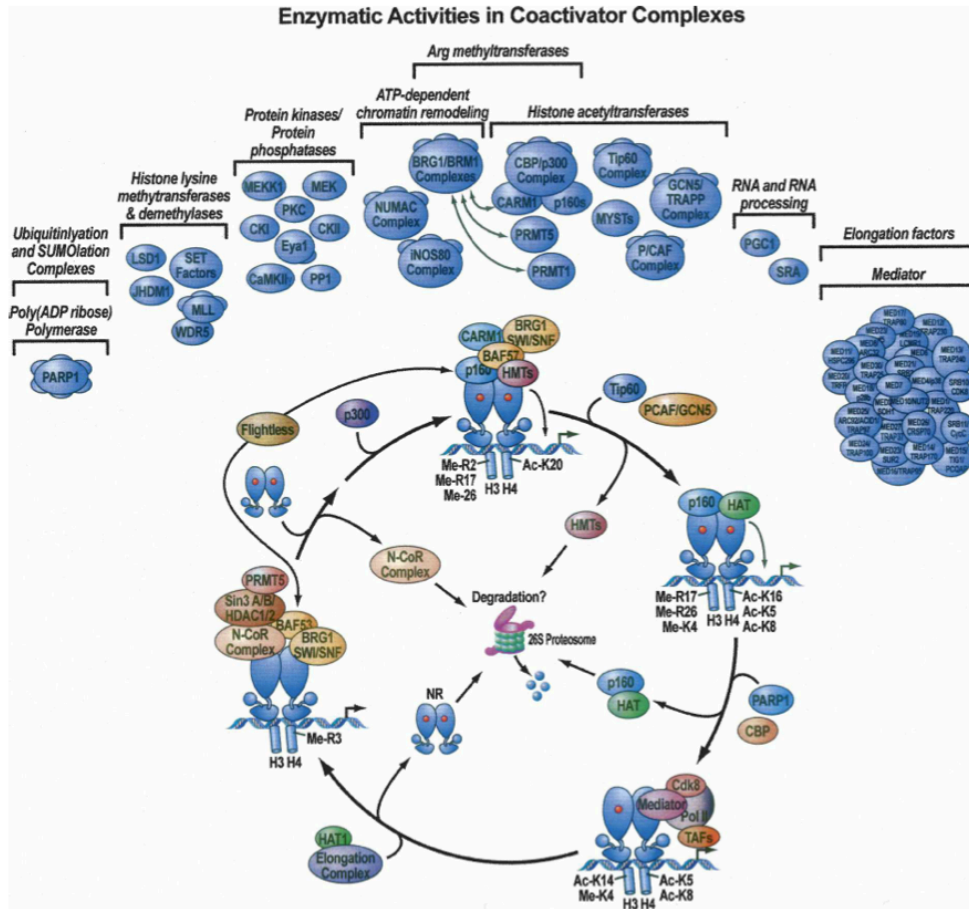
The histone code hypothesizes that crosstalk between histone PTMs orchestrates dynamic and context-specific reorganization of chromatin, an essential process for transcriptional regulation [5,15,122]. For example, it is suggested that histone methylation on specific residues is more upstream than acetylation in order to direct the chromatin state for gene activation/repression [123]. Notably, the roles of histone methylation/demethylation in ER α co-regulation are more dynamic [124]. HMTs/HDMs can be associated with either activation or repression, in a histone residue-, DNA sequence- and context-specific manner [33]. ER α co-activators are not only limited to HATs/HDACs and HMTs/HDMs, but also include histone kinases and histone phosphatases, ubiquitin, SUMO ligases and others. Modifiers of other histone PTMs functioning as ER α co-regulators are shown in Figure 2-2.

2.1.4. Chromatin remodeling and estrogen response

Chromatin remodelers play essential function in the process of chromatin reorganization, in an ATP-dependent manner [125,126]. By influencing histone-DNA interactions and sometimes through nucleosome sliding, this reversible process exposes naked DNA to a wide array of TFs and indirectly regulates transcription. This process can be mediated by three types of chromatin remodelers: Switch/Sucrose Non-Fermenting (SWI/SNF)-, Imitation Switch (ISWI)-, and Chromdomain Helicase DNA Binding Protein 4 (CHD4/MI2)-complexes [127]. Both SWI/SNF and ISWI can either activate or represses chromatin [125,128], while CHD4/MI2 is involved in chromatin inactivation [129].

Notably, the core subunits of these remodeler complexes can function as transcription coregulators. For example, BAF57, a subunit of the SWI/SNF complex, co-activates ER α -regulated transcription [130]. In addition, the association between ER α and these remodelers is believed to remodel the nucleosomes surrounding hormone-responsive DNA elements, and is indispensable for the binding of other ER co-regulators.

Figure 2-2. Co-activators of estrogen receptor- α . Reprinted with permission from Cold Spring Harbor Laboratory Press, *Genes and Development* **20**: 1405-1428, copyright (2006) [75].



2.1.5. Potential involvement of histone chaperones in ER α regulation

Effects of histone chaperones in transcriptional regulation also gained researchers' attention recently. By the regulation of chromatin reorganization through the eviction and reassembly of histones during replication, repair and transcription, chaperon proteins re-organize nucleosomal DNA to permit the accessibility of sequence-specific TFs and NR co-regulators during gene activation [131]. For examples, *Drosophila* DEK (dDEK) co-localizes with nuclear ecdysone receptor (EcR) in the salivary gland. Importantly, phosphorylation of *Drosophila* DEK (dDEK) induces complex formation with casein kinase 2; and this complex is known to associate with active histone marks. dDEK functions as a histone chaperon and facilitates H3.3 assembly [132]. Therefore histone chaperones such as dDEK may regulate gene activation and represent a distinct class of nuclear receptor co-regulators; but this potential still awaits further validation.

2.1.6. Timely and cyclical recruitment of ER α and its co-factors

Studies in MCF7 human breast cancer cells suggested that activation of ER α target genes exhibit distinct patterns of estrogen-mediated response, in a time-dependent manner [100,101]. It is therefore reasonable for estrogen to induce cyclical and sequential binding of ER α and its co-regulators. One study of the canonical *pS2* ERE in MCF7 human breast cancer cells led to a model where ER α binds to EREs in 3 distinct cycle of protein recruitment to chromatin (protein complexes involved illustrated in Figure 2-1) [73]. During the first “transcriptionally unproductive” cycle, initial engagement of the SWI/SNF

component BRG1 remodels the chromatin, and then H3K14 becomes acetylated and H4R3 becomes dimethylated, concurrent with the recruitment of acetyltransferases Tip60/p300 and arginine methyltransferase PRMT1, respectively. Transcription machinery regulators TATA-box binding protein (TBP, a subunit of transcription factor TFIID), TFIIA, mediator/TAF130, and acetyltransferase GCN5 are also recruited, all of which occur before the recruitment of activated RNA polymerase II [73]. During the second and third “transcriptionally productive” cycles, ER α is recruited every 40-50 minutes [73] and this recycling is dependent on proteasomal-mediated turnover of ER α [73,133]. Notably, every ER α recruitment coincides with the acetylation of H3K14 and H4K16, as well as the di-methylation of H3R17, and this process precedes the recruitment of activated RNA polymerase II. Moreover, timely recycling of p160 factors, histone methyltransferases (HMTs), and histone acetyltransferases is also observed on the *pS2* ERE.

Studies of histone methylation suggest that it is associated with either activation or repression of ER α -mediated response, in a histone residue-, DNA sequence-, and context-specific manner [31,33,124,134]. However, whether regulation of histone lysine methylation and demethylation is critical in the stepwise process of ER α -mediated transcriptional activation remains to be explored. Specifically, a comprehensive view of the kinetics of histone lysine demethylation through enzymatic activities and the recognition of demethylated histones by epigenetic reader proteins awaits further investigation, and thus is the central focus of this study.

2.1.7. TRIM24 functions as an ER α co-activator through chromatin recognition

Our lab recently identified an ER α co-activator, namely TRIM24. ChIP analysis showed that TRIM24 is co-recruited with ER α upon estrogen treatment to *GREB1* ERE sites (Figure 2-3A). Notably, ER α and TRIM24 are recruited as a complex, as revealed by sequential ChIP experiment (Figure 2-3B). TRIM24 depletion reduces recruitment of ER α to *GREB1* ERE (Figure 2-4B) and lead to down-regulation of estrogen-induced *GREB1* activation at $t = 3\text{hr}$ and $t = 6\text{hr}$ (Figure 2-4A, left). A detailed investigation of TRIM24 PHD-Bromo crystal structure establishes the simultaneous interaction of PHD-Bromo with unmethylated H3K4 (H3K4me0) and acetylated H3K23 (Figure 1-4B) [57]. I performed mutagenesis and generated TRIM24-PHD point mutation (C840W) and Dr. Tsai showed that reintroduction of WT-TRIM24, but not TRIM24-C840W, is able to fully rescue TRIM24 function in shTRIM24 cells.

Figure 2-3. ER α and TRIM24 are recruited together to EREs upon estrogen induction. (A) ChIP experiment showing both ER α (left) and TRIM24 (right) recruitment to *GREB1* distal and proximal EREs upon 15 min and 6 hours of estrogen (E₂) treatment. (B) Sequential ChIP showing that ER α and TRIM24 recruitment as a complex after 6 hours of E₂ activation. Reprinted by permission from Macmillan Publishers Ltd: *Nature* **468**:927-932, copyright (2009) [57].

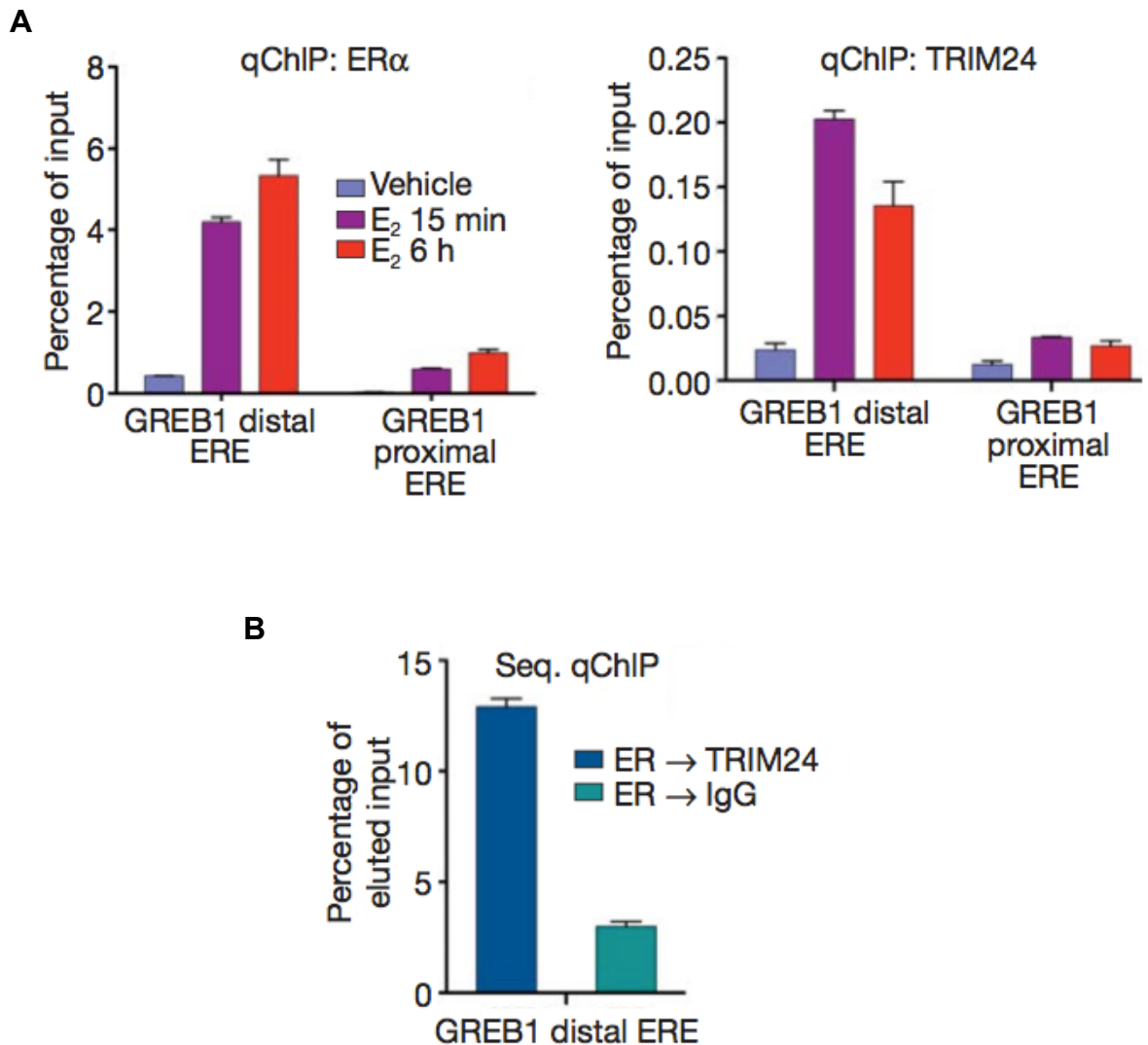
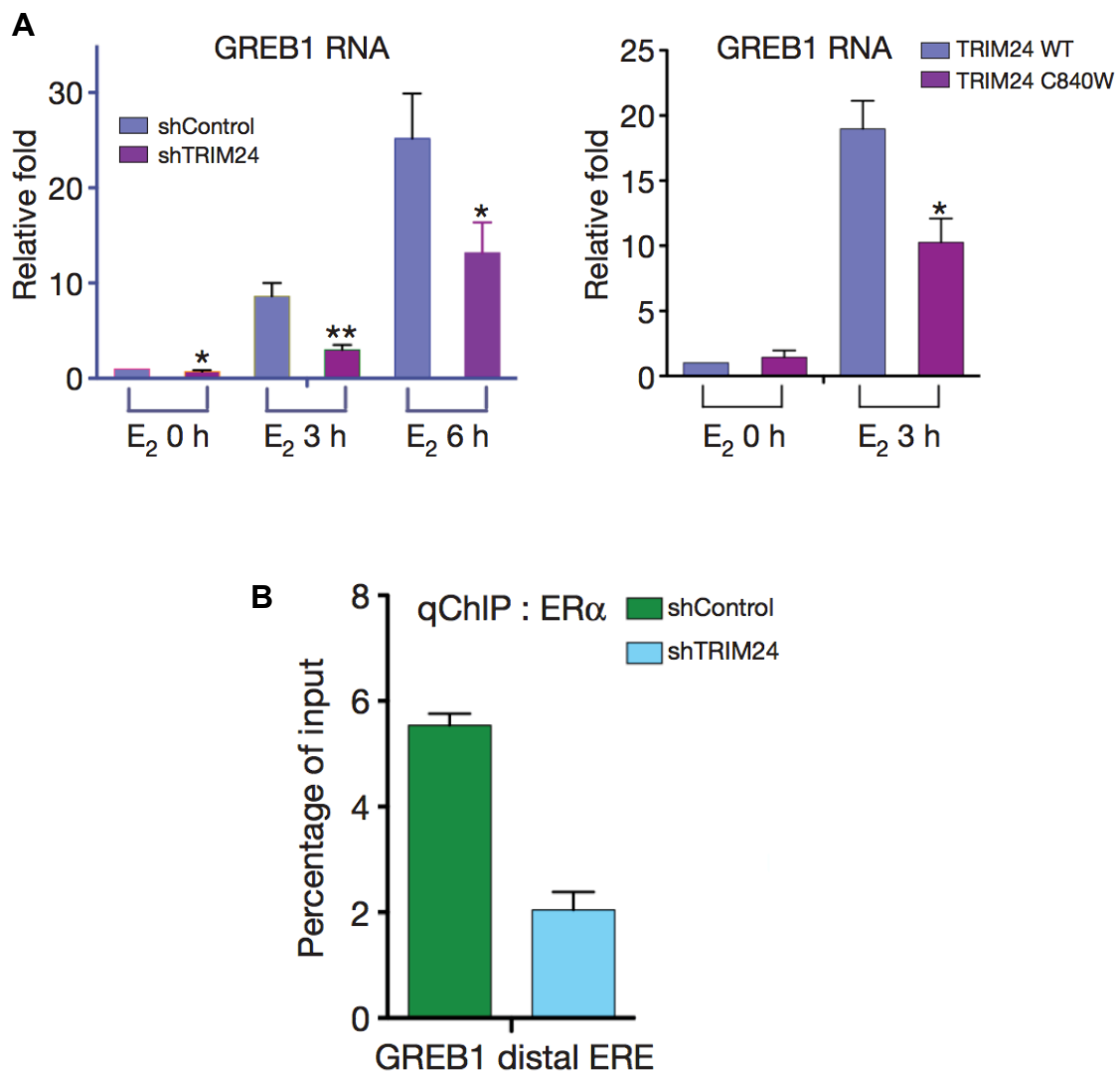


Figure 2-4. Depletion of TRIM24 decreases ER α binding to ERE and estrogen-activated gene induction. (A) qPCR: (left) depletion of TRIM24 by shRNA reduces E₂-induced activation of GREB1 at indicated time points; (right) re-introduction of wildtype (WT) but not PHD-finger mutant (C840W) rescues TRIM24-coactivated GREB1 induction. (B) ChIP: Knockdown of TRIM24 leads to decreased ER α recruitment to GREB1 distal ERE. Reprinted by permission from Macmillan Publishers Ltd: *Nature* **468**:927-932, copyright (2009) [57].



2.1.8. TRIM24 simultaneously recognizes two histone signatures on H3

Sequence alignment shows that TRIM24 PHD finger is highly similar to BHC80, especially the conserved residues critical for BHC80-H3K4me0 interaction. Binding of TRIM24 PHD-Bromo is abolished by H3K4 mono-, di-, or tri-methylation. In fact, TRIM24 PHD-Bromo binds to unmodified H3(1-15)K4 with a dissociation constant (K_D) of 8.6mM, as measured by isothermal titration calorimetry (ITC)-based binding assay. Even with the addition of one methyl group on H3K4, TRIM24 PHD-Bromo loses its binding ($K_D = 41\text{mM}$), the affinity is even weaker for di-methylated H3K4 peptide ($K_D = 198\text{mM}$), and with tri-methylation on H3K4 the interaction is totally abolished ($K_D > 400\text{mM}$). These observations suggest that TRIM24 PHD-Bromo specifically binds to unmethylated H3K4. Simultaneous with H3K4me0 recognition by TRIM24-PHD, TRIM24 bromodomain interacts with acetylated H3(13-21)K23ac peptide with a K_D of 8.8mM. Acetylation of H3K23 enhances the binding of TRIM24 to unmethylated H3K4. Interestingly, TRIM24 PHD-Bromo is tolerable with H3K4 tri-methylation in the presence of H3K23 acetylation (H3K4me3K23ac), suggesting that the combinatorial recognition of TRIM24 is dynamic and requires further investigation in the cellular context.

2.1.9. TRIM24 preferentially binds to regions depleted of H3K4me2

ChIP sequencing analyses of TRIM24 and H3K4me2 reveal that TRIM24 preferentially binds to genome-wide regions depleted of H3K4me2 [57]. As an example, Figure 2-5A shows TRIM24 binding and H3K4me2 occupancy at the estrogen responsive element (ERE) of an ER α target gene *IGFBP4*. TRIM24 is recruited to *IGFBP4*-ERE in response to estrogen stimulation. At the same ERE, demethylation of H3K4me2 is also prominent upon E₂. Figure 2-5B shows the global binding profile of TRIM24 in regions relative to H3K4me2 level. Corresponding number of tags sequenced for H3K4me2 occupancy is represented graphically on the y-axis, in relation to the distance to TRIM24 binding site (in terms of base pair, bp) on the x-axis (Figure 2-5B). It is clear that global demethylation in response to E₂ is observed, and TRIM24 preferentially binds to regions of low H3K4me2 occupancy. These observations, together with the peptide binding and ITC assays mentioned above, suggested that H3K4me2 must be demethylated in order for TRIM24 to bind to the chromatin, and targeting histone demethylases that mediate H3K4me2 demethylation may regulate the functions of TRIM24.

2.1.10. LSD1 as a transcription co-activator in androgen and estrogen receptors-mediated signaling

Among the four H3K4-specific demethylases, I focus on LSD1 in this study because it is the only enzyme capable of the demethylation from H3K4me2 to H3K4me1 and then to H3K4me0 [9,70,72], a preferential substrate for TRIM24 recognition, leading to TRIM24-regulated co-activation of ER α . Although LSD1 plays an important role in mediating gene repression under specific circumstances and in certain tissues, in hormone-responsive tissues, evidence showed that LSD1 mainly functions as a co-activator in nuclear receptor-mediated transcription activation. For example, estrogen induction leads to demethylation of H3K4me2 and H3K9me2/3 at ER α target genes *pS2* and *GREB1* EREs [124]. LSD1 interacts with ER α and co-activates estrogen-mediated expression of these genes [124]. However, whether LSD1 functions as an ER α by depleting H3K4 methylation has not been addressed. Another study of the ER α pioneer factor FOXA1 (Forkhead Box A1) showed that FOXA1 binding sites are enriched with H3K4me1/2 [135]. Notably, when LSD1 is overexpressed, H3K4me2 decreases while H3K9me2 remains unchanged, but FOXA1 recruitment is impaired [135]. These observations strongly suggested a role of LSD1 in ER α -regulated transcription through its ability to demethylate H3K4me2.

On the other hand, LSD1-mediated demethylation also generates the by-product hydrogen peroxide (H₂O₂), which has been shown in MCF7 cells to recruit 8-oxo-guanine–DNA glycosylase 1 (OGG1) and topoisomerase II β

(TopoII β), triggering chromatin looping for activated ER α binding [136]. In prostate cancer LNCaP cells, LSD1 interacts with androgen receptor (AR), binds to and co-activates AR target genes [134]. However, in both studies, LSD1 has been suggested to demethylate H3K9, a biochemically non-preferable substrate, instead of H3K4.

The enzymatic specificity of LSD1 has been debatable for awhile until a recent study showed that LSD1 interacts with H3K9me3-specific demethylase JMJD2C in prostate cancer cells, where JMJD2C also functions as a co-activator of AR [137]. Therefore, the change in H3K9 methylation when LSD1 is depleted could possibly be due to the loss of interaction with JMJD2C and other H3K9 demethylase(s), or even gain of H3K9 methyltransferase(s) recruitment. Although the conclusion from this study still emphasized the ability of LSD1 to demethylate mono- and di-methylated H3K9, and switch its substrate specificity with methyl-H3K4, how and whether substrate switch of LSD1 is possible and what unknown cofactors may be involved still remain unknown.

2.1.11. H3T6ph inhibits H3K4 demethylation mediated by LSD1 and chromatin binding by H3K4me0 reader proteins

LSD1-mediated demethylation can be regulated by several mechanisms [138,139,140]; one newly identified regulation is by phosphorylation of H3T6 (H3T6ph). Mass spectrometry analyses revealed that the presence of H3T6ph on H3K4me2 peptide inhibits LSD1-mediated demethylation [31]. H3T6ph is mediated by PKC family kinases PKC α , β I, and β II. In the absence of PKC β I and

H3T6ph, LSD1 is able to demethylate H3K4me2 on core histones or nucleosomes in demethylation assays. However, when PKC β I is added, LSD1 fails to mediate H3K4me2 demethylation. The same histone mark also influences the histone recognition of several PHD-finger reader proteins, such as BHC80 and AIRE [29], as well as ARTX-ADD [141], which specifically bind to unmethylated H3K4. Therefore, it is plausible to postulate that functions of H3K4me0 reader TRIM24 in estrogen response may be intrinsically regulated by LSD1-mediated H3K4me2 demethylation and H3T6 phosphorylation.

2.1.12. Hypothesis: Function of TRIM24 is dependent on LSD1-mediated H3K4 demethylation

Despite the many functions mediated by TRIM24 and LSD1, and their respective roles in estrogen response, no study has focused on the potential cooperation of TRIM24 and LSD1 in mediating ER α target gene activation through changes and recognition of specific histone modifications. Through its recognition of unmethylated H3K4, TRIM24 functions as a chromatin reader and an ER α co-activator. However, it is unknown whether LSD1-mediated demethylation of H3K4me1/2 leads a favorable histone substrate for TRIM24 binding and orchestrated ER α -mediated transcriptional activation. Therefore, I ***hypothesize*** that *the function of TRIM24 as an ER α co-activator is dependent on LSD1-mediated H3K4 demethylation*. To test the hypothesize, I have formulated the following specific aims and test them using several approaches in human tumor-derived MCF7 breast cancer cells:

- Establish the time-dependent profile of ER α target gene activation when TRIM24 or LSD1 is depleted
- Establish a cyclical recruitment profile of TRIM24 and LSD1, as well as dynamic H3K4 methylation over a time course of E₂ stimulation
- Screen for potent LSD1 inhibitors and their effects on H3K4me₂ on EREs and ER α -mediated transcription activation
- Determine whether inhibition of LSD1 prevents TRIM24 from binding to EREs on the chromatin
- Investigate how H3T6 affects TRIM24-regulated ER α -mediated transcription

In summary, the results presented in this chapter suggested that TRIM24 and LSD1 are cyclically recruited to EREs in response to E₂ stimulation. Estrogen induction mediates dynamic H3K4 methylation/demethylation events over a time course. Moreover, inhibition of LSD1 enzymatic activity results in re-methylated H3K4me₂, decreased binding of TRIM24 and ER α , leading to down-regulation of TRIM24-regulated ER α -mediated transcription activation. Finally, H3T6ph impairs TRIM24 binding to histone H3 and may play a critical role in ER α -mediated transactivation.

2.2. MATERIALS AND METHODS

2.2.1. Cell culture

MCF7 cells are obtained from ATCC and cultured in Dulbecco's Modified Eagle Medium (DMEM) supplemented with 10% fetal bovine serum (FBS), as previously described [57,68]. For hormone depletion, cells are changed to charcoal-stripped hormone-free medium (Gibco) supplemented with 10% charcoal dextran-treated FBS (Hyclone) for 96h. Estrogen induction is performed in the presence of 17 β -estradiol (Sigma) for the indicated times. Ethanol is used as a vehicle control.

2.2.2 Mutagenesis

Site-specific point mutations are introduced to wildtype and FLAG-tagged TRIM24 plasmid using QuickChange® Site-Directed Mutagenesis Kit (Stratagene), according to manufacturer's suggestions. Each transformation reaction is then plated on LB-ampicillin agar plates and incubated at 37°C overnight. DNA isolated from *E. coli* culture is purified using DNA Miniprep Kit (Qiagen). Sequences of specific point mutation have been confirmed by M.D. Anderson DNA Analysis Core Facility.

2.2.3. Transient DNA plasmid transfection

MCF7 cells cultured in 6-well plates in the presence of hormone-depleted medium are transfected with FLAG-TRIM24 using Effectene (Qiagen), according to manufacturer's instructions. Briefly, 2 μ g of DNA plasmid is resuspended in

300 μ L EC Buffer, together with 16 μ L Enhancer and vortexed for 1 sec. After 5 min of incubation at room temperature (RT), 60 μ L of Effectene Transfection Reagent is added to the mixture, and vortexed for 10 sec. At the end of 10 min incubation at RT, medium is added to reach 500 μ L total and pipetted evenly onto the cells. Cells are treated with estrogen or control, as indicated. RNA is harvested 48 hr after transfection.

2.2.4. Transient knockdown by siRNAs

MCF7 cells cultured at 6-well plates are transfected with siControl, siTRIM24, or siLSD1 (ON-TARGETplus SMARTpool, Dharmacon) using LipofectamineTM 2000 (Invitrogen), according to manufacturer's instructions. Briefly, cells are changed to Pen/Strep-free medium 2 to 3 hr prior to transfection. For each transfection, 100 pmol of siRNA and 5 μ L LipofectamineTM 2000 are first individually resuspended into 250 μ L medium and incubated at RT separately for 5 min. Then, siRNA and LipofectamineTM 2000 are mixed together and further incubated at RT for 20 min. Cells covered with 250 μ L medium are then transfected with the siRNA-Lipofectamine mixture for 4 to 6 hr. Medium is changed and cells are cultured for a total of 72 hr before harvest. Estrogen treatment is added prior to harvest for indicated time points.

2.2.5. RNA extraction, cDNA, and real-time RT-PCR

RNA in each 6-well plate is isolated using Trizol reagent (Invitrogen), according to manufacturer's suggestions. 3 μ g of RNA are used to synthesize

cDNA using RT-PCR kit (Invitrogen), according to manufacturer's suggestions. Each real time PT-PCR reaction mix, containing 2 μ L of dilutes cNDA (1:10 dilution), 5 μ L SYBR Green Reaction Mix (Applied Biosystems), 0.25 μ L forward primer (20 μ M), 0.25 μ L reverse primer (20 μ M), and 2.5 μ L sterile water, is set up in a 96-well plate and performed in a 7500 Fast Real Time PCR instrument (Applied Biosystems). Primer sequences are listed below:

Gene	Forward Sequence	Reverse Sequence
GREB1	GGCAGGACCAGCTTCTGA	CTGTTCCCACCACCTTGG
PR	GTGCCTATCCTGCCTCTCAATC	CCCGCCGTCGTAACITTCG
pS2	TTGTGGTTTTCTGGTGCA	CCGAGCTCTGGGACTAATCA
IGFBP4	AGAGCGAAGGGGGTCAAAGGAAGA	TGGGGAGGGAGGTGTAGGGGAAGG
BCAS4	CCTGGCCGGGGCTGATGGA	GGCACCGAGGTCTGGAGGCAACA
TRIM24	TATCTCCAGAGGCAGTTG	CTCACAGTACAGCTTCAG
LSD1	TCCTGGCCCCTCGATTC	ATGTTCTCCCGCAAAGAAGAGT
GAPDH	GAAGGTGAAGGTCGGAGTC	GAAGATGGTGATGGGATTC

2.2.6. Chromatin immunoprecipitation (ChIP)

MCF7 cells are cultured in 150 mm² plates for ChIP experiments as previously described^{58,70}. Essentially, after 96 h of hormone depletion, cells are treated with indicated treatment or corresponding control, in addition to 20nM 17 β -estradiol (Sigma) or ethanol, for indicated time course. Upon harvest, cells

are cross-linked with 556 μ L 37% formaldehyde (in 20 mL medium) and rotated at RT for 15 min. Cross-linking is stopped with 6.8 mL of glycine (0.5M stock) and rotated at RT for an additional 10 min. The media on the plates are then removed and washed with chilled sterile PBS twice before scrapping in 5 mL PBS (with 1X PMSF). Cells pellets are spun down 2K rpm for 5 min at 4°C. After the supernatant has been discarded, cells are lysed with 1 mL Cell Lysis Buffer (5mM PIPES pH 8.0, 85mM KCl, 0.5% NP-40, fresh protease inhibitors) and incubated on ice for 15 min. Then the cell lysates are collected after centrifugation at 5K rpm for 5 min and resuspended in 300 μ L Nuclear Lysis Buffer (50mM Tris pH 8.1, 10mM EDTA, 1% SDS, and fresh protease inhibitors). 100mg glass beads (Sigma) are added to the samples. Sonication is performed using a bioruptor (Diagenode, Bioruptor Twin #UCD-400) at high input for 36 min (in a 30 sec ON, 30 sec off mode). After sonication, the tubes are spun at 14K for 15 min at 4°C. Supernatant is transferred to a new tube to check for fragment size. For ChIP experiments, lysates are divided and diluted using ChIP Lysis Buffer (150mM NaCl, 25mM Tris pH 7.5, 5mM EDTA, 1% TritonX 100, 0.1% SDS, 0.5% Deoxycholate, and fresh protease inhibitors). After IgG preclearing (2.5 μ g for 1 hr at 4°C), immunoprecipitation is performed overnight (O/N) with specific antibodies: ER α (F-10, Santa Cruz), TRIM24 (ProteinTech), LSD1 (Abcam), histone H3 (Abcam), H3K4me1 (Abcam), H3K4me2 (Active Motif), H3K4me3 (Active Motif), H3T6ph (Abcam), H3K9me2 (Abcam) or normal sheep IgG (Upstate/Millipore). The next day, pre-washed Protein A Sepharose beads (GE Health) are incubated with antibody/protein bound complexes for 2 hr at 4°C.

Then, Protein A beads are washed once with RIPA Buffer (50mM Tris pH 8.0, 150mM NaCl, 0.1% SDS, 0.5% Deoxycholate, 1% NP-40, and 1mM EDTA), once with High Salt Buffer (50mM Tris pH 8.0, 500mM NaCl, 0.1% SDS, 0.5% Deoxycholate, 1% NP-40, and 1mM EDTA), once with LiCl Wash (50mM Tris pH 8.0, 1mM EDTA, 250mM LiCl, 1% NP-40, and 0.5% Deoxycholate), and twice with TE Buffer, each wash for 10 min at 4°C. The input and the ChIP samples are resuspended into 300µL TE Buffer and incubated with 1.5µL RNaseA (10mg/mL stock) for 30 min at 37°C and then with 15µL SDS (10% stock) and 7.5µL ProteaseK (10mg/mL stock) for 2 hr at 55°C.

The crosslinks are reversed by incubating the samples at 65°C O/N. The next day, Protein/antibody bound DNA fragments are extracted with 300µL Phenol/Chloroform twice and 300µL Chloroform once. Precipitation is performed using 30 µL NaOAc (3M stock), 600 µL ethanol (100% stock) and 25 µL glycogen (1mg/mL stock) for 1 hr at -80°C. qPCR analyses are performed to analyze specific antibody- and protein-bound DNA using SYBR Green Reaction Mix (Applied Biosystems) in a 7500 Fast Real Time PCR instrument (Applied Biosystems). Sequences of ChIP primers are listed below:

Region	Forward Sequence	Reverse Sequence
GREB1- distal ERE	GAGCTGACCTTGTGGTAGGC	GGTTTTTAAGCAGCCAGCAG
GREB1- proximal ERE	TTGTTGTAGCTCTGGGAGCA	CAACCAGCCAAGAGGCTAAG
GREB1 +54kb	ACCTGTCATCCCAGCTACTCG	GCTGTCTGGCAAGGTGAGTT
PR-221kb	GGGAAATTGCCTCTCCTCACTTTG	CCAAGGATTAGGGCAGTTCAGAAG
PR-205kb	AAAGAGAGTGAGTCATTTGTG	CAGGAGATCCGTGAGTTC
PR +4kb	TTGGTTCTGCTTCGGAATCTG	CCTCCTCTCCTCACTCTTGG
pS2-ERE	GCTTAGGCCTAGACGGAATGGGC	CCAGGTCCTACTCATATCTGAGAG
IGFBP4- ERE	GGTGCAGAGAAGCTGTTGAAG	AGACAGGCTCAGGCTCAAGA
GAPDH	GAAGGTGAAGGTCGGAGTC	GAAGATGGTGATGGGATTTTC

2.2.7. GST-tagged protein expression and purification

GST-only and GST-tagged TRIM24 recombinant proteins are expressed using BL21-AI strains of *E. coli* (Invitrogen) and cultured in 2X LB media in the presence of 100 ug/mL Ampicillin at 37°C. When the overnight culture reaches OD₆₀₀ of 0.5 to 0.6, it is induced with final concentration 0.2% L-arabinose (Sigma) and 100 µM ZnCl (for PHD zinc finger expression), and subsequently cultured at RT for 24 hr. The cell pellets are collected by spinning at 4K rpm for

15 min at 4°C and snap-freeze at -80°C. The frozen pellets are resuspended in cold lysis buffer (50mM Tris pH 7.5, 150mM NaCl, 0.05% NP-40, 1X PMSF and protease inhibitors) in the presence of final concentration 0.5mg/mL lysozyme solution and sonicated at an output of 18% for 40 sec (in a 1 sec on, 1 sec off manner) on ice. The supernatant is collected by centrifugation at 12K rpm for 15 min at 4°C, and incubated with washed 50% slurry mix of glutathione (GST) beads (AmerSham) O/N at 4°C. The GST-beads are washed three times with lysis buffer, then once with elution buffer (100mM Tris pH 8.0) at 4°C for 5 min. Finally, the GST-proteins are eluted with elution buffer containing 10mM fresh glutathione. Concentration is measured using Bradford protein assay at A280 and analyzed by Coomassie blue staining of SDS-PAGE gel, in comparison to BSA standards. Final concentration of 10% glycerol is added to the recombinant proteins for long-term storage at -80°C.

2.2.8. Biotinylated peptide pulldown assay

GST-RBP2 (PHD1 or PHD2) recombinant proteins are obtained from Dr. Xiaobing Shi's laboratory, GST-JMJD2A-Double Tudor Domain (DTD) from Dr. Mark Bedford's laboratory and GST-LSD1 from Dr. Yang Shi's laboratory. Peptides are biotin-labeled and custom-made by peptide synthesis facility at Yale University.

In each binding assay, 2 µg of GST-tagged recombinant proteins and 1 µg of biotinylated histone peptides (1mg/mL) are incubated together in 500µL NTP binding buffer (50mM Tris PH 7.5, 200mM NaCl, 0.1% NP-40) O/N at 4°C. For

input, no peptide is added. On the next day, 20 μ L of washed 50% slurry of Streptavidin beads (GE Heath) are added into each binding assay and rotated at 4°C for 1 hr. The beads are washed with NTP binding buffer and rotated at 4°C for 10 min. Flowthrough (FT) is saved. After three washes, the beads are resuspended in 60 μ L of 2X SDS loading dye, boiled and loaded on a 10% SDS-PAGE gel, together with 10% input and FT for each binding assay. The peptide-bound GST proteins are detected by GST-antibody (Cell Signaling, 1:1000).

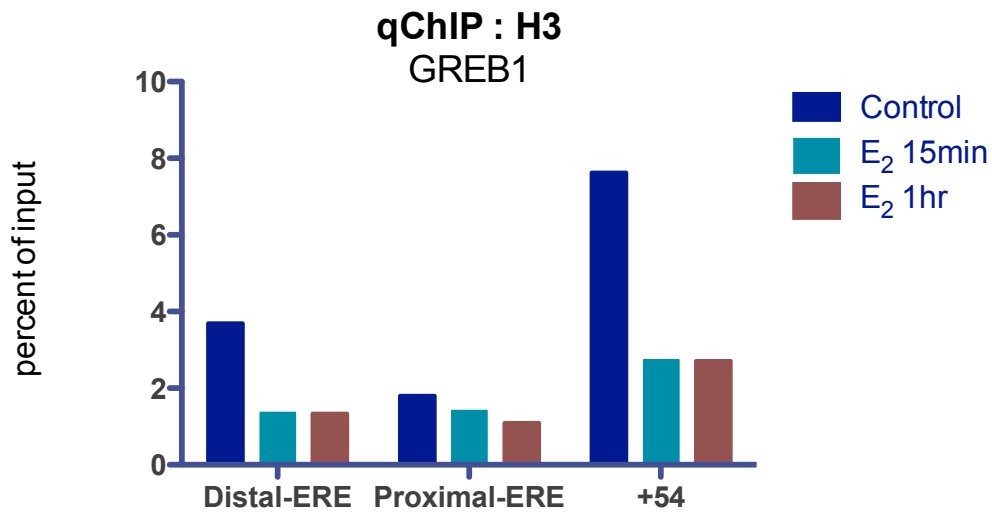
2.3. RESULTS

2.3.1. Estrogen triggers immediate dynamic histone modifications

The addition of an ER α agonist, 17 β -estradiol (estrogen, E₂), immediately triggers changes in the chromatin architecture. First, total H3 at ER α target genes, *GREB1* and *PR* estrogen responsive elements (EREs), decreases as early as 15 min of E₂ treatment, and the low levels of H3 persist until 1 hr after E₂ induction (Figure 2-6). The decrease in total suggests that the chromatin may employ a more “open” conformation for the recruitment of co-activator proteins and transcription machinery for ER-regulated gene activation. Consistent with this notion, active histone marks such as H3K23ac (Figure 2-7) and H3K27ac (Figure 2-8) are also enriched at *GREB1* and *PR* EREs and promoters. Consistently, ER α is recruited to *GREB1* and *PR* EREs at $t = 15$ min and $t = 1$ hr. Notably, dynamic H3K4me_{2/3} levels are also observed at these time points, suggesting that H3K4 methylation may be involved in the regulation of ER α -mediated transcription activity.

Figure 2-6. Total H3 decreases immediately upon estrogen treatment.
qChIP: H3 occupancy at (A) *GREB1* and (B) *PR* EREs and promoters at untreated (Control) or estrogen (E_2) treated for 15 min or 1 hr.

A



B

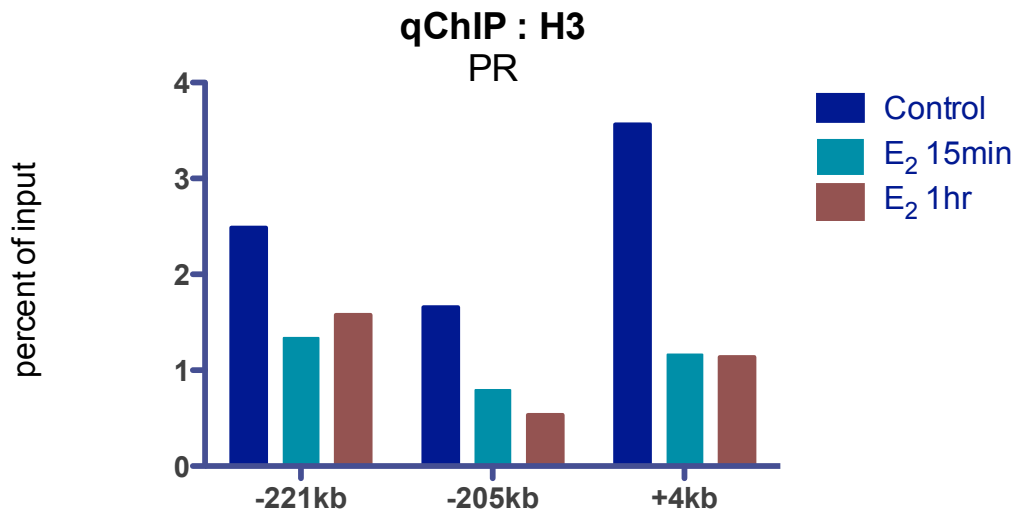
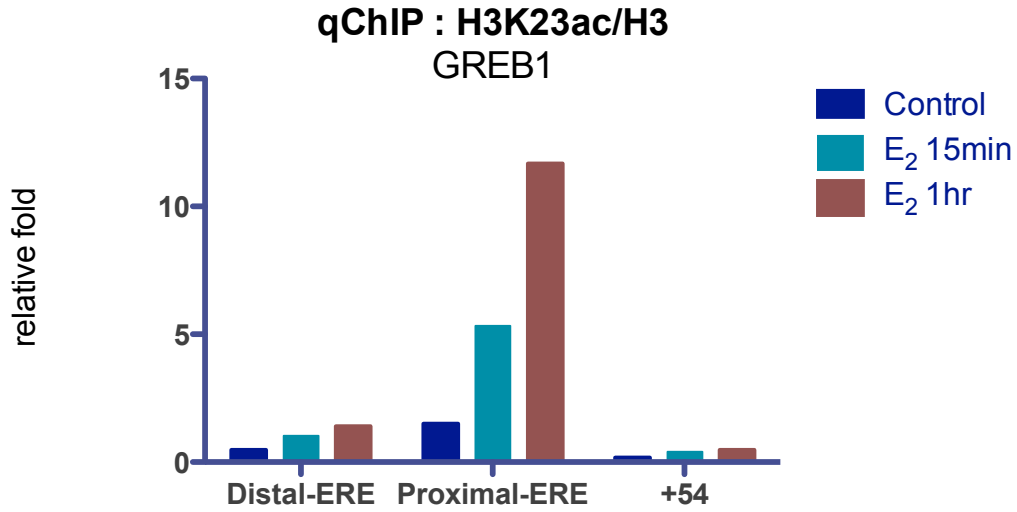


Figure 2-7. Changes of H3K23ac levels upon estrogen treatment. qChIP: H3K23ac levels, normalized with H3, at (A) *GREB1* and (B) *PR* EREs and promoters at untreated (Control) or estrogen (E_2) treated for 15 min or 1 hr.

A



B

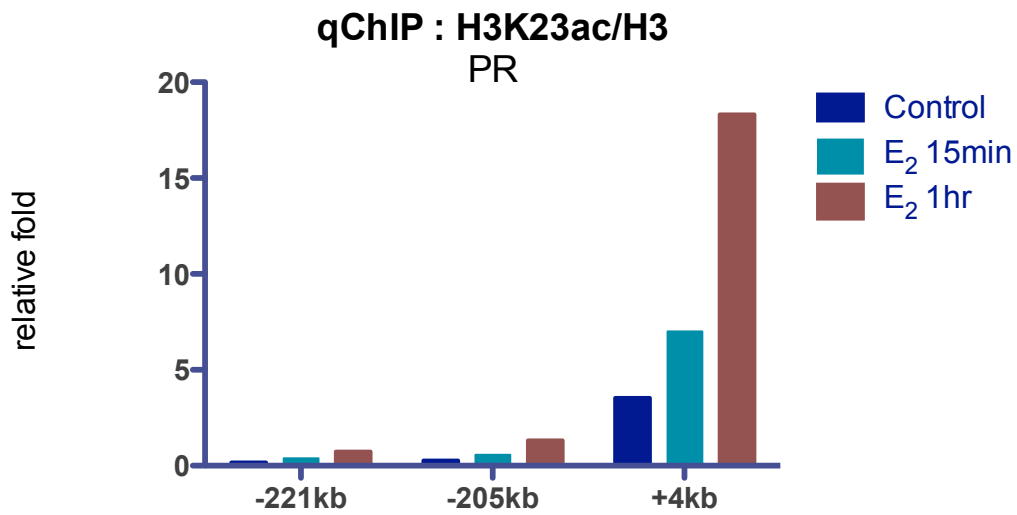
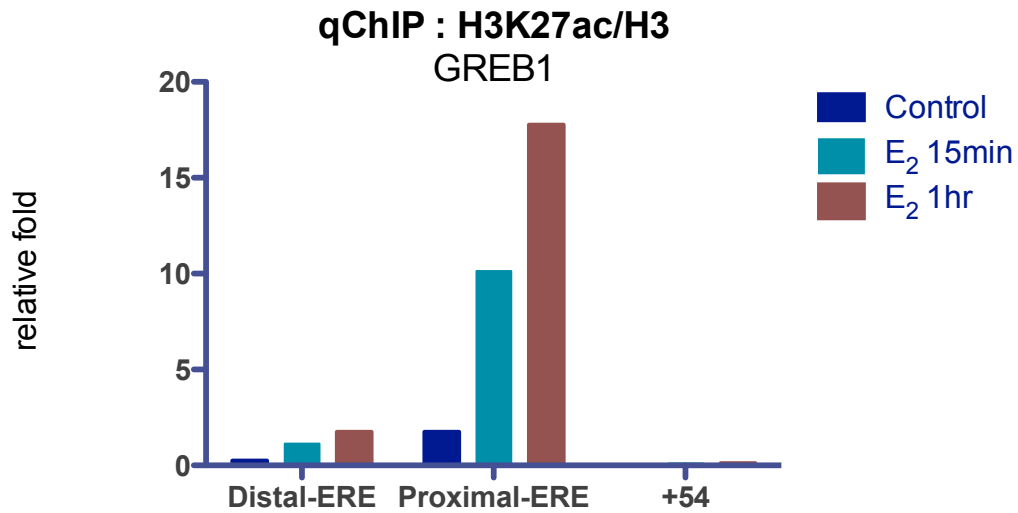


Figure 2-8. Changes of H3K27ac levels upon estrogen treatment. qChIP: H3K27ac levels, normalized with H3, at (A) *GREB1* and (B) *PR* EREs and promoters at untreated (Control) or estrogen (E_2) treated for 15 min or 1 hr.

A



B

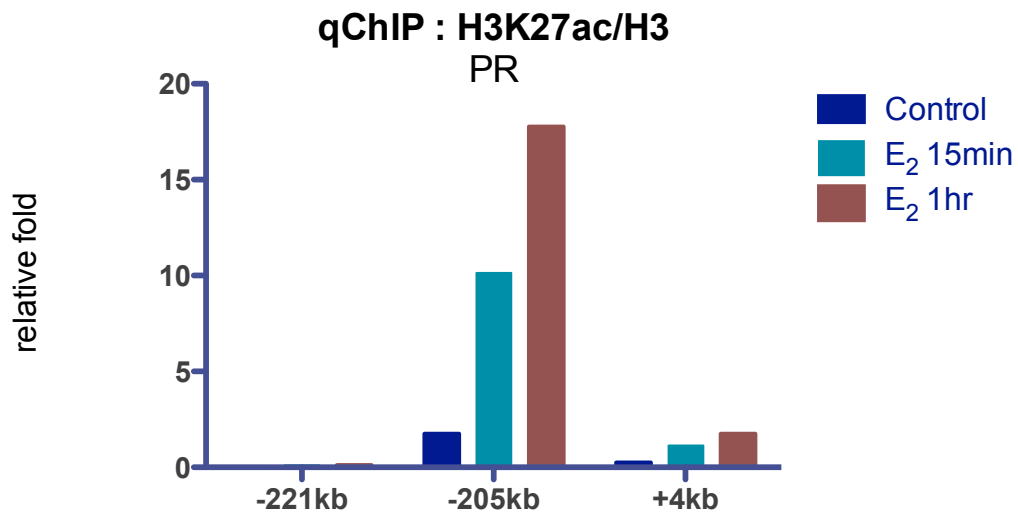
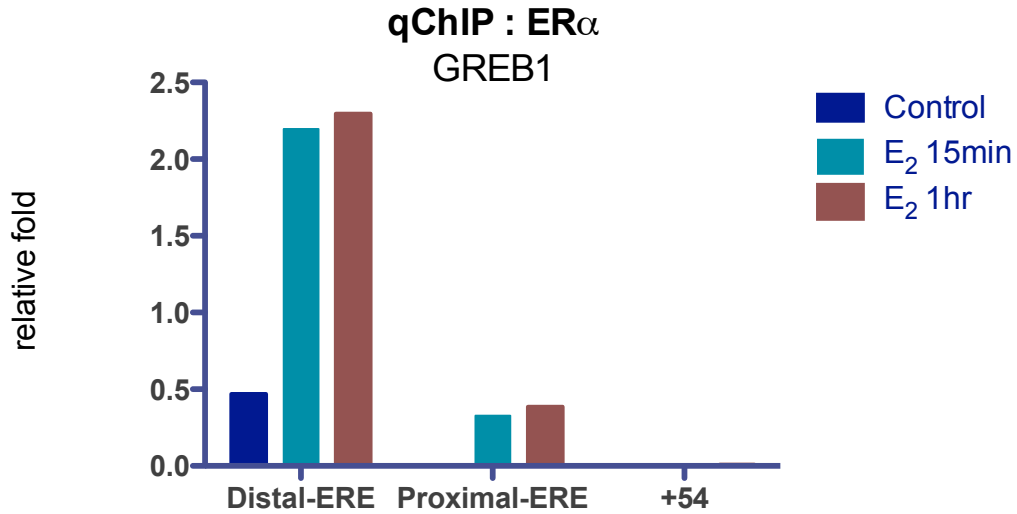


Figure 2-9. Recruitment of ER α upon estrogen treatment. qChIP: ER α recruitment at (A) *GREB1* and (B) *PR* EREs and promoters at untreated (Control) or estrogen (E₂) treated for 15 min or 1 hr.

A



B

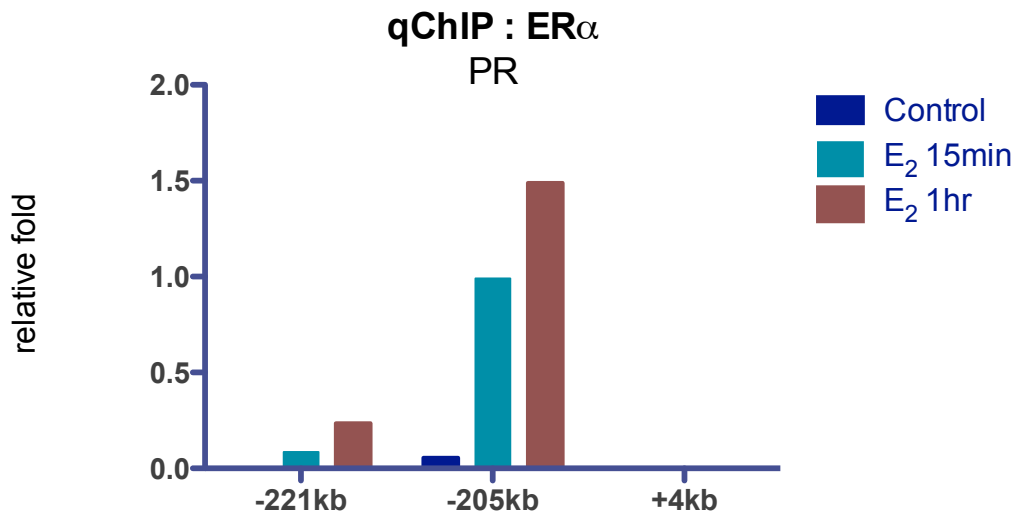
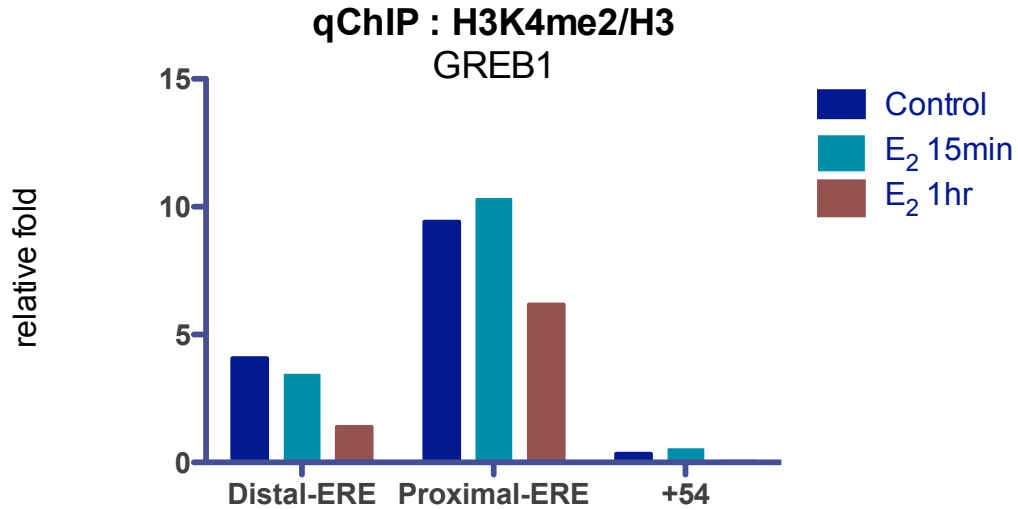


Figure 2-10. Changes of H3K4me2 levels upon estrogen treatment. qChIP: H3K4me2 levels, normalized with H3, at (A) *GREB1* and (B) *PR* EREs and promoters at untreated (Control) or estrogen (E_2) treated for 15 min or 1 hr.

A



B

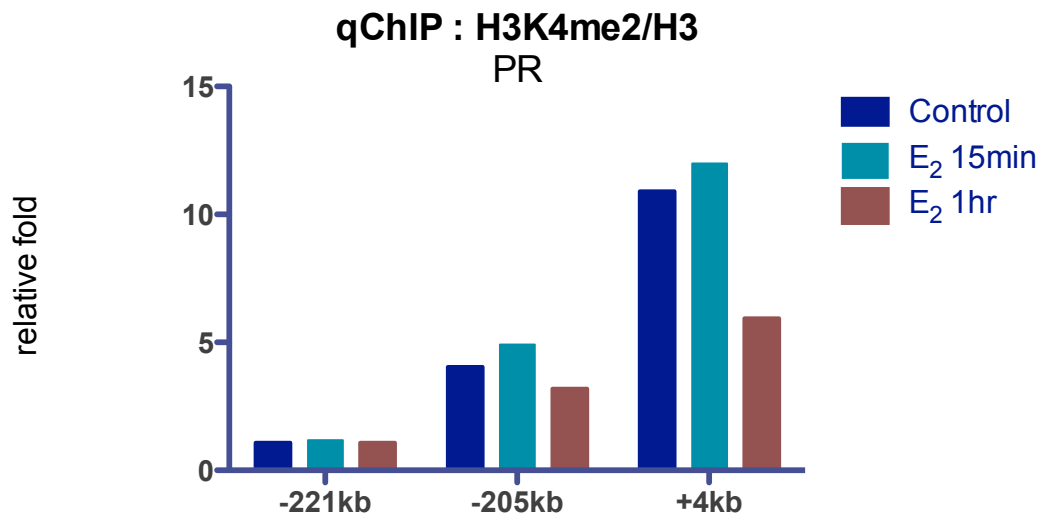
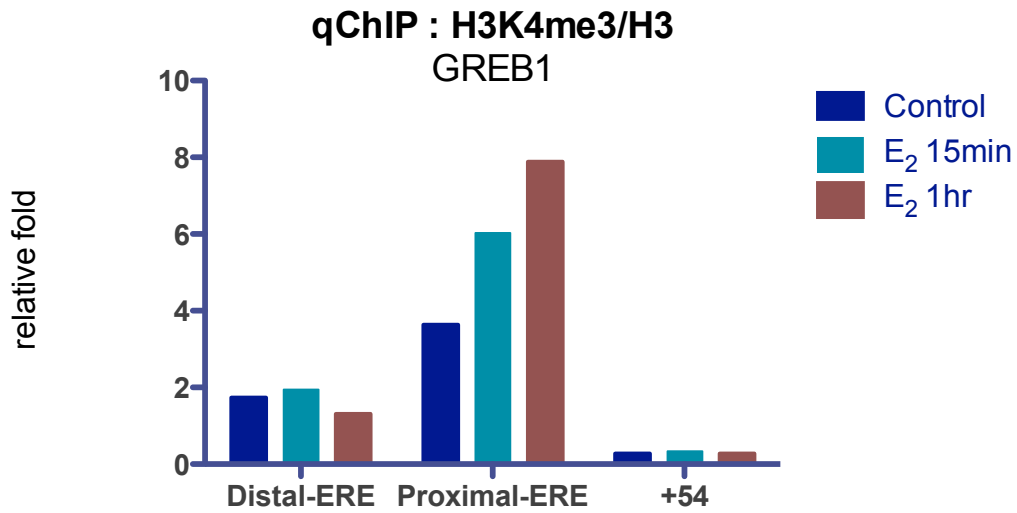
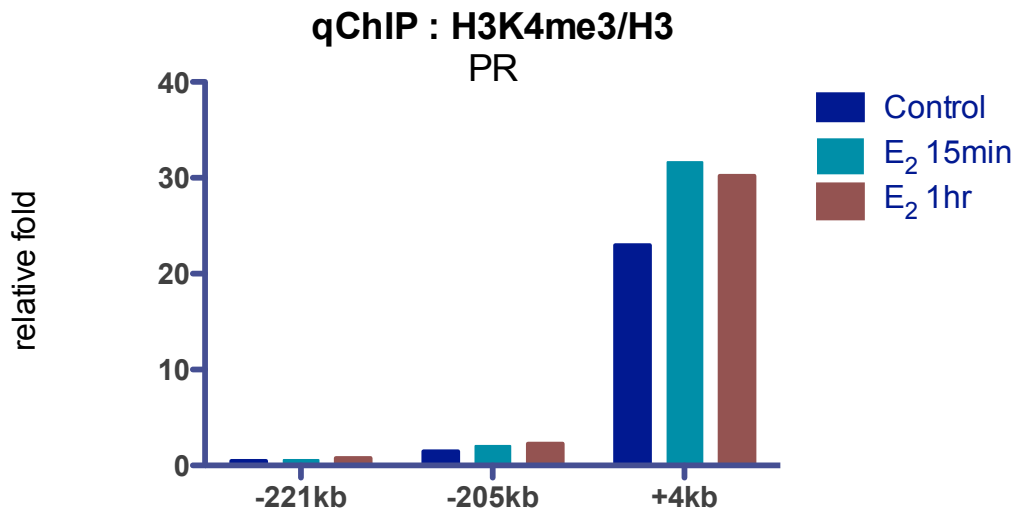


Figure 2-11. Changes of H3K4me3 levels upon estrogen treatment. qChIP: H3K4me3 levels, normalized with H3, at (A) *GREB1* and (B) *PR* EREs and promoters at untreated (Control) or estrogen (E_2) treated for 15 min or 1 hr.

A



B



2.3.2. TRIM24 expression is essential for timely estrogen response

TRIM24 and ER α co-occupy nearly 1600 genes when ER α is activated by estrogen (E₂) [57]. Among these genes, I first focused on *GREB1* and studied the mechanism of TRIM24-regulated transcription. Previous study by Dr. Tsai suggested that TRIM24 depletion reduces E₂-induced GREB1 activation at $t = 3$ hr and $t = 6$ hr. Here I re-introduced WT-TRIM24 or EGFP (plasmid control) into shTRIM24 MCF7 cells (48 hr transfection) and treated with different doses of estrogen (E₂) before assaying *GREB1* activation with qPCR. When I compared *GREB1* induction in shControl and shTRIM24 cells, TRIM24 expression is essential for response at lower level of estrogen (Figure 2-13, E₂ = 10⁻¹⁰M). Rescue of WT-TRIM24 expression (Figure 2-12) is able to fully rescue estrogen response at sub-nanomolar of E₂ (Figure 2-13). When TRIM24 is depleted (Figure 2-14) and *GREB1* transactivation assayed over a time course of $t = 0$ hr, 1hr, 2hr, 3hr, 4hr, and 5hr, it suggested that TRIM24 expression is essential for timely estrogen response (Figure 2-16A). Taken together, TRIM24 expression allows timely activation of *GREB1* expression at lower levels of E₂. In fact, depletion of TRIM24 or LSD1 also reduces estrogen-induced *PR* activation (Figure 2-16B). However, only LSD1, but not TRIM24 regulates *IGFBP4* transactivation (Figure 2-17). As a control, neither TRIM24 nor LSD1 knockdown affects non-estrogen responsive gene *BCAS4* (Figure 2-18). Therefore, LSD1 and TRIM24 may cooperatively regulate the time-dependent activation on a subset of ER α target genes.

Figure 2-12. Ectopic expression of TRIM24 in MCF7 depleted of endogenous TRIM24. qPCR analyses of cDNA prepared from TRIM24 knockdown cells transfected with exogenous TRIM24-WT or EGFP control vector for 48 hours. Cells are pretreated with vehicle, or indicated concentration of Estrogen (E_2), and/or 4-hydroxy-Tamoxifen (Tam) before assaying for TRIM24 expression. RNA levels are normalized to *GAPDH*; value from EGFP-transfected cells is set as one. Averaged results from duplicates; error bars = SEM.

Overexpression of TRIM24

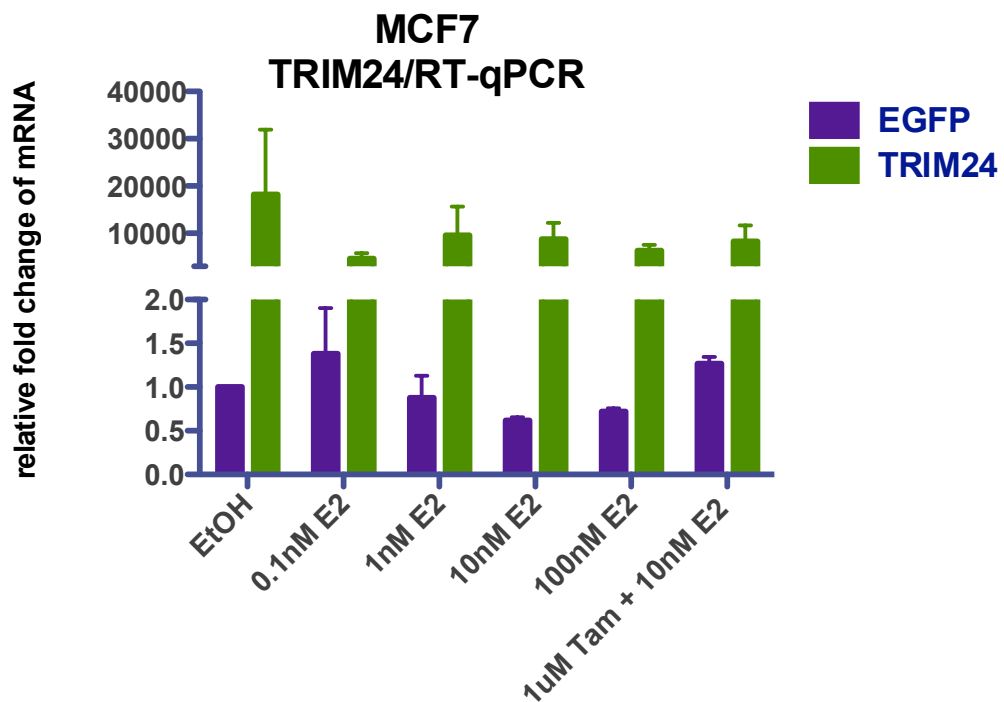


Figure 2-13. TRIM24 expression allows estrogen response at lower levels of hormone. qPCR analyses of cDNA prepared from shControl or shTRIM24 cells transfected with exogenous TRIM24-WT or EGFP control vector for 48 hours. Cells are pretreated with vehicle, or indicated concentration of Estrogen (E_2) before assaying for *GREB1* induction. RNA levels are normalized to *GAPDH*; untreated shControl MCF7 is set as one. Averaged results from duplicates; error bars = SEM.

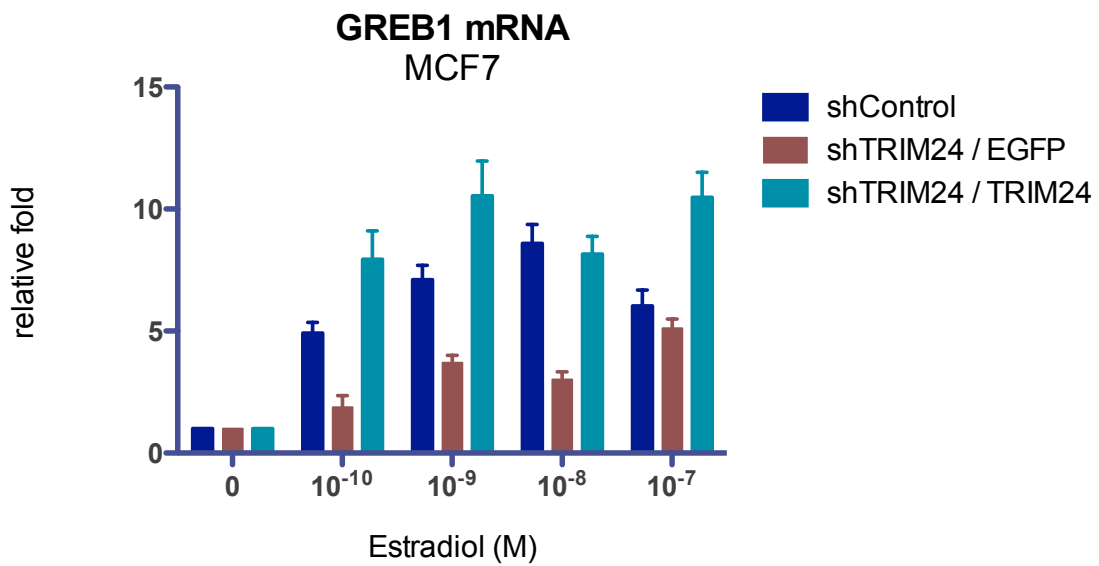
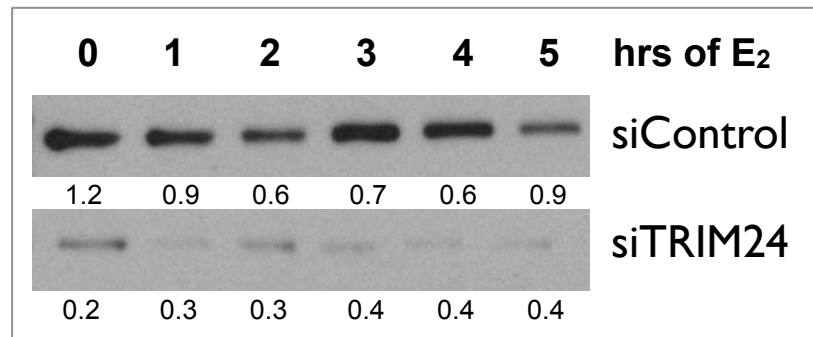


Figure 2-14. Western blot analysis revealed decreased TRIM24 protein level mediated by siRNA in MCF7 cells. (A) Western blot showing knockdown efficiency of TRIM24 by siRNA (for 72 hours) at indicated time of estrogen (E₂) treatment. (B) Quantification of TRIM24 expression as normalized to β-ACTIN control in siControl and siTRIM24 cells.

A

TRIM24 protein (normalized with ACTIN):



B

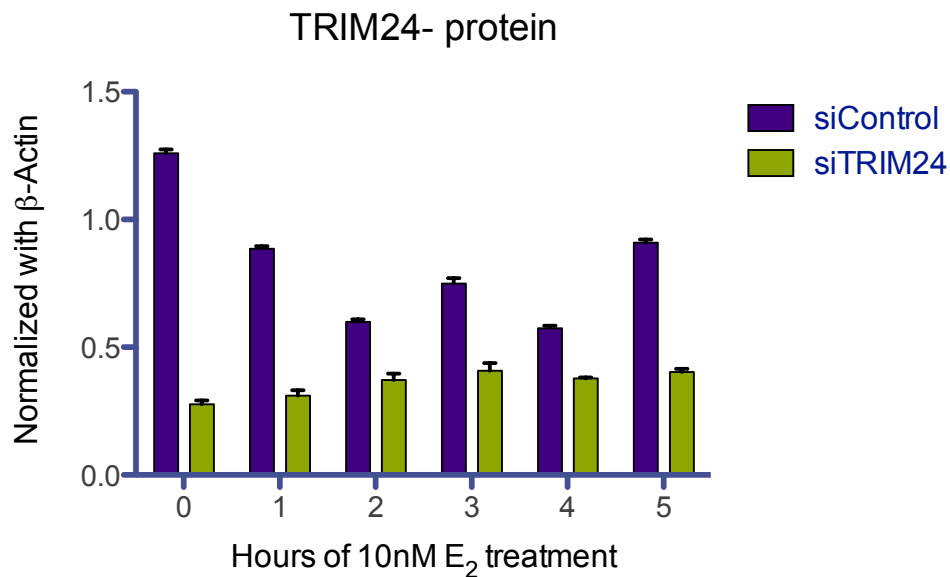


Figure 2-15. Knockdown of LSD1 by siRNAs. qPCR analyses of cDNA prepared from MCF7 cells transfected with siControl or siLSD1 for 48 hr and treated with of 10 nM estrogen at the indicated time points before assaying for *LSD1* expression. RNA levels are normalized to *GAPDH*; siControl at each time point is set as one. Average results from triplicates; error bars = SEM.

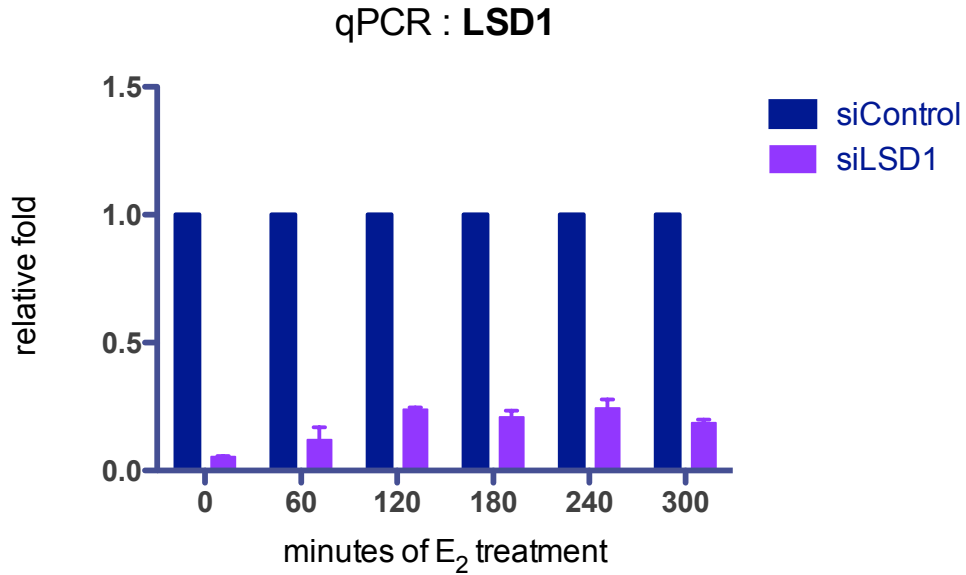


Figure 2-16A. Effects of siTRIM24 or siLSD1 on ER α target gene activation. qPCR analyses of cDNA prepared from MCF7 cells transfected with siControl, siTRIM24, or siLSD1 for 48 hr and treated with of 10 nM estrogen at the indicated time points before assaying for (A) *GREB1*, (B) *PR* expression. RNA levels are normalized to *GAPDH*; vehicle-treated MCF7 is set as one. Average results from triplicates; error bars = SEM (Student *t* test: *p-value<0.05).

A

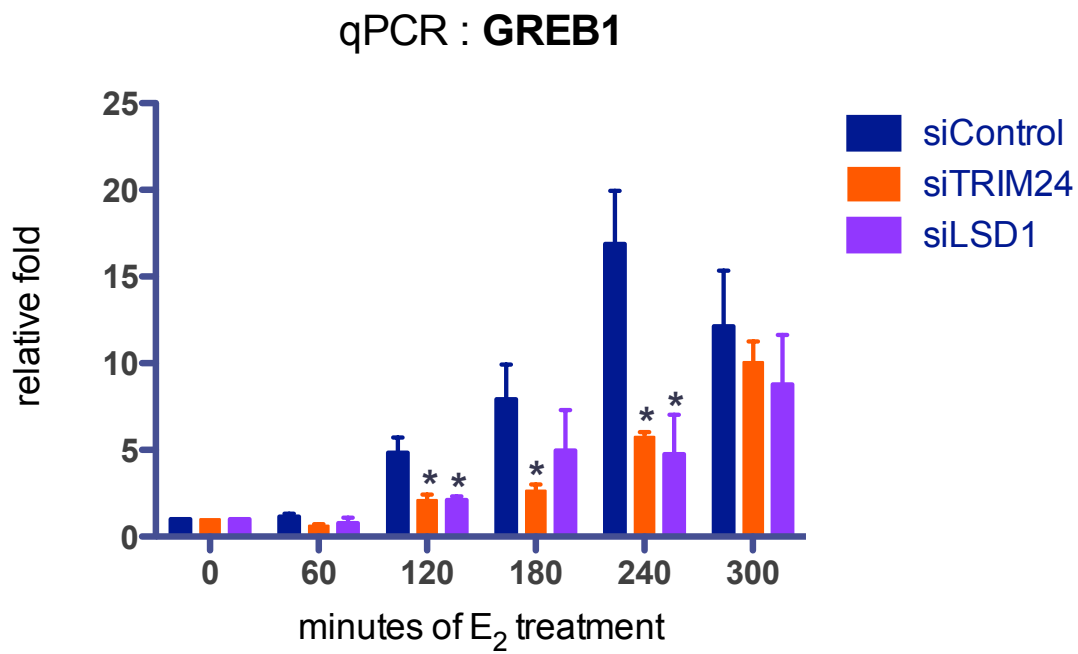


Figure 2-16B. Effects of siTRIM24 or siLSD1 on ER α target gene activation. qPCR analyses of cDNA prepared from MCF7 cells transfected with siControl, siTRIM24, or siLSD1 for 48 hr and treated with of 10 nM estrogen at the indicated time points before assaying for (A) *GREB1*, (B) *PR* expression. RNA levels are normalized to *GAPDH*; vehicle-treated MCF7 is set as one. Average results from triplicates; error bars = SEM (Student *t* test: *p-value<0.05; *** p-value<0.001).

B

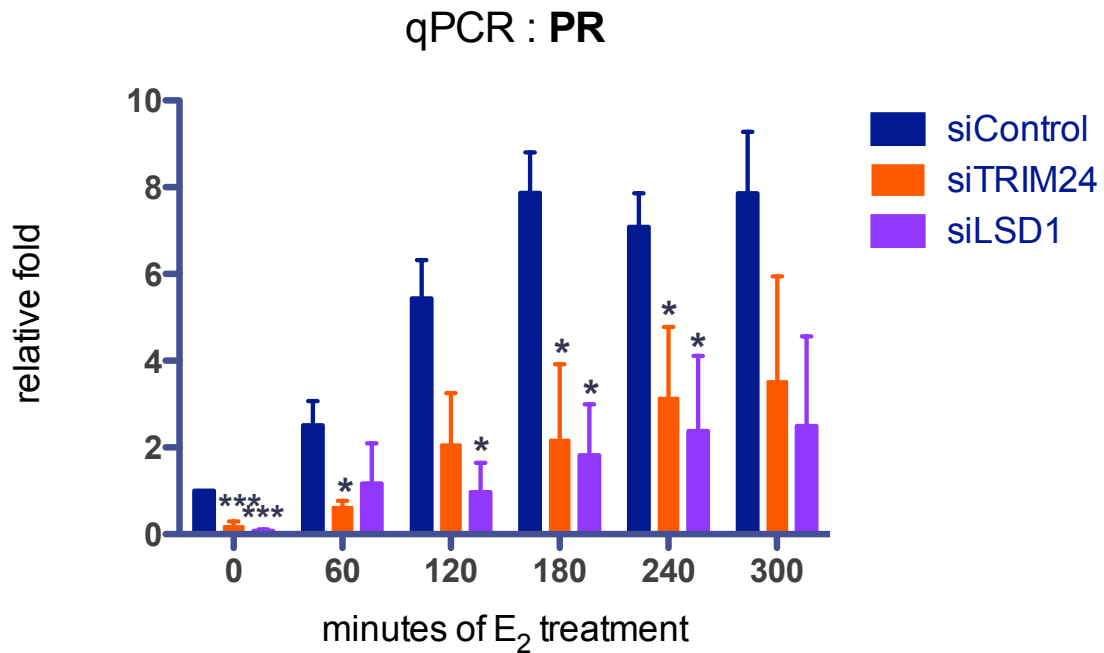


Figure 2-17. Effects of siTRIM24 or siLSD1 on ER α target gene activation. qPCR analyses of cDNA prepared from MCF7 cells transfected with siControl, siTRIM24, or siLSD1 for 48 hr and treated with of 10 nM estrogen at the indicated time points before assaying for *IGFBP4* expression. RNA levels are normalized to *GAPDH*; vehicle-treated MCF7 is set as one. Average results from triplicates; error bars = SEM.

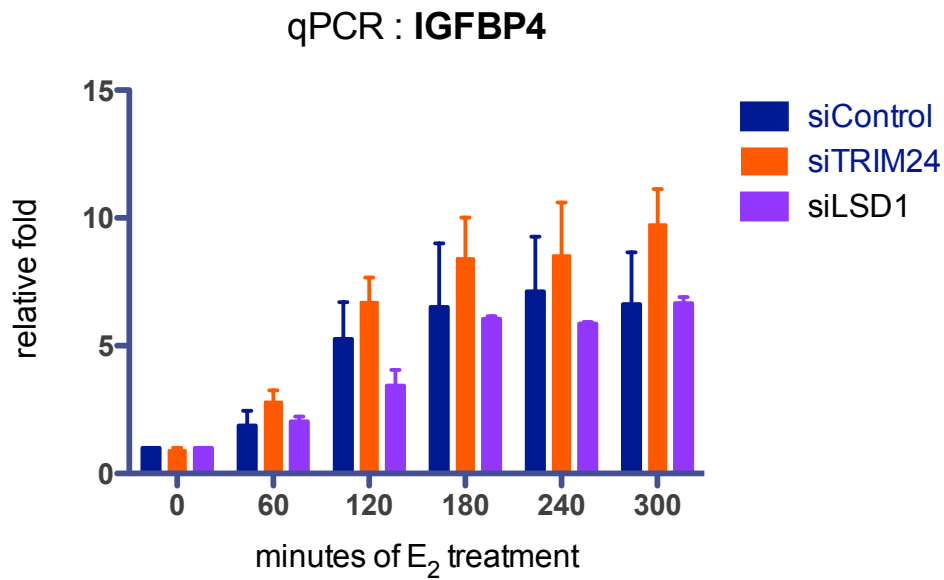
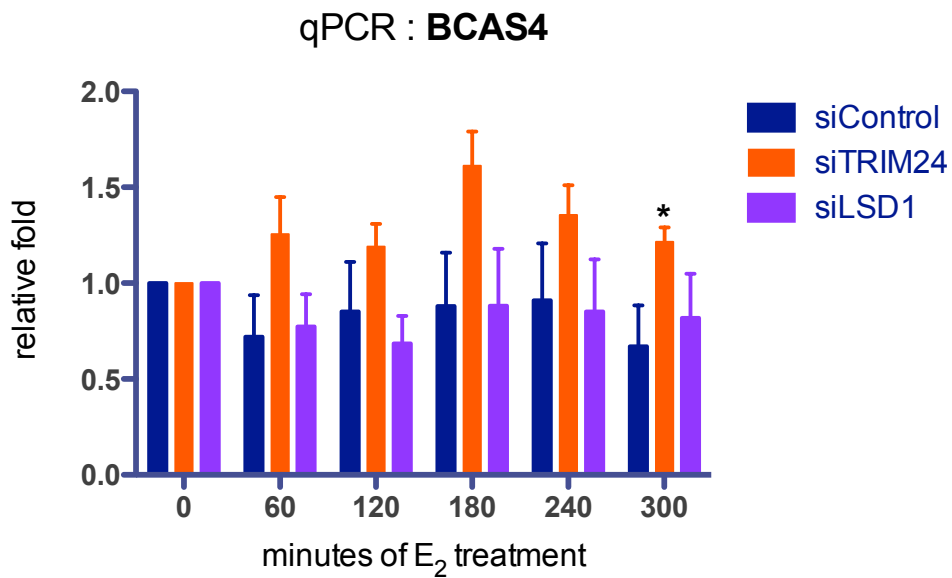


Figure 2-18. Effects of siTRIM24 or siLSD1 on non-E₂ response gene *BCAS4*. qPCR analyses of cDNA prepared from MCF7 cells transfected with siControl, siTRIM24, or siLSD1 for 48 hr and treated with of 10 nM estrogen at the indicated time points before assaying for *BCAS4* expression. RNA levels are normalized to *GAPDH*; vehicle-treated MCF7 is set as one. Average results from triplicates; error bars = SEM (Student *t* test: *p-value<0.05).

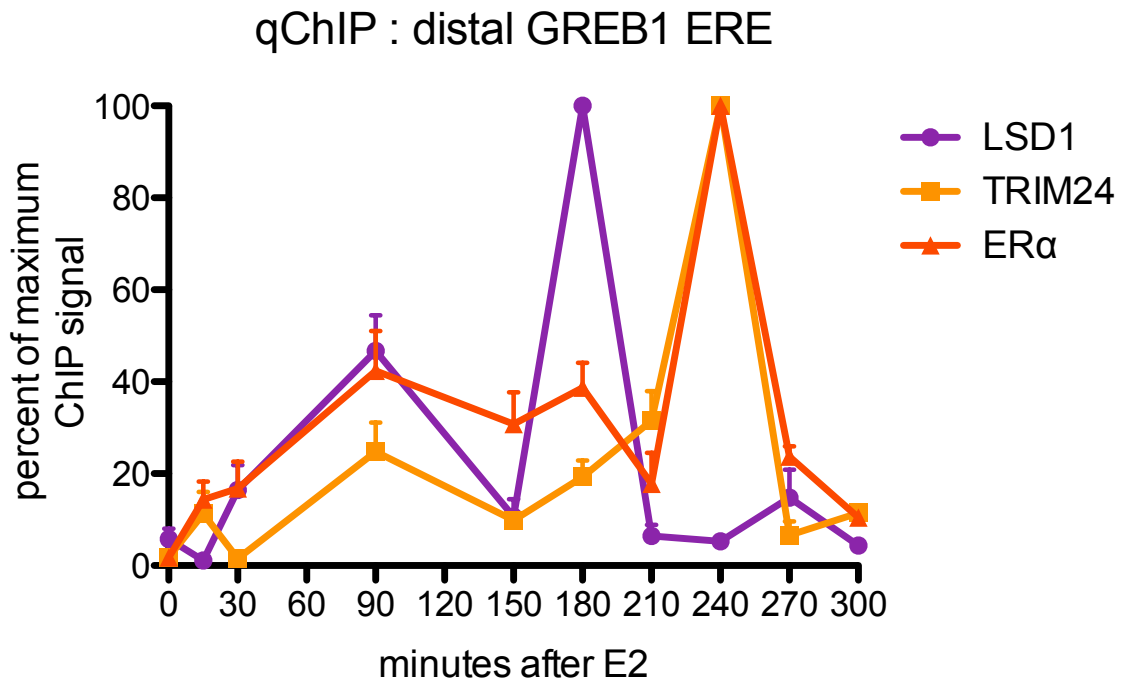


2.3.3. Recruitment of LSD1 and TRIM24 and changes of H3K4 methylation at *GREB1* ERE upon estrogen induction

Although global binding of TRIM24 preferentially concentrates on demethylated regions, no change of H3K4me2 was observed at *GREB1* ERE sites after 6 hours of E₂ treatment [57]. Therefore, I decided to expand our profile and perform ChIP analyses and examined the snapshots of ER α , LSD1, and TRIM24 recruitment on the chromatin at $t = 15$ min, 30 min, 90 min, 150 min, 180 min, 210 min, 240 min, 270 min, and 300 min after E₂. In hormonally synchronized MCF7 cells, estrogen-induced transcriptional activation of *GREB1* occurs as early as 60 min and continues to up-regulate until 240 min (Figure 2-16A). At 300 min, ER α -mediated activated *GREB1* expression levels off (Figure 2-16A). I also aimed to detect any methylation/demethylation events of histone H3 lysine 4 (H3K4) at these time points.

Upon estrogen stimulation, LSD1 and TRIM24 are naturally recruited to *GREB1* distal ERE in non-identical cyclical patterns (Figure 2-19). The engagement of LSD1 occurs every 90 min while TRIM24 is bound at 15 min, 90 min, and 240 min. As for ER α , estrogen-induced recruitment is initiated at 15 min, which persists and fluctuates until 210 min, followed by a sharp peak at 240 min, then maintains at low levels from 270 min to 300 min. Previous study suggested that total H3 methylation is cyclical [73]. Here, I provided a detailed profile of mono-, di-, and tri-methylated H3K4 (H3K4me_{1/2/3}) after E₂ treatment and detected dynamic methylation/demethylation events at specific time points.

Figure 2-19. Cyclical recruitments of LSD1 and TRIM24 to *GREB1* distal ERE site. Percent of maximum ChIP signals for recruitments of LSD1, TRIM24 and ER α to *GREB1* distal ERE at indicated time points of estrogen (E₂) treatment.

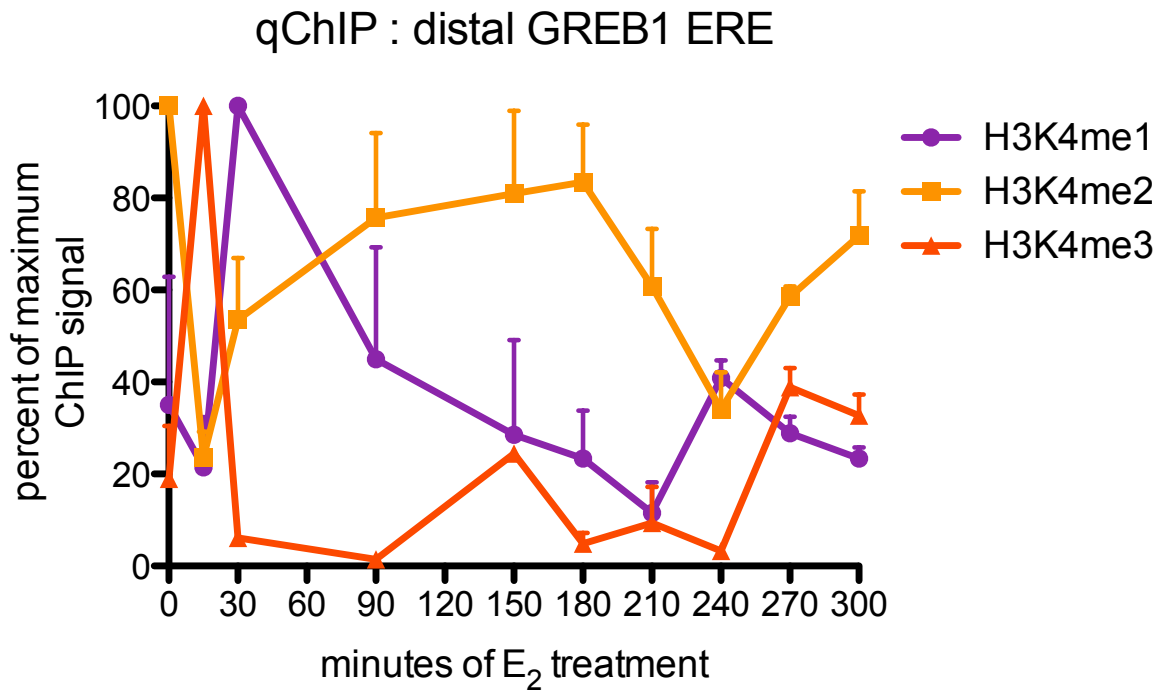


The pre-E₂ recruitment of LSD1 has been previously reported. Here, I observed high level of H3K4me₂ and co-occupancy of LSD1 before E₂ induction (Figures 2-19 and 2-20). As soon as 15 min post-E₂, LSD1 immediately disengages *GREB1* ERE and the reason still remains unclear. On the chromatin, the loss of H3K4me_{2/1} is accompanied by gain of H3K4me₃, suggesting that unknown lysine methyltransferases(s) may be involved. Notably, both TRIM24 and ER α are recruited at $t = 15$ min (Figure 2-19), the previously described “transcriptionally unproductive cycle” [73].

From 15 min to 30 min, LSD1 is re-engaged on *GREB1* ERE; ER α accumulates while TRIM24 cycles off the chromatin (Figure 2-19). At the same time, rapid demethylation events from H3K4me₃ to H3K4me₂, as well as from H3K4me₂ to H3K4me₁, are observed. Because LSD1 is unable to demethylate trimethyl-H3K4, I suspected that another unknown lysine demethylases(s) might also be present on the chromatin at this interval.

The first synchronized recruitments of ER α , LSD1 and TRIM24 occur from 30 min to 180 min (Figure 2-19). Consistent with the observation, knockdown of LSD1 or TRIM24 during this period leads to down-regulation of *GREB1* induction (Figure 2-16A). During this period, the successive enrichment of H3K4me₂ is concurrent with gradual loss of H3K4me_{3/1}, possibly through demethylation of H3K4me₃ and re-methylation of H3K4me₁.

Figure 2-20. Dynamic changes in H3K4 methylation levels at *GREB1* distal ERE site. Percent of maximum ChIP signals for H3K4me1, H3K4me2, and H3K4me3, normalized with total H3, to *GREB1* distal ERE at indicated time points of estrogen (E_2) treatment.



The second cycle and maximum recruitment of LSD1 occurs at $t = 180$ min, when TRIM24 and ER α are accumulating on the chromatin (Figure 2-19). From 180 min to 210 min, immediate loss of H3K4me2 is accompanied by gain of TRIM24 recruitment, while ER α partially cycles off the chromatin.

From 210 to 240 min, TRIM24 continues to accumulate and ER α cycles back to *GREB1* ERE. Highest magnitude of TRIM24 and ER α binding is observed at 240 min, while minimal level of LSD1 is detectable. From 240 min to 300 min, LSD1, TRIM24 and ER α are gradually dis-engaged from the chromatin, while H3K4me2 continues to increase.

2.3.4. Recruitment of LSD1 and TRIM24 and changes of H3K4 methylation at *PR* ERE upon estrogen induction

The recruitment profile of LSD1 and TRIM24 to *PR* ERE (Figure 2-21) is similar but not identical to *GREB1* (Figure 2-19). Similar to *GREB1*, the cycling time for LSD1 is 90 min while TRIM24 engagement peaks at $t = 150$ min, 210min, and 300min (Figure 2-21), suggesting that there are intrinsic differences of LSD1 and TRIM24 recruitment in a gene-specific manner. For ER α , estrogen-induced recruitment occurs as early as $t = 15$ min, which persists and continues to be enriched until $t = 180$ min, and maintains at detectable levels from 210 min to 300 min (Figure 2-21). Essentially, pre-E₂ recruitment of LSD1 is also observed on *PR* ERE. Disengagement of LSD1 at $t = 15$ min (Figure 2-21) is accompanied by loss of H3K4me2 and gain of H3K4me1/3 (Figure 2-22), suggesting dynamic changes in chromatin architecture during immediate estrogen response. From 30 min to 150 min, H3K4me1/2 dominant while H3K4me3 is kept at barely

detectable level (Figure 2-22). During the same period, ER α , LSD1, and TRIM24 are co-recruited to *PR* ERE (Figure 2-21). Notably, the second cycle and maximum recruitment of LSD1 occurs at $t = 180$ min, preceding that of TRIM24 at $t = 210$ min (Figure 2-21). From 180 min to 210 min, the loss of H3K4me2 is concurrent with gain of H3K4me1, suggesting that demethylation of H3K4me2 is actively ongoing (Figure 2-22). Interestingly, TRIM24 has a third recruitment peak at $t = 300$ min on *PR* ERE (Figure 2-19), which is not observed on *GREB1* ERE (Figure 2-21).

Figure 2-21. Cyclical recruitments of LSD1 and TRIM24 to *PR* ERE site. Percent of maximum ChIP signals for recruitments of LSD1, TRIM24 and ER α to *PR* ERE (205kb upstream of promoter) at indicated time points of estrogen (E_2) treatment.

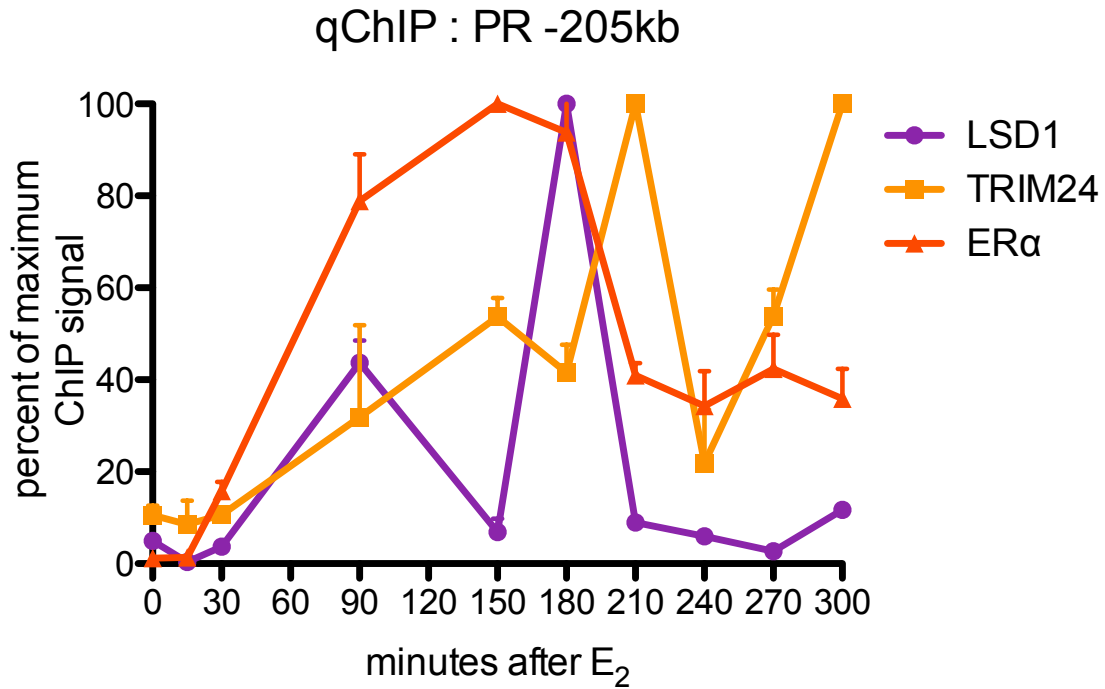
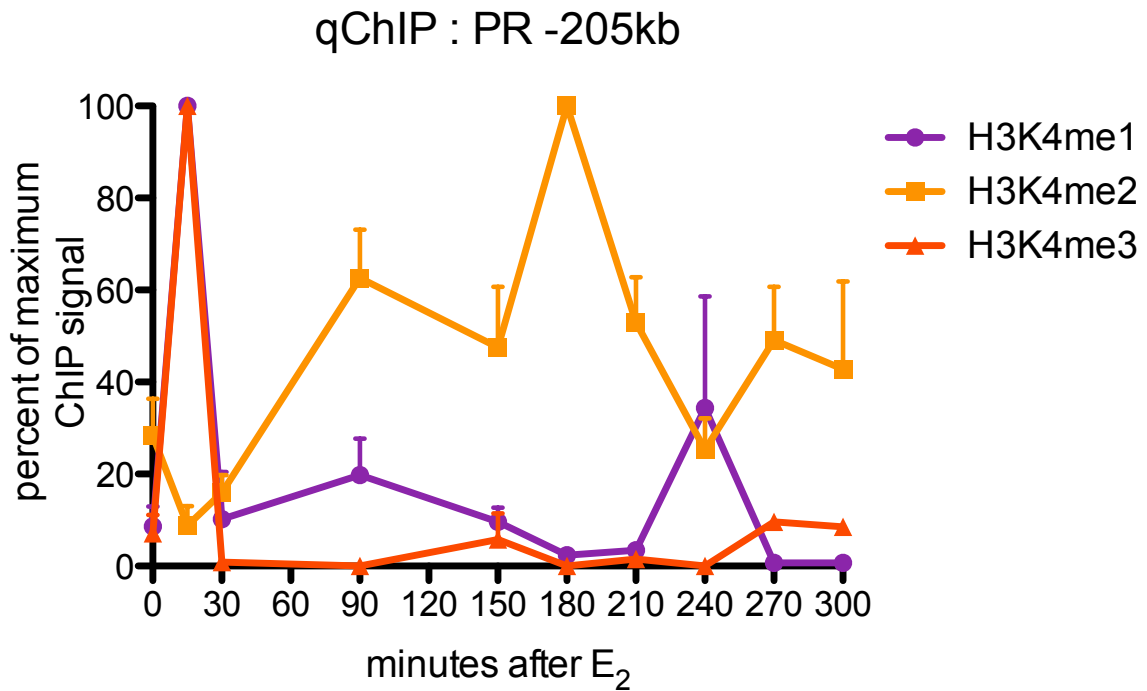


Figure 2-22. Dynamic changes in H3K4 methylation levels at *PR* ERE site. Percent of maximum ChIP signals for H3K4me1, H3K4me2, and H3K4me3, normalized with total H3, to *PR* ERE (205kb upstream of promoter) at indicated time points of estrogen (E_2) treatment.



2.3.5. Recruitment of LSD1 and TRIM24 and changes of H3K4 methylation at *pS2 ERE* upon estrogen induction

As for *pS2 ERE*, LSD1 also has a recruitment cycle of 90min and pre-occupied the chromatin before estrogen stimulation. The disengagement of LSD1 at $t = 15$ min (Figure 2-23) is accompanied by loss of H3K4me2 and gain of H3K4me3 (Figure 2-24), suggesting that methylation of H3K4me2 to H3K4me3 is activated. From 15 min to 30 min, loss of H3K4me3 is concurrent with gain of H3K4me1/2 (Figure 2-24), implying demethylation of H3K4me3 is ongoing. Again, the first synchronized recruitment of LSD1, TRIM24, and ER α occur from 30min 150min (Figure 2-23). From 30 min to 60 min, H3K4me2 is accumulating while H3K4me1/3 is gradually lost (Figure 2-24). From 60 min to 150min, occupancies of H3K4me1/2/3 are all decreasing (Figure 2-24). The second synchronized peak for LSD1, TRIM24, and ER α is from 150 min to 240 min (Figure 2-23), which is not observed in neither *GREB1* (Figure 2-19) nor *PR* EREs (Figure 2-21). During this time, H3K4me2 is first being accumulated, and then H3K4me3 is enriched as H3K4me2 is gradually weakening (Figure 2-24). The third synchronized peak for LSD1 and ER α at $t = 270$ min. From 270 min to 300 min, LSD1 and ER α are disengaged from the chromatins and H3K4me2/3 marks are accumulating. During this time, TRIM24 recruitment is still lagging behind.

Figure 2-23. Cyclical recruitments of LSD1 and TRIM24 to *pS2* proximal ERE site. Percent of maximum ChIP signals for recruitments of LSD1, TRIM24 and ER α to *pS2* proximal ERE at indicated time points of estrogen (E_2) treatment.

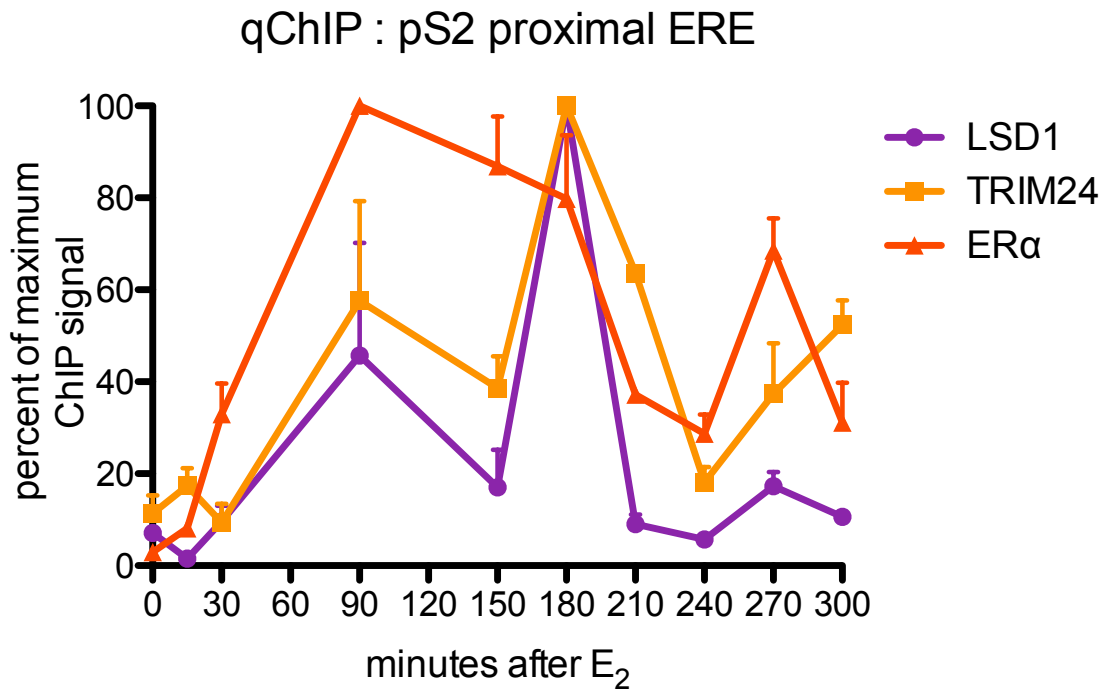
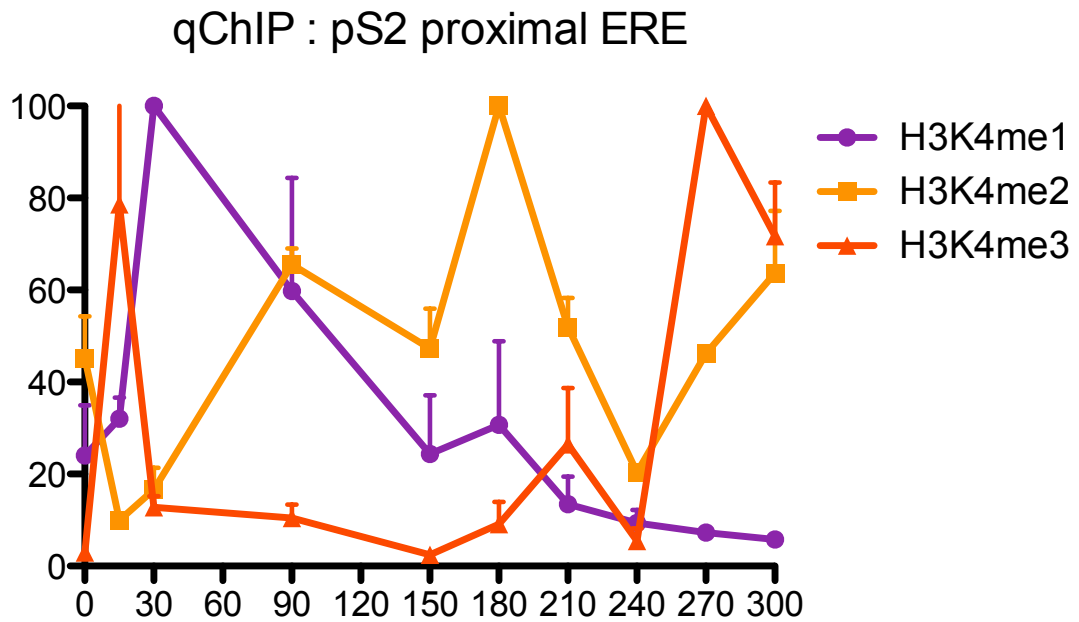


Figure 2-24. Dynamic changes in H3K4 methylation levels at *pS2* proximal ERE site. Percent of maximum ChIP signals for H3K4me1, H3K4me2, and H3K4me3, normalized with total H3, to *pS2* proximal ERE at indicated time points of estrogen (E_2) treatment.

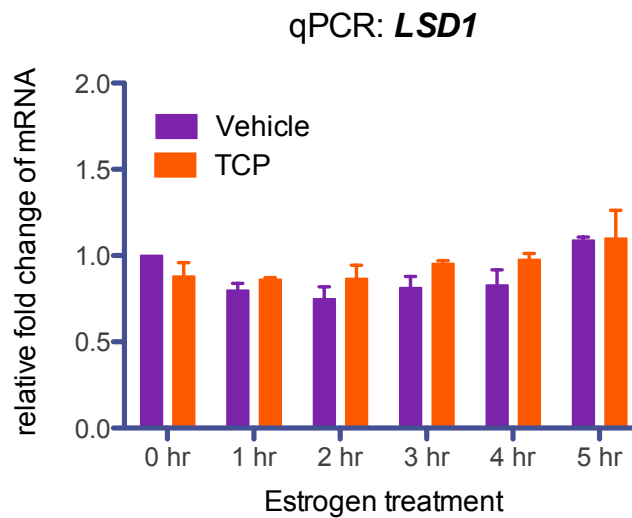


2.3.6. LSD1 enzymatic activity is critical for ER α -mediated transcription

In 2006, LSD was discovered to share close homology with monoamine oxidases (MAO), and MAO inhibitors, often used as antidepressants, can effectively inhibit the enzymatic activity of LSD1 [140]. Among these inhibitors, Tranylcypromine (TCP) is the only one that specifically inhibits LSD1 for the demethylation of H3K4 but not H3K9. After consulting with the author Dr. Min Gyu Lee, we were advised to pretreat cells with 2 μ M TCP for 24 hr for optimal inhibitory effects. Using this condition, I tracked estrogen-induced ER α target gene activation at $t = 0$ hr, 1hr, 2hr, 3hr, 4hr or 5hr after estrogen stimulation. First, TCP treatment does not affect LSD1 RNA level (Figure 2-25A). However, TCP-treated cells responds slowly to estrogen, compared to vehicle control (Figure 2-25) and the most significant down-regulation of *GREB1* gene occurs at $t = 3$ hr (Figure 2-25B), *PR* gene at $t = 3$ hr (Figure 2-25C) and *IGFBP4* gene at $t = 2$ hr (Figure 2-25D). However, TCP treatment does not affect estrogen-irresponsive gene *BCAS4* (Figure 2-25E). This is the first use of TCP to inhibit LSD1 in breast cancer cells and the first evidence that TCP can affect estrogen response, similar to siLSD1 in ER α target genes at specific time points (Figures 2-16 and 2-17).

Figure 2-25 (A-B). Effects of LSD1 inhibitor TCP on ER α target gene activation. qPCR analyses of cDNA prepared from MCF7 cells pretreated with vehicle (DMSO) or 100 μ M AH124 for 24 hr and treated with of 10 nM estrogen at the indicated time points before assaying for (A) *LSD1*, (B) *GREB1*, (C) *PR*, (D) *IGFBP4*, or (E) *BCAS4* expression. RNA levels are normalized to *GAPDH*; vehicle-treated MCF7 is set as one. Average results from triplicates; error bars = SEM (Student *t* test: *p-value<0.05).

A



B

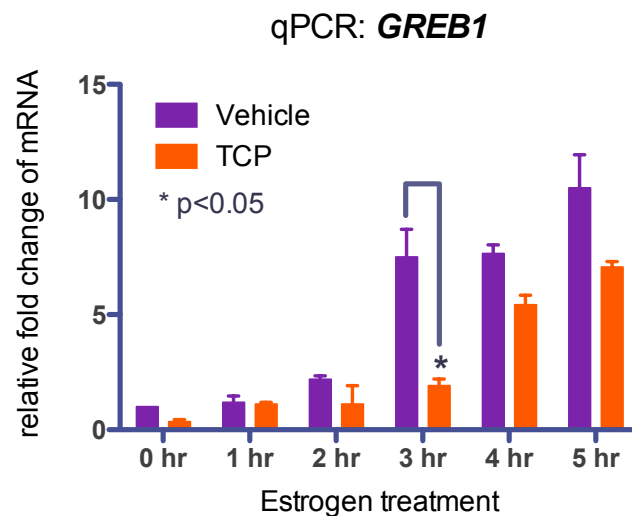
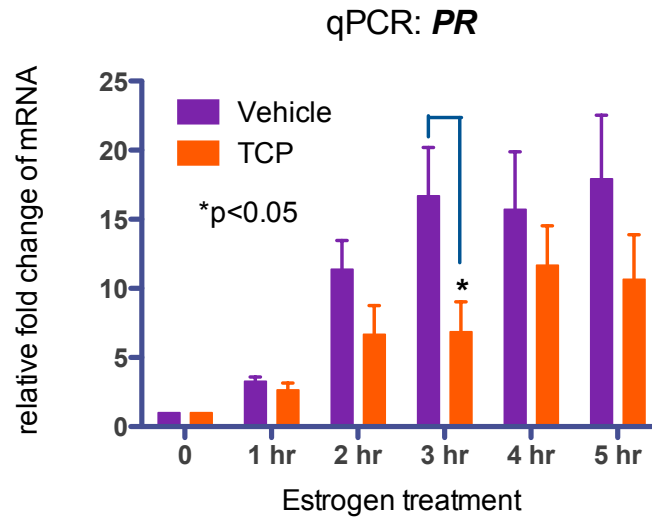


Figure 2-25 (C-D). Effects of LSD1 inhibitor TCP on ER α target gene activation. qPCR analyses of cDNA prepared from MCF7 cells pretreated with vehicle (DMSO) or 100 μ M AH124 for 24 hr and treated with of 10 nM estrogen at the indicated time points before assaying for (A) *LSD1*, (B) *GREB1*, (C) *PR*, (D) *IGFBP4*, or (E) *BCAS4* expression. RNA levels are normalized to *GAPDH*; vehicle-treated MCF7 is set as one. Average results from triplicates; error bars = SEM (Student *t* test: **p*-value<0.05).

C



D

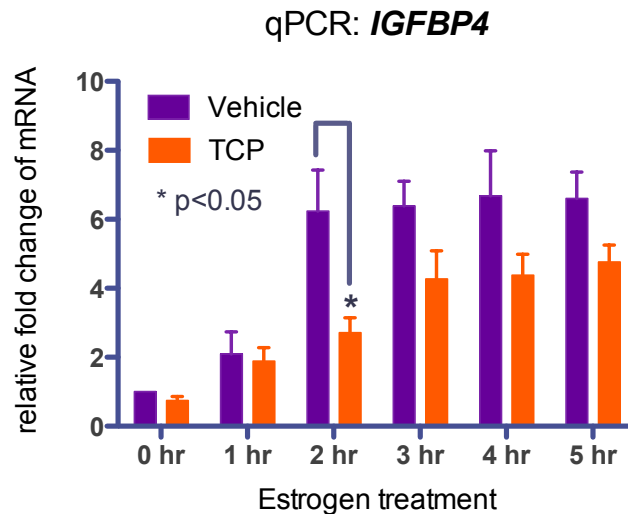
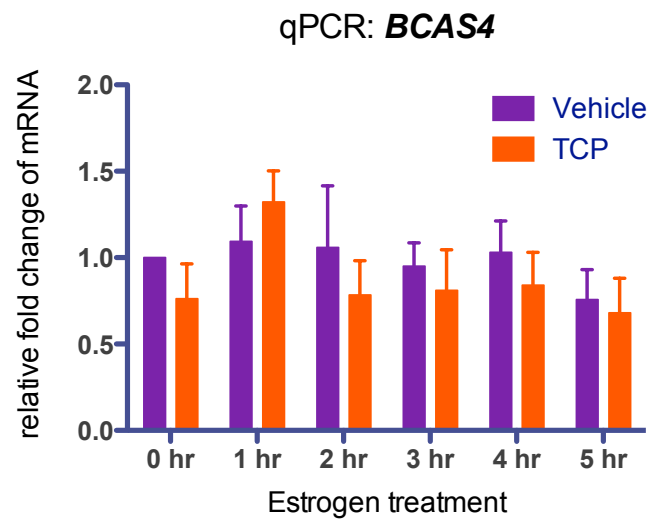


Figure 2-25 (E). Effects of LSD1 inhibitor TCP on ER α target gene activation. qPCR analyses of cDNA prepared from MCF7 cells pretreated with vehicle (DMSO) or 100 μ M AH124 for 24 hr and treated with of 10 nM estrogen at the indicated time points before assaying for (A) *LSD1*, (B) *GREB1*, (C) *PR*, (D) *IGFBP4*, or (E) *BCAS4* expression. RNA levels are normalized to *GAPDH*; vehicle-treated MCF7 is set as one. Average results from triplicates; error bars = SEM (Student *t* test: *p-value<0.05).

E



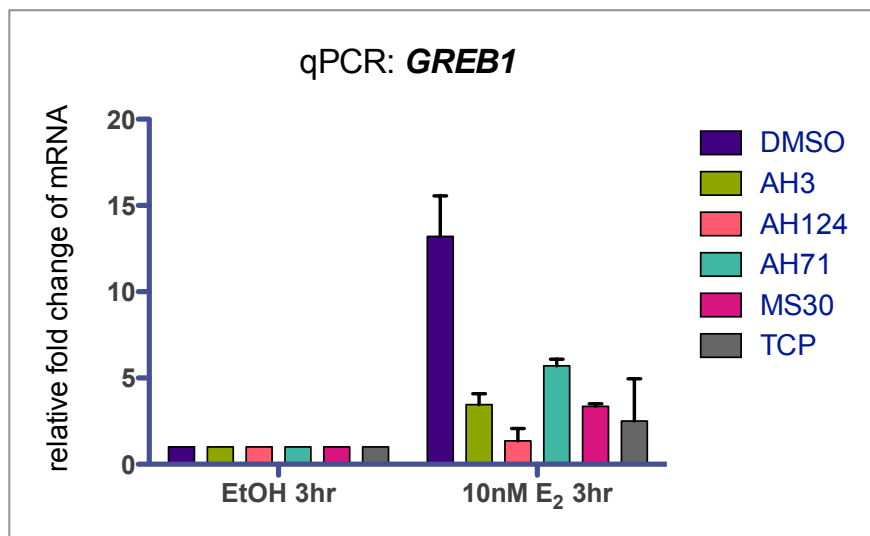
As more and more of LSD1 functions are implicated in cancer biology, recently there is a growing interest in generating specific LSD1 inhibitors for treating cancer cells. In collaboration with Dr. Manfred Jung (Institute of Pharmaceutical Sciences, University of Freiburg, Freiburg, German), I obtained several biochemically verified but unpublished LSD1 inhibitors: AH3, AH124, AH71, and MS30. I pre-treated MCF7 cells with these inhibitors (100 μ M, the recommended dosage) and induced with 10 nM E₂ for 3 hr. qPCR analyses demonstrated that these potent LSD1 inhibitors are able to down-regulate ER α target genes *GREB1* (Figure 2-26A), *PR* (Figure 2-26B), *IGFBP4* (Figure 2-26C), but not the control gene *BCAS4* (Figure 2-26D), similar to TCP treatment. Protein level of LSD1 before and after estrogen treatment does not change in DMSO (vehicle)-, AH3, or AH124-treated cells (Figure 2-27). Global H3K4me2 (by Western blot) slightly increases in the presence of AH124 and MS30 (Figure 2-28). I selected AH124 to perform a detailed time course of estrogen treatment. Preliminary results from qPCR analyses demonstrated that AH124 down-regulates ER α target genes at wider range of time points (Figure 2-29), while LSD1 RNA expression does not change in the presence or absence of AH124 or E₂. Taken together, I have validated the ability of AH124 and MS30 to down-regulate ER α target gene activation and to increase global H3K4me2 levels in MCF7 cells.

Similarly, chemicals that share similar structure to the above LSD1 inhibitors, such as Chem778 and Chem779 (from Chembridge Inc.), are tested in this screening (Figure 2-30). The addition of Chem778 or Chem779 down-

regulates estrogen-induced expression of *GREB1* at $t = 180$ min and 240 min (Figure 2-30A); PR at $t = 120$ min, 180 min, 240 min, and 300 min (Figure 2-30B); IGFBP4 at $t = 180$ min and 240 min (Figure 2-30C); and *pS2* at $t = 240$ min (Figure 2-30D). These observations suggested that Chem788 and Chem779 can potentially be potent LSD1 inhibitors, but future biochemical validations are required. Results obtained from these experiments showed that potent and potential LSD1 inhibitors can also effectively down-regulates estrogen-induced ER α target gene activation in MCF7 cells.

Figure 2-26 (A-B). Pilot study of LSD1 inhibitors and their effects on ER α target gene activation. qPCR analyses of cDNA prepared from MCF7 cells pretreated with vehicle (DMSO), 100 μ M of AH3, AH124, Chem778, Chem779 or Chem782 for 24 hr, and treated with 10 nM estrogen for 3 hr before assaying for (A) *GREB1*, (B) *PR*, (C) *pS2*, or (D) *IGFBP4* expression. RNA levels are normalized to *GAPDH*; vehicle-treated MCF7 is set as one. Average results from duplicates; error bars = SEM.

A



B

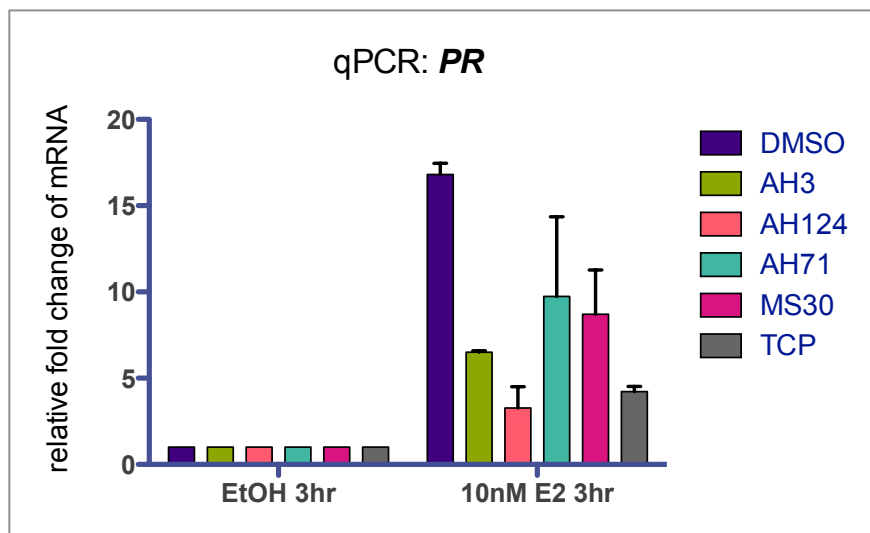
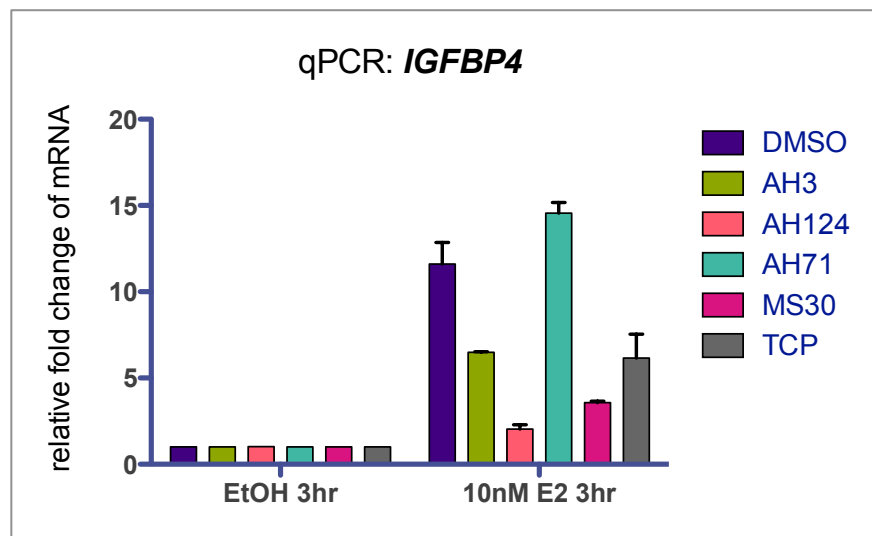


Figure 2-26 (C-D). Pilot study of LSD1 inhibitors and their effects on ER α target gene activation. qPCR analyses of cDNA prepared from MCF7 cells pretreated with vehicle (DMSO), 100 μ M of AH3, AH124, Chem778, Chem779 or Chem782 for 24 hr, and treated with 10 nM estrogen for 3 hr before assaying for (A) *GREB1*, (B) *PR*, (C) *pS2*, or (D) *IGFBP4* expression. RNA levels are normalized to *GAPDH*; vehicle-treated MCF7 is set as one. Average results from duplicates; error bars = SEM.

C



D

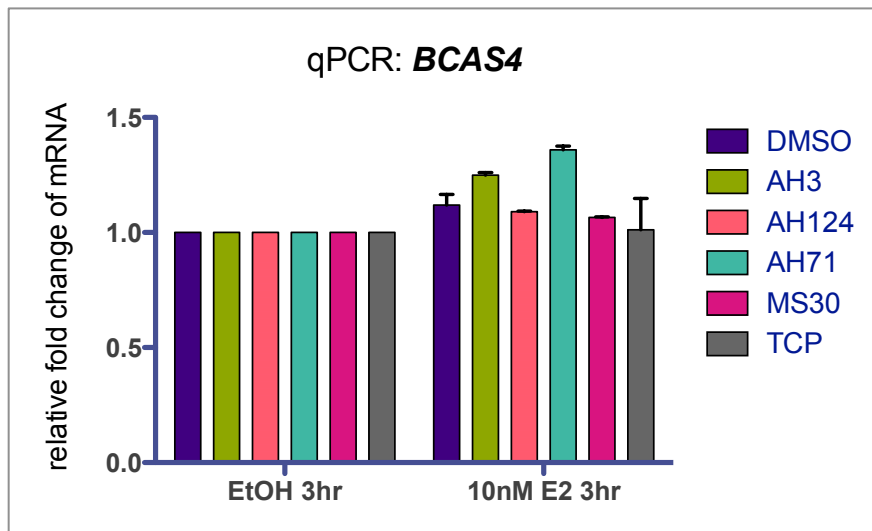


Figure 2-27. Effects of potent LSD1 inhibitors on LSD1 protein expression in MCF7 cells. Cell lysates were prepared from MCF7 cells pretreated with vehicle (DMSO), 100 μ M AH3 or AH124 for 24 hr and treated with ethanol control (E0) or 10 nM estrogen for 3 hr (E3). Western blot analysis reveals LSD1 protein level and TUBULIN (loading control).

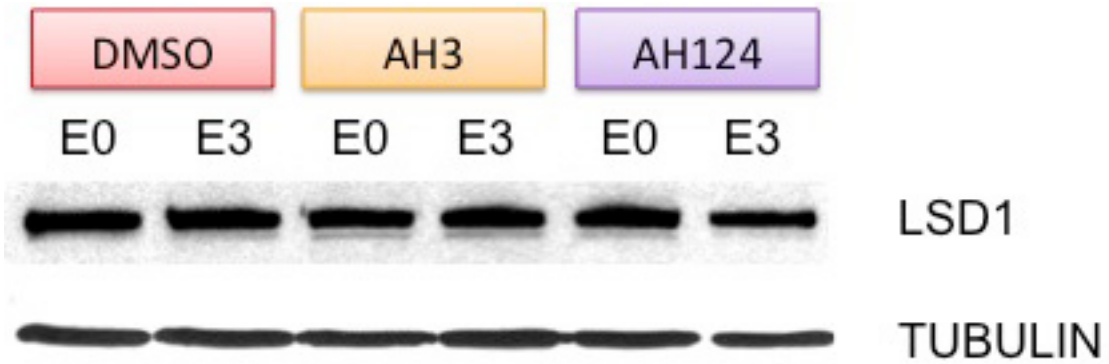


Figure 2-28. Effects of potent LSD1 inhibitors on global H3K4me2 in MCF7 cells. Cell lysates were prepared from MCF7 cells pretreated with vehicle (DMSO), AH124 (100 μ M or 200 μ M), or MS30 (30 μ M or 100 μ M) for 24 hr. Western blot analysis reveals global H3K4me2 level and H3 loading control (at short and long exposure).

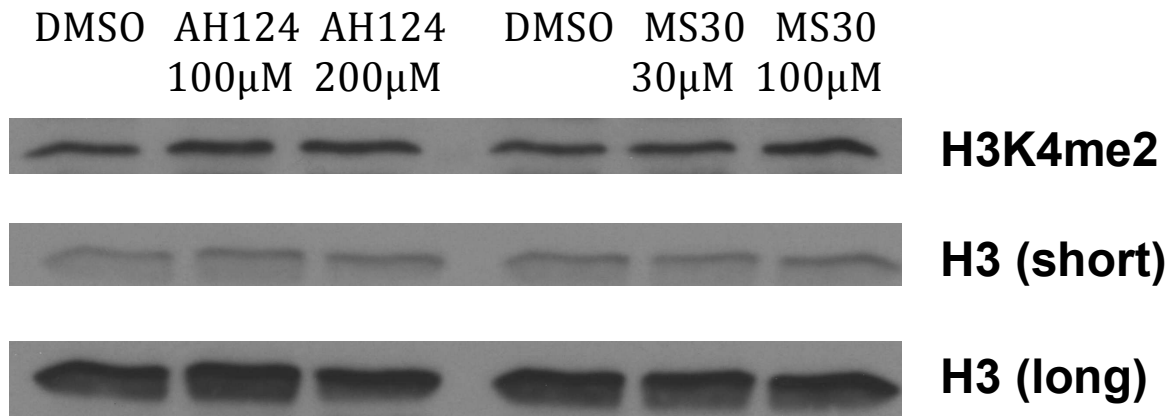
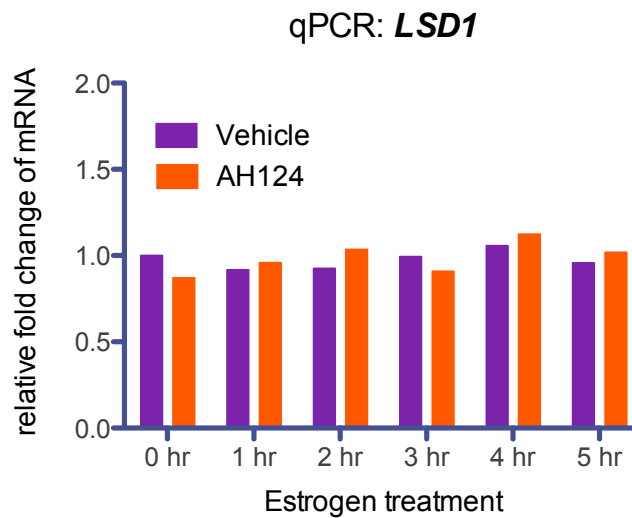


Figure 2-29 (A-B). Effects of potent LSD1 inhibitor AH124 on ER α target gene activation. qPCR analyses of cDNA prepared from MCF7 cells pretreated with vehicle (DMSO) or 100 μ M AH124 for 24 hr and treated with of 10 nM estrogen at the indicated time points before assaying for (A) *LSD1*, (B) *GREB1*, (C) *IGFBP4*, or (D) *pS2* expression. RNA levels are normalized to *GAPDH*; vehicle-treated MCF7 is set as one. Gene induction in the presence of TCP is shown as a control.

A



B

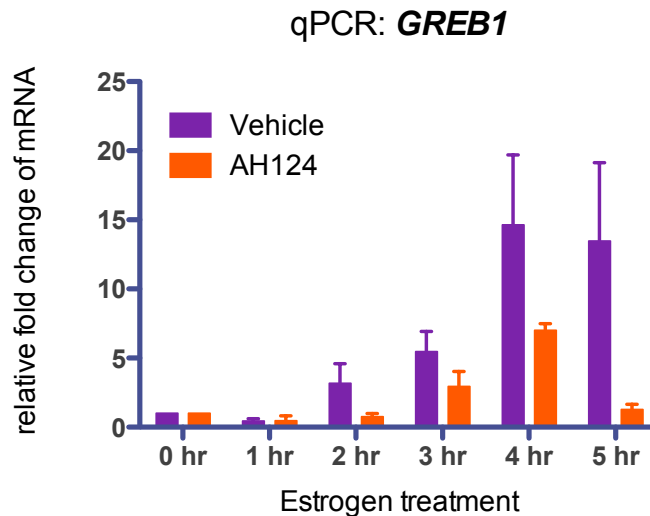
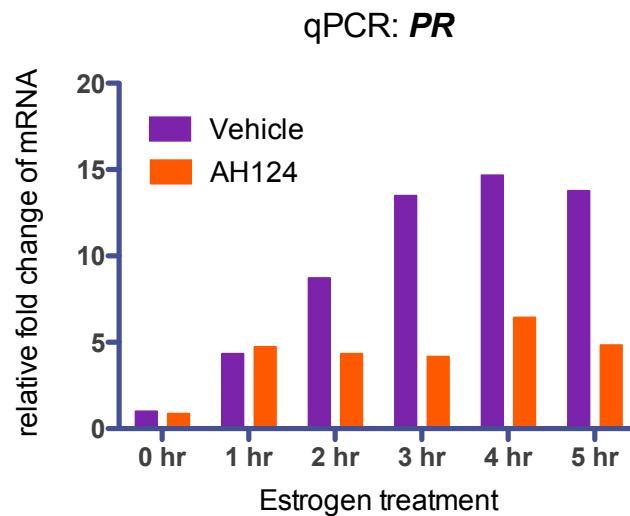


Figure 2-29 (C-D). Effects of potent LSD1 inhibitor AH124 on ER α target gene activation. qPCR analyses of cDNA prepared from MCF7 cells pretreated with vehicle (DMSO) or 100 μ M AH124 for 24 hr and treated with of 10 nM estrogen at the indicated time points before assaying for (A) *LSD1*, (B) *GREB1*, (C) *IGFBP4*, or (D) *pS2* expression. RNA levels are normalized to *GAPDH*; vehicle-treated MCF7 is set as one. Gene induction in the presence of TCP is shown as a control.

C



D

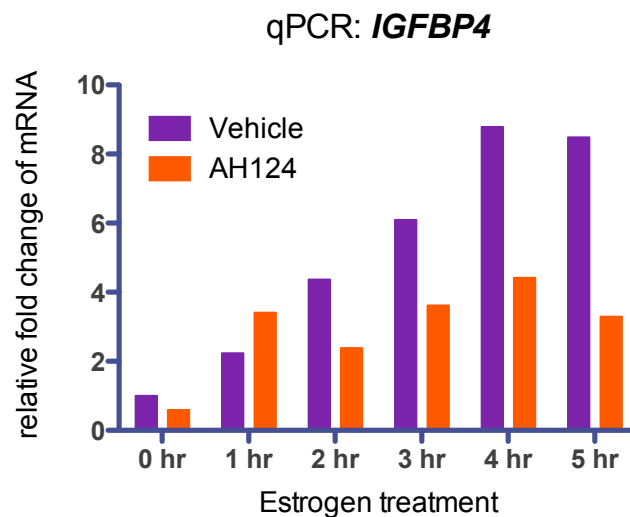
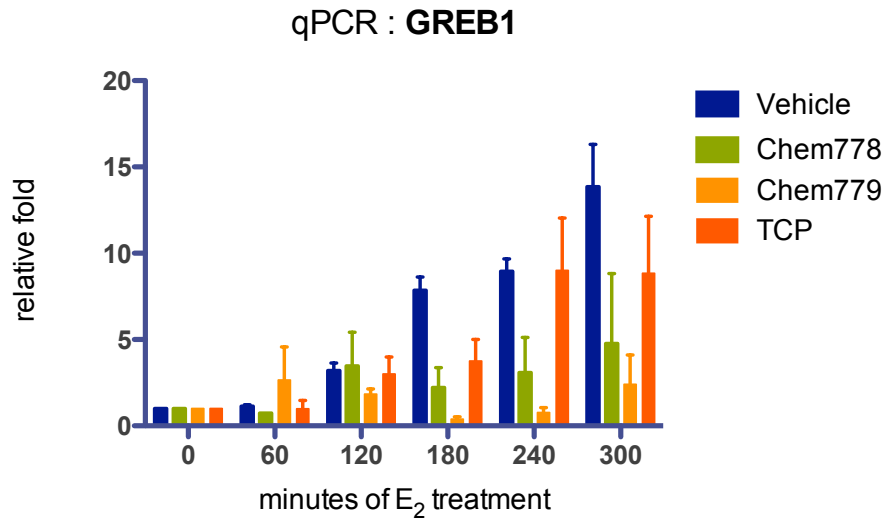


Figure 2-30 (A-B). Effects of potential LSD1 inhibitors Chem778 and Chem779 on ER α target gene activation. qPCR analyses of cDNA prepared from MCF7 cells pretreated with vehicle, 100 μ M Chem778 or Chem779 for 24 hr and treated with 10 nM estrogen at the indicated time points before assaying for (A) *GREB1*, (B) *PR*, (C) *IGFBP4*, or (D) *pS2* expression. RNA levels are normalized to *GAPDH*; vehicle-treated MCF7 is set as one. Gene induction in the presence of TCP is shown as a control. Average results from duplicates; error bars = SEM.

A



B

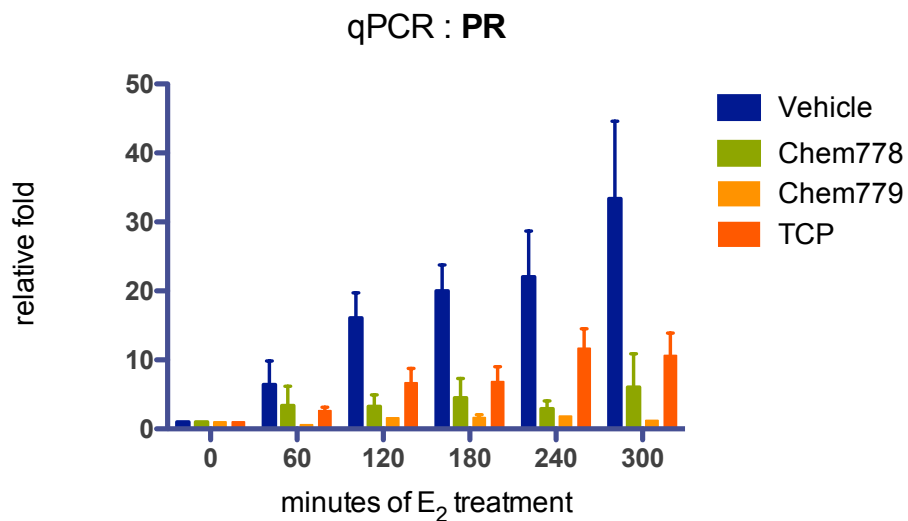
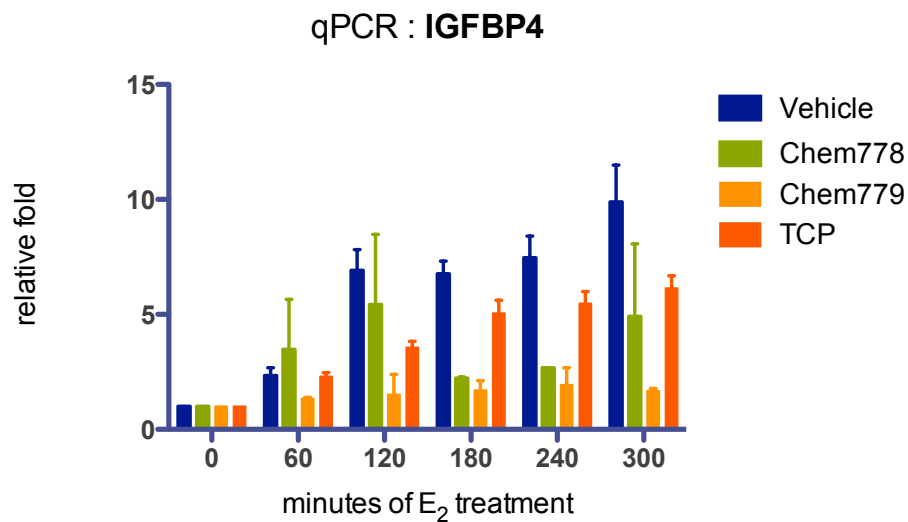
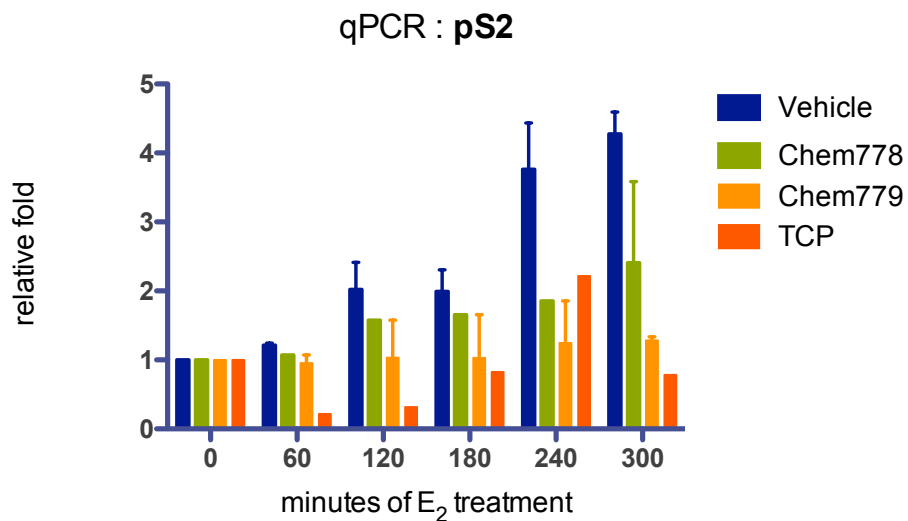


Figure 2-30 (C-D). Effects of potential LSD1 inhibitors Chem778 and Chem779 on ER α target gene activation. qPCR analyses of cDNA prepared from MCF7 cells pretreated with vehicle, 100 μ M Chem778 or Chem779 for 24 hr and treated with 10 nM estrogen at the indicated time points before assaying for (A) *GREB1*, (B) *PR*, (C) *IGFBP4*, or (D) *pS2* expression. RNA levels are normalized to *GAPDH*; vehicle-treated MCF7 is set as one. Gene induction in the presence of TCP is shown as a control. Average results from duplicates; error bars = SEM.

C



D



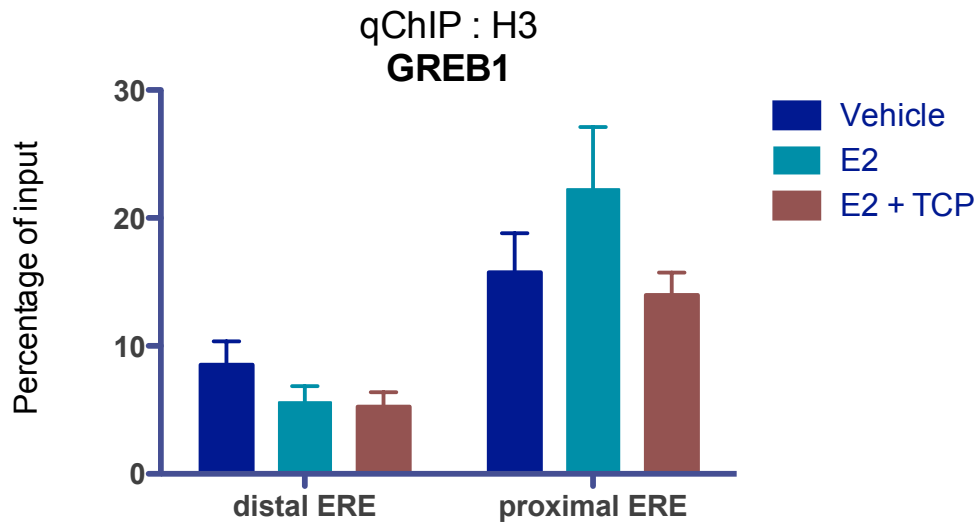
2.3.7. Chromatin-binding ability of TRIM24 is dependent on the enzymatic activity of LSD1

The effects of LSD1 inhibitors on ER α gene activation led to the question of how these inhibitors work mechanistically and whether TRIM24 is involved. The kinetic recruitment of transcription factors (Figures 2-19, 2-21, and 2-23) and dynamic H3K4 methylation (Figures 2-20, 2-22, and 2-24) represents valuable information in guiding the time-specific ChIP experiments in the presence of Tranylcypromine (TCP, an inhibitor of LSD1). For *GREB1*, the maximum recruitment of LSD1 occurs at 180 min post-E₂ (Figure 2-21), so I sought to determine how LSD1 affects the accumulation of TRIM24 and ER α on the chromatin at this time point. When I pre-treated MCF7 cells with 1 μ M of TCP, estrogen-induced transcriptional activation of *GREB1* is down-regulated, most significantly at $t = 180$ min. (Figure 2-16A). Consistently, at $t = 180$ min, ChIP assays reveal that TCP treatment leads to re-methylation of H3K4me₂ (Figure 2-31C), but not H3K4me₃ (Figure 2-31D), at *GREB1* EREs. I also observed a reduction in H3K4me₁ in the presence of TCP at $t = 180$ min (Figure 2-31B), possibly due to the inhibition of demethylation from H3K4me₂ to H3K4me₁. Importantly, inhibition of LSD1 by TCP does not affect H3K9me₂ levels at *GREB1* distal ERE (Figure 2-33), suggesting that TCP only induces changes in H3K4 (a preferable substrate of LSD1) but not H3K9 methylation (a biochemically non-preferred LSD1 substrate). Notably, gain of H3K4me₂ is concurrent with decreased binding of TRIM24 (Figure 2-32A) and ER α (Figure 2-32B), as well as LSD1 (Figure 2-32C) to the chromatin. Similar effects of TCP

on H3K4me2 occupancy (Figure 2-36), TRIM24 (Figure 2-37) and ER α (Figure 2-38) recruitment are also observed in *PR*, *pS2*, and *IGFBP4* ERE sites, but not at unspecific site *GAPDH* (negative control). A summary of TCP-induced changes in histone modifications and recruitments of TRIM24 and ER α is presented in Figure 2-39. These observations confirmed the gene- and time-specific dependence on chromatin structure for unique TRIM24 and ER α binding events.

Figure 2-31 (A-B). LSD1 inhibitor Tranylcypromine (TCP) leads to changes in H3K4 methylation. ChIP assays for (A) total H3, (B) H3K4me1, (C) H3K4me2, (D) H3K4me3 at *GREB1* distal and proximal ERE sites with the indicated treatment: vehicle (ethanol), estrogen (E_2), or E_2 + TCP. Cells are pre-treated with 2 μ M TCP for 24 hr and treated with 20 nM E_2 for 3 hr. Average results from triplicates; error bars = SEM.

A.



B.

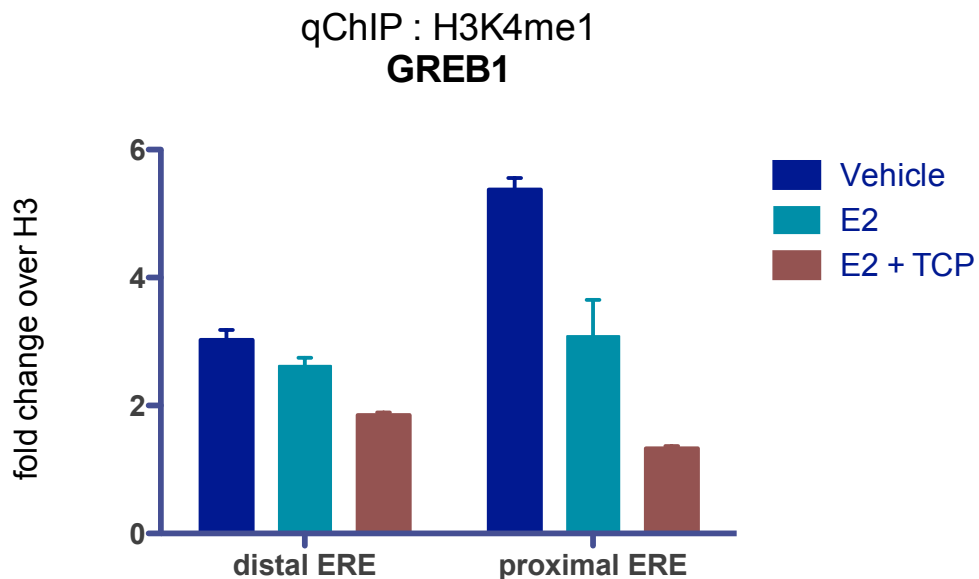
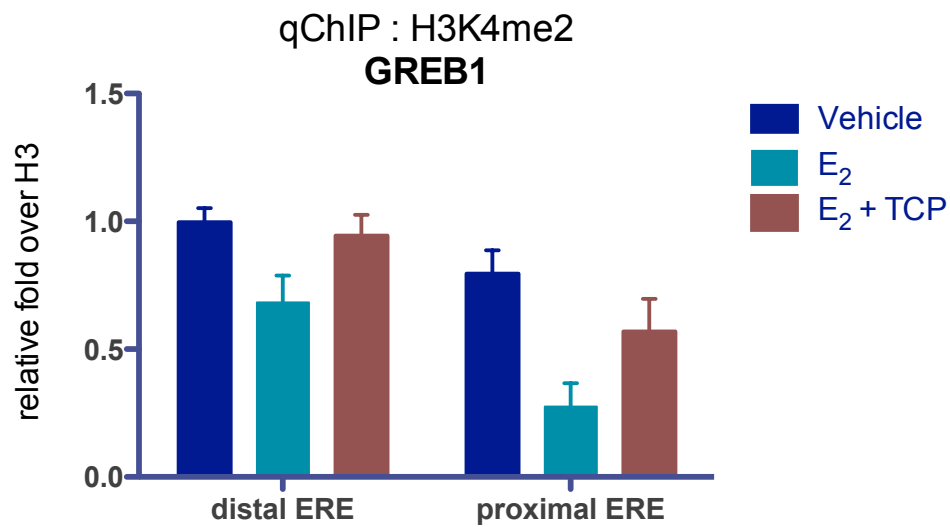


Figure 2-31 (C-D). LSD1 inhibitor Tranylcypromine (TCP) leads to changes in H3K4 methylation. ChIP assays for (A) total H3, (B) H3K4me1, (C) H3K4me2, (D) H3K4me3 at *GREB1* distal and proximal ERE sites with the indicated treatment: vehicle (ethanol), estrogen (E_2), or E_2 + TCP. Cells are pre-treated with 2 μ M TCP for 24 hr and treated with 20 nM E_2 for 3 hr. Average results from triplicates; error bars = SEM.

C.



D.

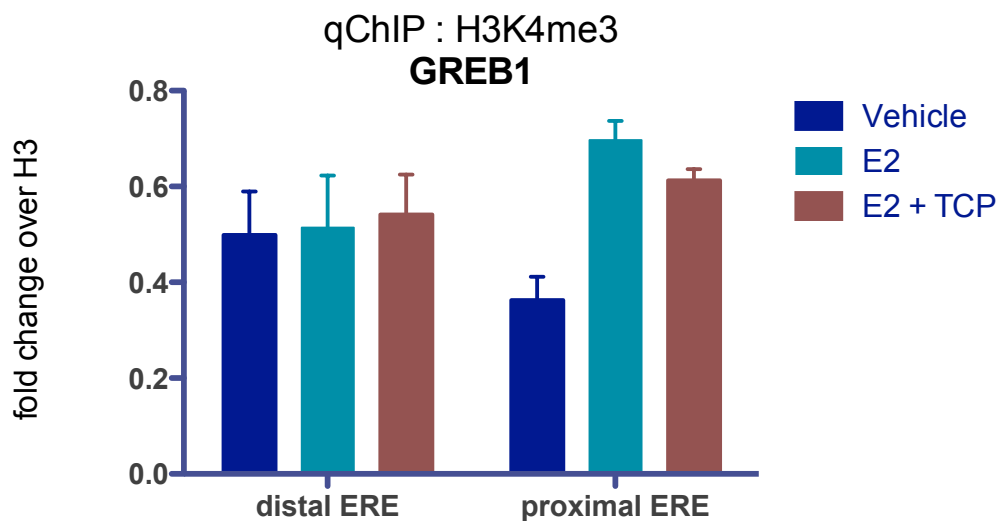
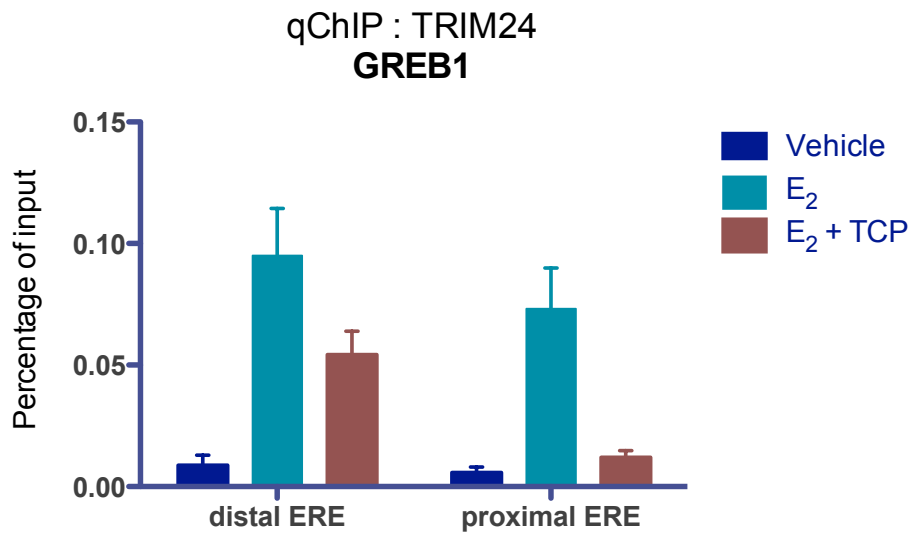


Figure 2-32 (A-B). LSD1 inhibitor Tranylcypromine (TCP) impairs recruitment of TRIM24 and ER α . ChIP assays for (A) TRIM24, (B) ER α , and (C) LSD1 at *GREB1* distal and proximal ERE sites with the indicated treatment: vehicle (ethanol), estrogen (E₂), or E₂ + TCP. Cells are pre-treated with 2 μ M TCP for 24 hr and treated with 20 nM E₂ for 3 hr. Average results from triplicates; error bars = SEM.

A.



B.

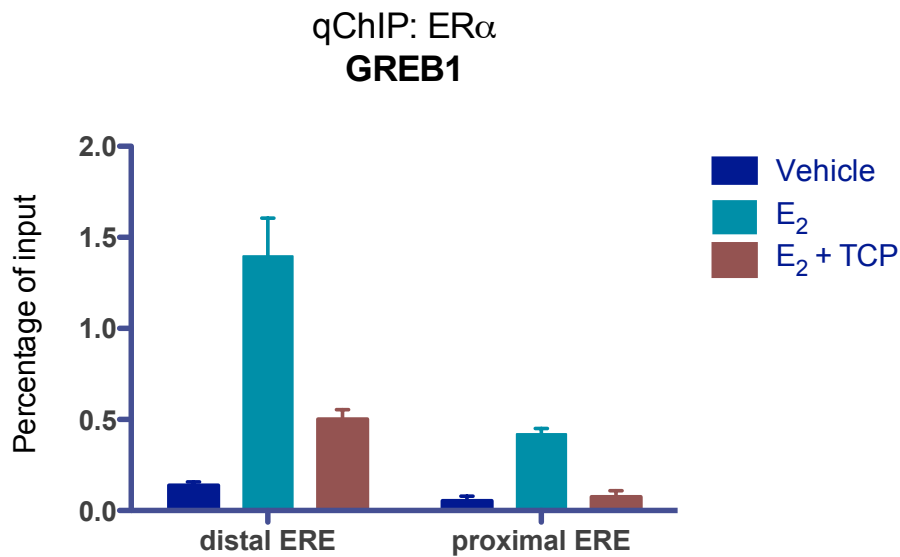


Figure 2-32C. LSD1 inhibitor Tranylcypromine (TCP) impairs recruitment of TRIM24 and ER α . ChIP assays for (A) TRIM24, (B) ER α , and (C) LSD1 at *GREB1* distal and proximal ERE sites with the indicated treatment: vehicle (ethanol), estrogen (E₂), or E₂ + TCP. Cells are pre-treated with 2 μ M TCP for 24 hr and treated with 20 nM E₂ for 3 hr. Average results from triplicates; error bars = SEM.

C.

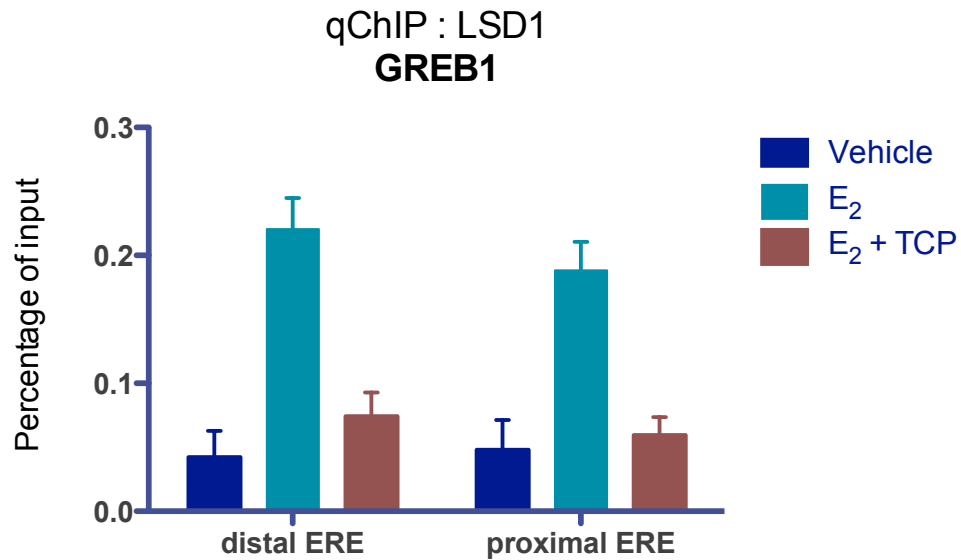


Figure 2-33. LSD1 inhibitor Tranylcypromine (TCP) does not affect H3K9 methylation. ChIP assays for H3K9me (normalized with total H3) at *GREB1*, *PR*, *pS2*, and *IGFBP4* ERE sites with the indicated treatment: vehicle (ethanol), estrogen (E_2), or E_2 + TCP. Cells are pre-treated with 2 μ M TCP for 24 hr and treated with 20 nM E_2 . Average results from duplicates; error bars = SEM.

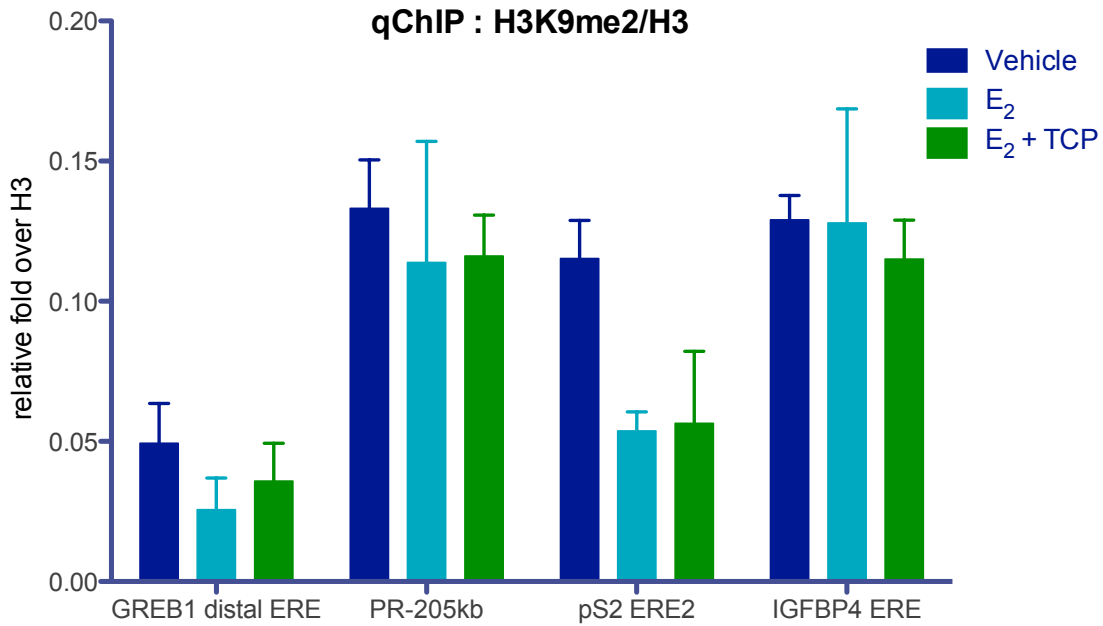
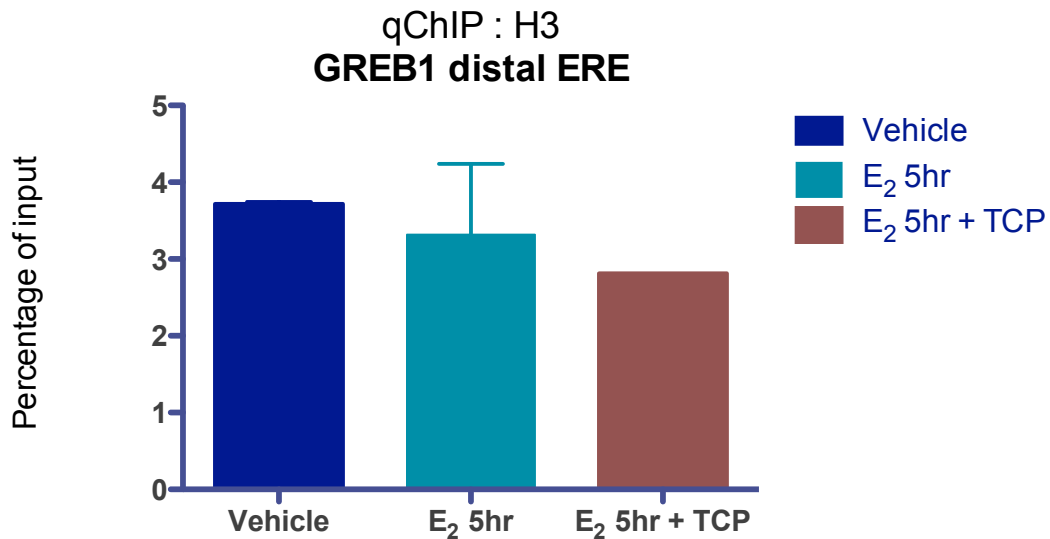


Figure 2-34 (A-B). LSD1 inhibitor Tranylcypromine (TCP) leads to changes in H3K4 methylation. ChIP assays for (A) total H3, (B) H3K4me1, and (C) H3K4me2 at *GREB1* distal and proximal ERE sites with the indicated treatments: vehicle (ethanol), estrogen (E_2), or E_2 + TCP. Cells are pre-treated with 2 μ M TCP for 24 hr and treated with 20 nM E_2 for 5 hr. Average results from triplicates; error bars = SEM.

A.



B.

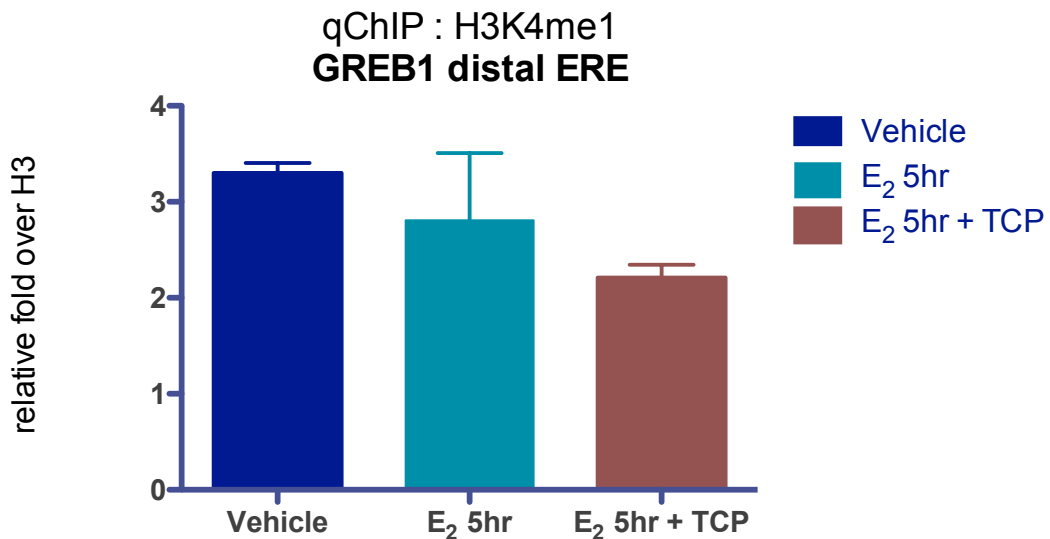


Figure 2-34C. LSD1 inhibitor Tranylcypromine (TCP) leads to changes in H3K4 methylation. ChIP assays for (A) total H3, (B) H3K4me1, and (C) H3K4me2 at *GREB1* distal and proximal ERE sites with the indicated treatment: vehicle (ethanol), estrogen (E₂), or E₂ + TCP. Cells are pre-treated with 2 μM TCP for 24 hr and treated with 20 nM E₂ for 5 hr. Average results from triplicates; error bars = SEM.

C.

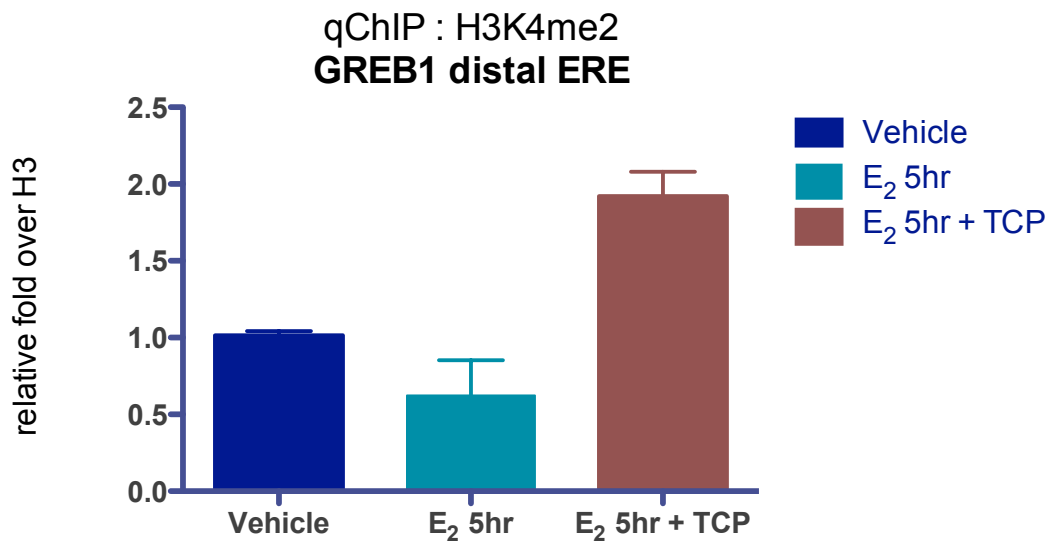
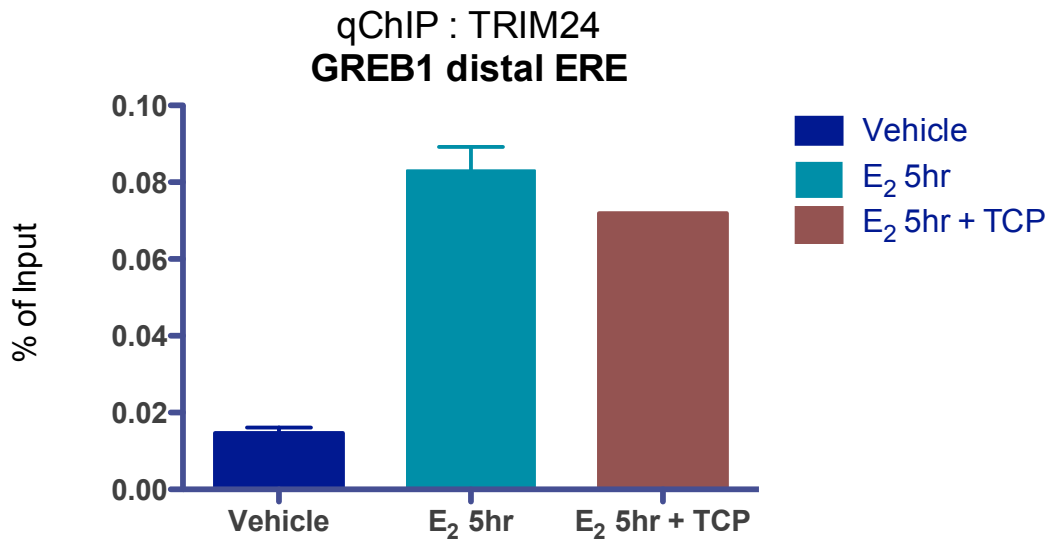


Figure 2-35 (A-B). LSD1 inhibitor Tranylcypromine (TCP) impairs recruitment of TRIM24 and ER α . ChIP assays for (A) TRIM24, (B) ER α , and (C) LSD1 at *GREB1* distal and proximal ERE sites with the indicated treatment: vehicle (ethanol), estrogen (E₂), or E₂ + TCP. Cells are pre-treated with 2 μ M TCP for 24 hr and treated with 20 nM E₂ for 5 hr.

A.



B.

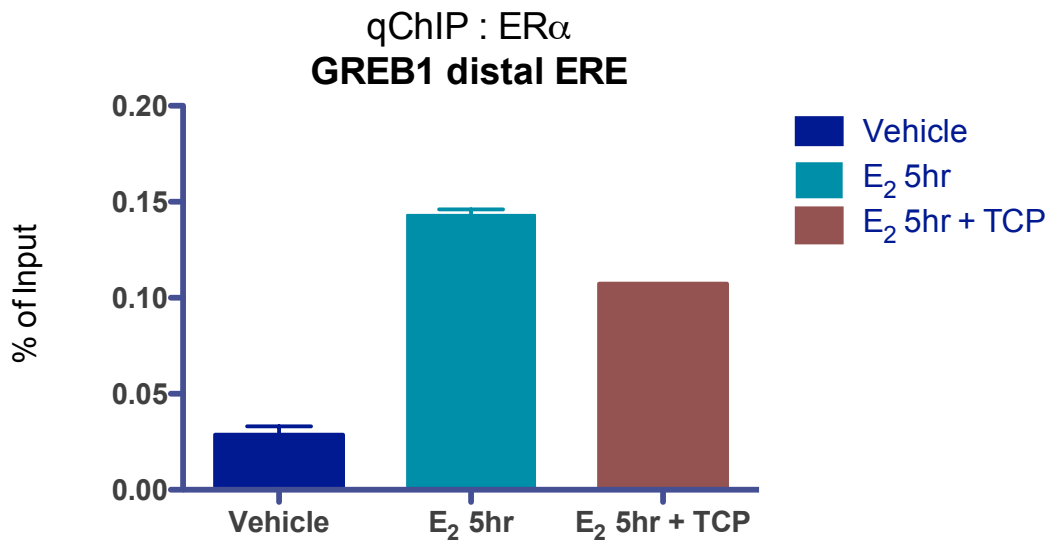


Figure 2-35C. LSD1 inhibitor Tranylcypromine (TCP) impairs recruitment of TRIM24 and ER α . CHIP assays for (A) TRIM24, (B) ER α , and (C) LSD1 at *GREB1* distal and proximal ERE sites with the indicated treatment: vehicle (ethanol), estrogen (E₂), or E₂ + TCP. Cells are pre-treated with 2 μ M TCP for 24 hr and treated with 10 nM E₂ for 5 hr.

C.

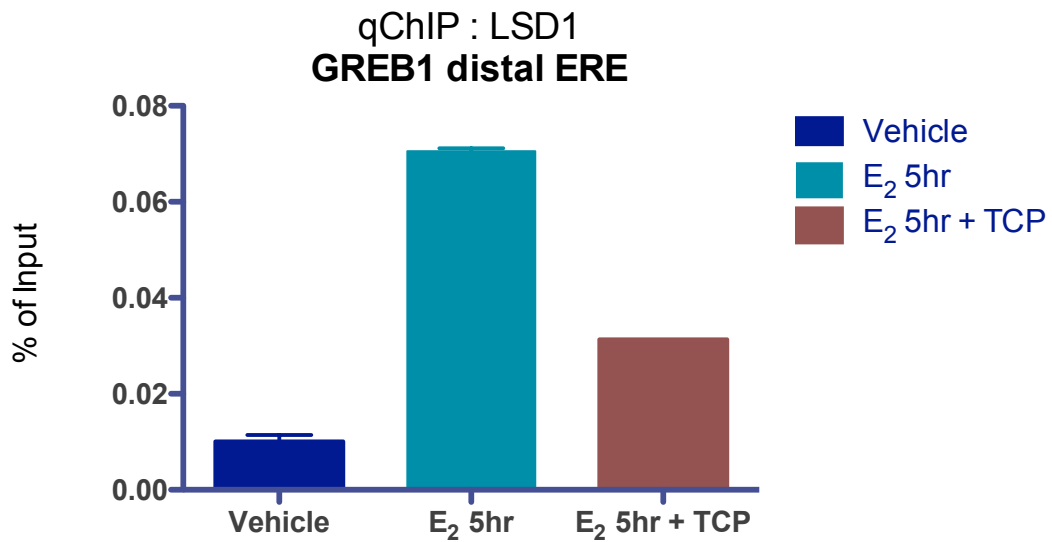
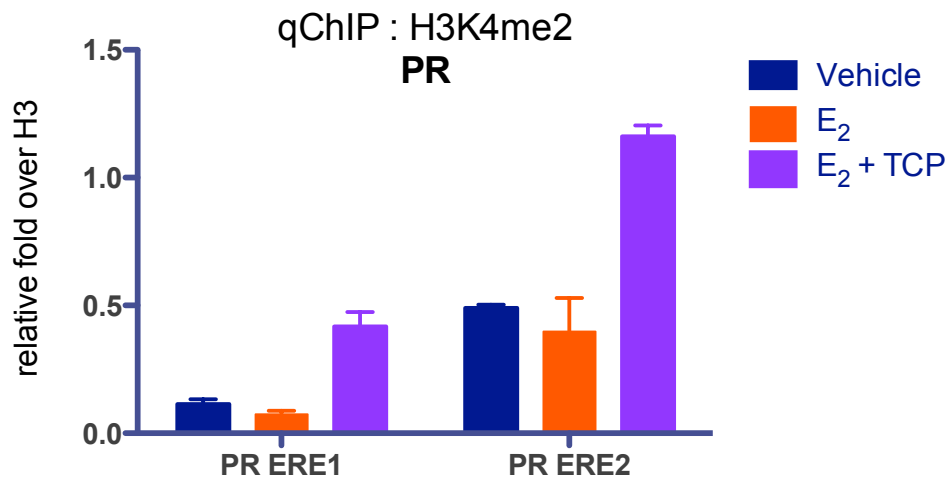


Figure 2-36 (A-B). LSD1 inhibitor Tranylcypromine (TCP) leads to re-methylation of H3K4me2. ChIP assays for H3K4me2 occupancy (normalized with total H3) at (A) *PR*, (B) *pS2*, and (C) *IGFBP4* ERE sites, or negative control (D) *GAPDH*, with the indicated treatment: vehicle (ethanol), estrogen (E_2), or E_2 + TCP. Cells are pre-treated with 2 μ M TCP for 24 hr and treated with 20 nM E_2 . Average results from duplicates; error bars = SEM.

A.



B.

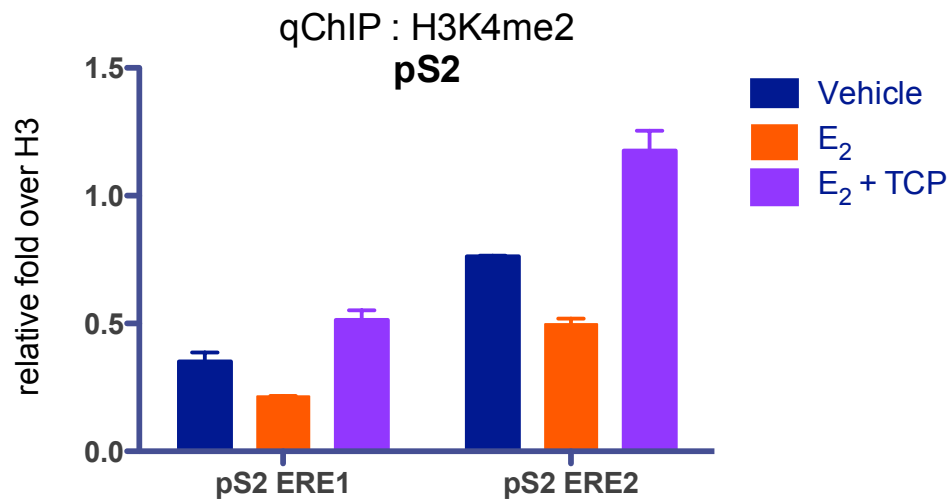
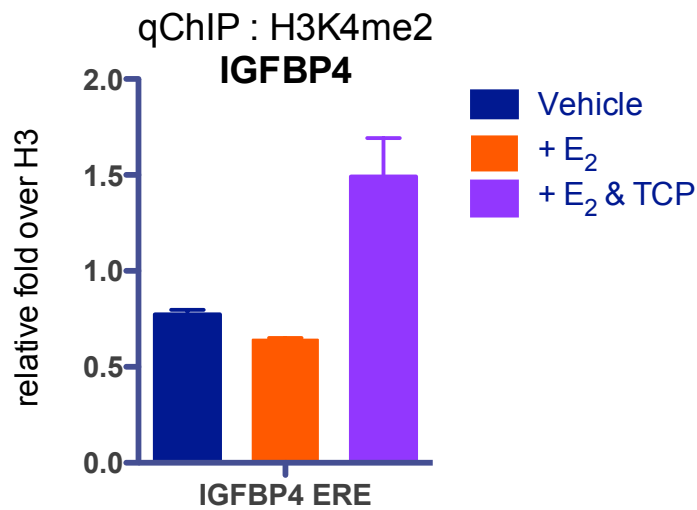


Figure 2-36 (C-D). LSD1 inhibitor Tranylcypromine (TCP) leads to re-methylation of H3K4me2. ChIP assays for H3K4me2 occupancy (normalized with total H3) at (A) *PR*, (B) *pS2*, and (C) *IGFBP4* ERE sites, or negative control (D) *GAPDH*, with the indicated treatment: vehicle (ethanol), estrogen (E_2), or E_2 + TCP. Cells are pre-treated with 2 μ M TCP for 24 hr and treated with 20 nM E_2 . Average results from duplicates; error bars = SEM.

C.



D.

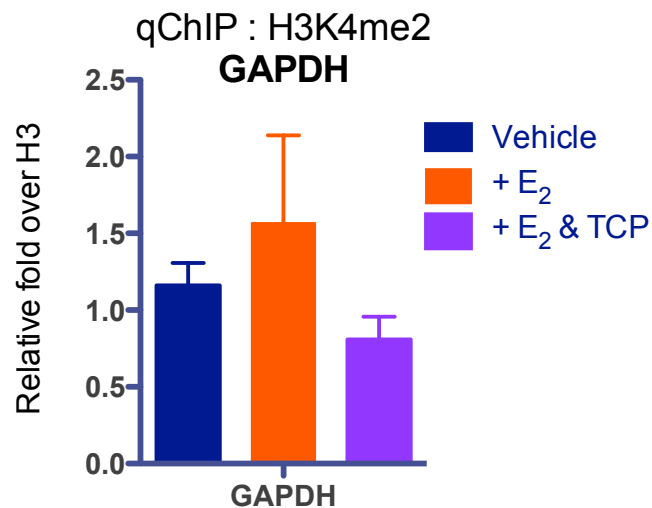
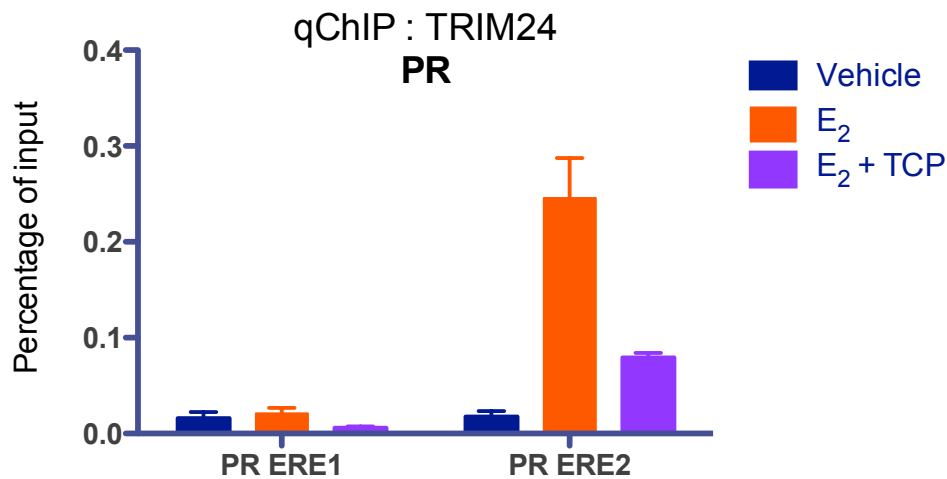


Figure 2-37 (A-B). LSD1 inhibitor Tranylcypromine (TCP) impairs TRIM24 recruitment. ChIP assays for TRIM24 recruitment (normalized with input) at (A) *PR*, (B) *pS2*, and (C) *IGFBP4* ERE sites, or negative control (D) *GAPDH*, with the indicated treatment: vehicle (ethanol), estrogen (E_2), or E_2 + TCP. Cells are pre-treated with 2 μ M TCP for 24 hr and treated with 20 nM E_2 . Average results from duplicates; error bars = SEM.

A.



B.

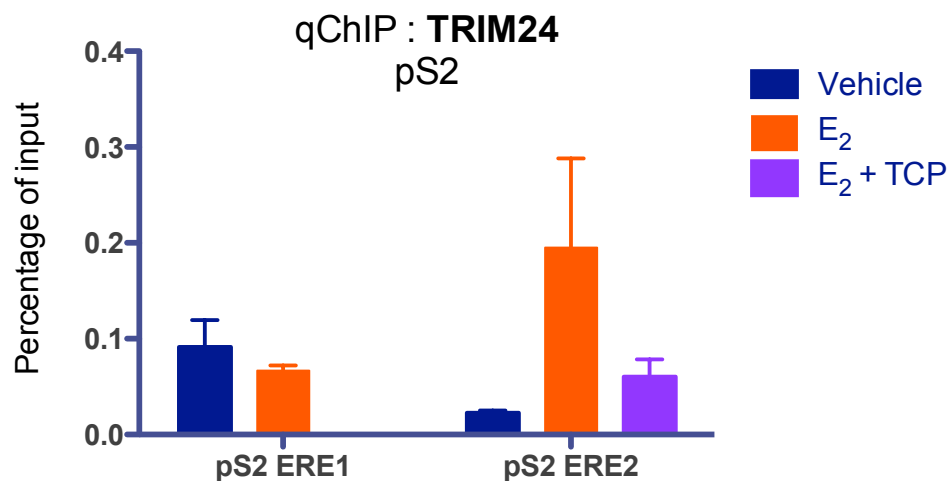
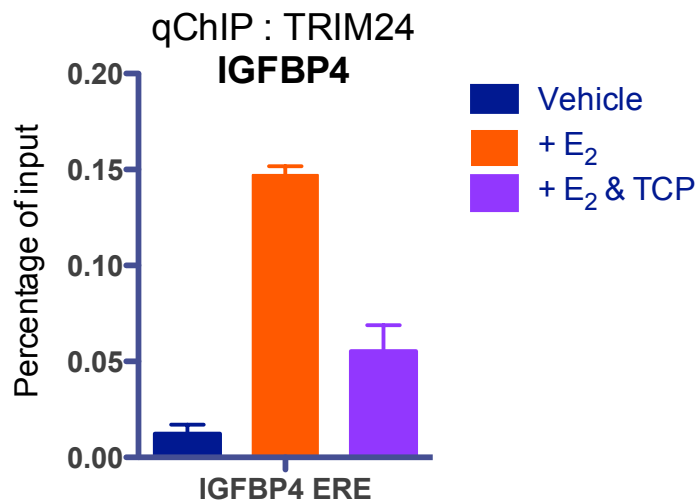


Figure 2-37 (C-D). LSD1 inhibitor Tranylcypromine (TCP) impairs TRIM24 recruitment. ChIP assays for TRIM24 recruitment (normalized with input) at (A) *PR*, (B) *pS2*, and (C) *IGFBP4* ERE sites, or negative control (D) *GAPDH*, with the indicated treatment: vehicle (ethanol), estrogen (E_2), or E_2 + TCP. Cells are pre-treated with 2 μ M TCP for 24 hr and treated with 20 nM E_2 . Average results from duplicates; error bars = SEM.

C.



D.

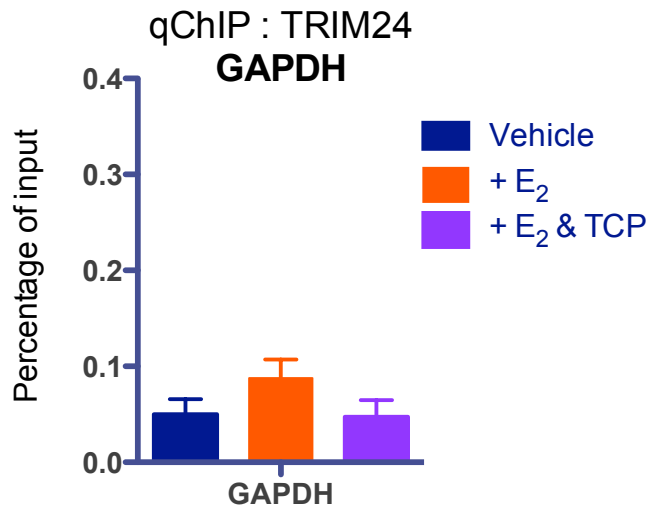
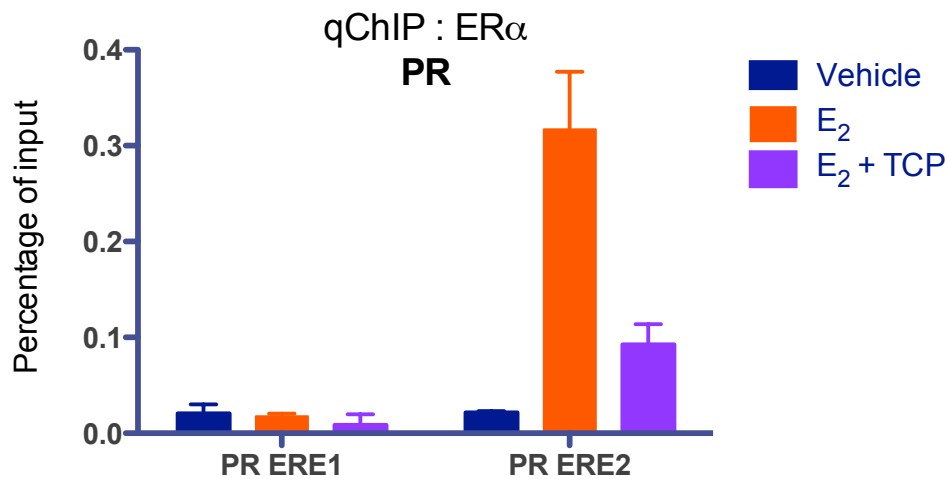


Figure 2-38 (A-B). LSD1 inhibitor Tranylcypromine (TCP) impairs ER α recruitment. ChIP assays for ER α binding (normalized with input) at (A) *PR*, (B) *pS2*, and (C) *IGFBP4* ERE sites, or negative control (D) *GAPDH*, with the indicated treatment: vehicle (ethanol), estrogen (E₂), or E₂ + TCP. Cells are pre-treated with 2 μ M TCP for 24 hr and treated with 20 nM E₂. Average results from duplicates; error bars = SEM.

A.



B.

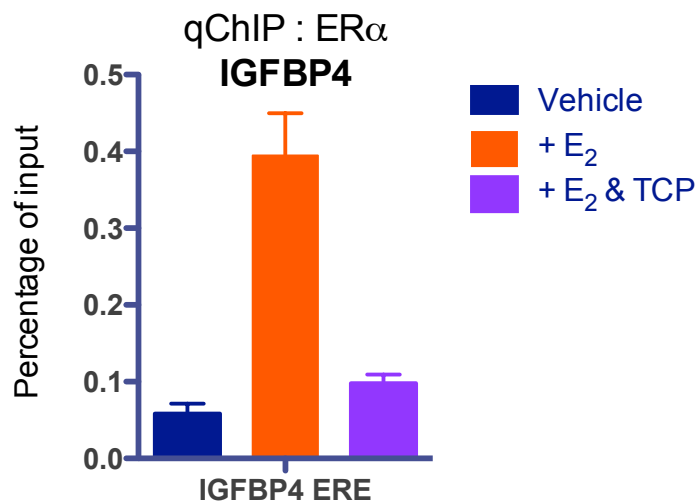
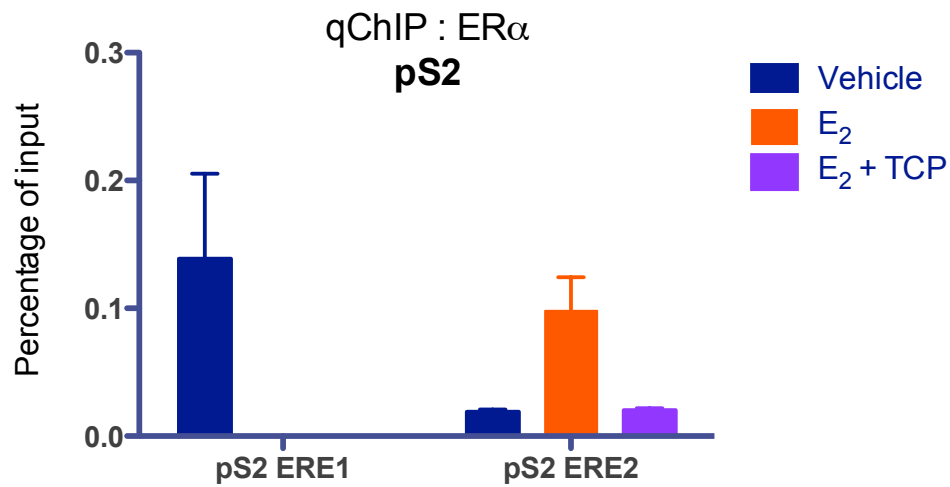


Figure 2-38 (C-D). LSD1 inhibitor Tranylcypromine (TCP) impairs ER α recruitment. ChIP assays for ER α binding (normalized with input) at (A) *PR*, (B) *pS2*, and (C) *IGFBP4* ERE sites, or negative control (D) *GAPDH*, with the indicated treatment: vehicle (ethanol), estrogen (E_2), or E_2 + TCP. Cells are pre-treated with 2 μ M TCP for 24 hr and treated with 20 nM E_2 . Average results from duplicates; error bars = SEM.

C.



D.

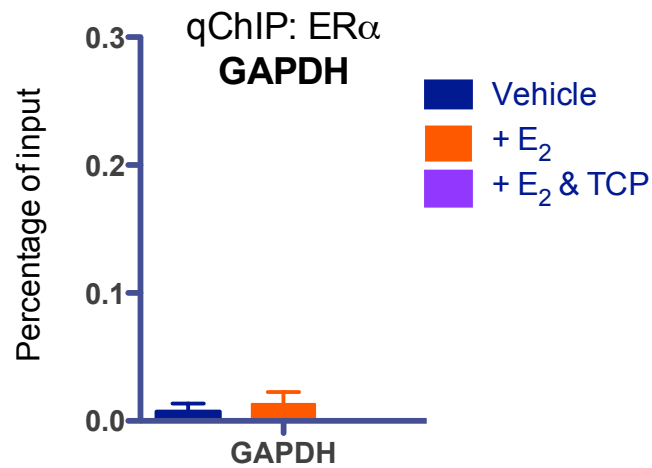


Figure 2-39. Summary of changes in histone modifications and recruitment of TRIM24 and ER α in the presence of Tranylcypramine (TCP). Summarized results for ChIP assays from Figures 2-31 to 2-36.

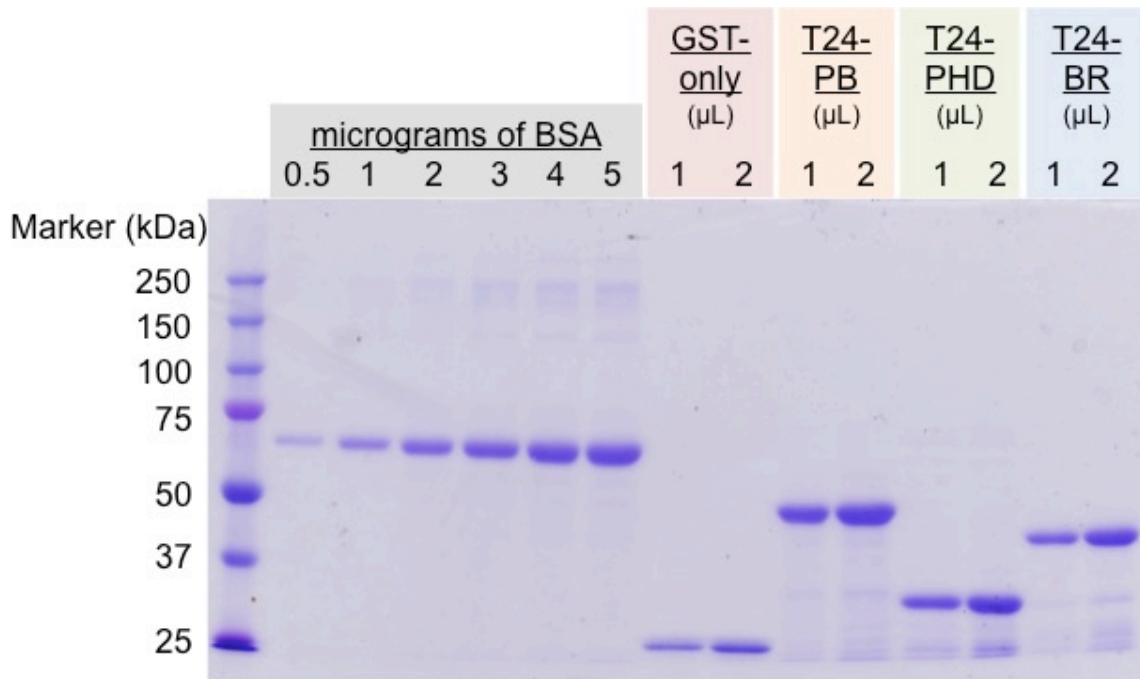
Transcription factor binding or histone modification	Changes in the presence of TCP
H3K4me1	No change
H3K4me2	Increase
H3K4me3	No change
H3K9me2	No change
TRIM24	Decrease
ERα	Decrease
LSD1	Decrease

2.3.8. H3T6ph disrupts TRIM24 from binding to histone peptide

LSD1-mediated demethylation of H3K4me2 is dependent on H3T6 dephosphorylation [31] and H3T6 phosphorylation inhibits H3K4me0 readers BHC80- and AIRE-PHD from binding to H3 [29]. Since chromatin binding of TRIM24 follows LSD1 pre-recruitment and H3K4me2 demethylation (Figure 2-19), and TRIM24 preferentially recognizes H3K4me0, it is reasonable that H3T6ph will disrupt the interaction between TRIM24 and unmodified H3.

To determine whether H3T6ph has any effects on TRIM24 binding, I performed biotinylated peptide pulldown assays to study the biophysical interaction between TRIM24 and modified histone peptides. I used purified GST-tagged TRIM24 recombinant protein (Figure 2-40) in the assays, as well as GST-only, GST-RBP2 (PHD1 or PHD2), GST-JMJD2A-Double Tudor Domain (DTD) as controls. I also included full-length LSD1 for reference. These GST-proteins are individually incubated with commercially available histone peptides: unmodified H3 (1-21), H3K4me2, H3T6ph, or H3K4me2T6ph. The pulldown assays shown in Figure 2-41 suggested that GST-only protein does not interact with any peptides (negative controls) and confirmed that methylated H3K4 disrupts the binding of TRIM24-PB and RBP2-PHD1 (lane 3, H3K4me2), which preferentially recognize unmodified H3K4 (lane 2, H3₁₋₂₁). As a control, I also examined readers that specifically bind to methyl-H3K4, such as RBP2-PHD3 and JMJD2A-DTD. These H3K4me readers are also pulled down with methylated-H3K4 (lane 3, H3K4me2), but not unmodified H3 (lane 2, H3₁₋₂₁). The

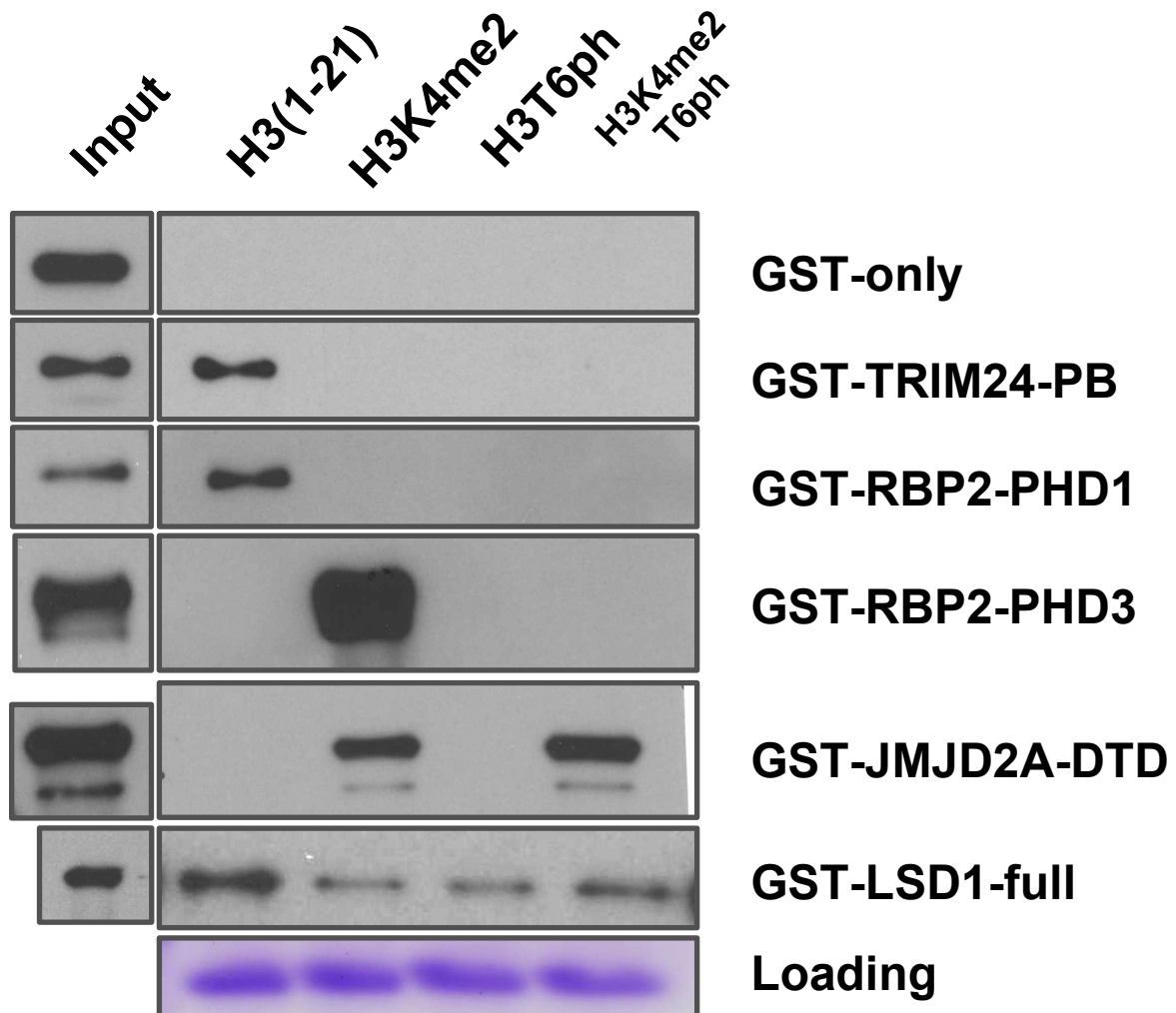
Figure 2-40. Purification of GST-only and GST-tagged TRIM24 recombinant proteins. Coomassie staining shows the purity and approximate concentration of GST-only and GST-tagged TRIM24-PHD-Bromo (T24-PB), TRIM24-PHD (T24-PHD), and TRIM24-Bromo (T24-BR), as compared to BSA controls.



quality control confirms that these GST-proteins and histone peptides are functional.

Next, the question is whether peptides phosphorylated at H3T6 disrupts the interaction with the readers. Both TRIM24-PB and RBP2-PHD1 lose binding in the presence of H3T6ph (Figure 2-41, lane 4). As for H3K4-methyl readers, RBP2-PHD3 and JMJD2A-DTD, H3T6ph only inhibits the binding of RBP2-PHD3 to H3K4me2, but does not affect JMJD2A-DTD (Figure 2-41, lane5). Therefore, H3T6 phosphorylation selectively disrupts binding of some but not all readers. Importantly, TRIM24 fails to bind to histone H3 (residues 1-21) in the presence of H3K4me2 (Figure 2-41, lane3), H3T6oh (lane 4), or both (lane 5, H3K4me2T6ph). Taken together, the inhibitory mark H3T6 is possibly significant for the biological functions of TRIM24 and RBP2.

Figure 2-41. H3T6 phosphorylation and/or H3K4 methylation hinder TRIM24 from binding to H3. Biotinylated peptide pulldown assay: 2 μ g of GST-only, GST-tagged TRIM24-PHD/Bromo (PB), GST-RBP2-PHD1, GST-RBP2-PHD3, GST-JMJD1A-Double Tudor Domain (DTD) or full-length LSD1 (GST-LSD1-full) is incubated with 1 μ g biotinylated-labeled histone peptides: unmodified H3 (1-21), H3K4me2, H3T6ph, or H3K4me2T6ph. The complex is pulled down by Streptavidin beads, and shown here is a Western blot probed with GST-antibody. 10% input is used as a positive control.



2.3.9. H3T6ph and its potential role in ER α target gene activation

If H3T6 phosphorylation is critical for ER α -mediated transcription activation, I expect that upon estrogen stimulation, dephosphorylation will occur to allow for H3K4 demethylation by LSD1 and chromatin binding of TRIM24. Using an antibody specific for H3T6ph (Figure 2-42), I sought to determine the potential roles of H3T6 in ER α target gene activation. Although estrogen treatment does not change the global H3T6 phosphorylation level in MCF7 cells (data not shown), it triggers dynamic H3T6ph in a gene-specific manner. For example, upon E₂ stimulation, phosphorylation of H3T6 at *GREB1* EREs exhibits a cyclical pattern from 0 hr to 3 hr, and dephosphorylation occurs from 1 hr to 2 hr (Figure 2-43 A-B). The pattern is slightly different at *PR* EREs, where H3T6ph slightly increases at $t = 1$ hr and then dramatically decreases at $t = 2$ hr and $t = 3$ hr (Figure 2-43 C-D). Taken together, dephosphorylation of H3T6 does not happen immediately after E₂ stimulate, but occurs from 1 hr to 2 hr, at *GREB1* and *PR* EREs.

PKC kinases PKC- α , - β 1 and β II have been previously shown to be specific for H3T6 phosphorylation [31]. To determine how ER α -regulated transcription will be affected by H3T6 phosphorylation, I performed a pilot study using a potent PKC inhibitor, bis-indolylmaleimide I (Bis I), that inhibits the kinase activity of $\alpha/\beta/\gamma$ isoforms. Bis I treatment dramatically dephosphorylates H3T6 at the EREs of target genes *GREB1*, *PR*, *pS2* and *IGFBP4*, compared to DMSO control (Figure 2-44) but the effects on estrogen-induced transcription is gene- and time-specific.

Figure 2-42. Specificity of H3T6ph antibody. Dot blot analysis is performed to determine the specificity of H3T6 antibody (Abcam) on recognizing H3T6 phosphorylation on different peptides: unmodified H3 (1-21), H3K4me2, H3T6ph, and H3K4me2T6ph. A five-fold dilution of BSA is used.

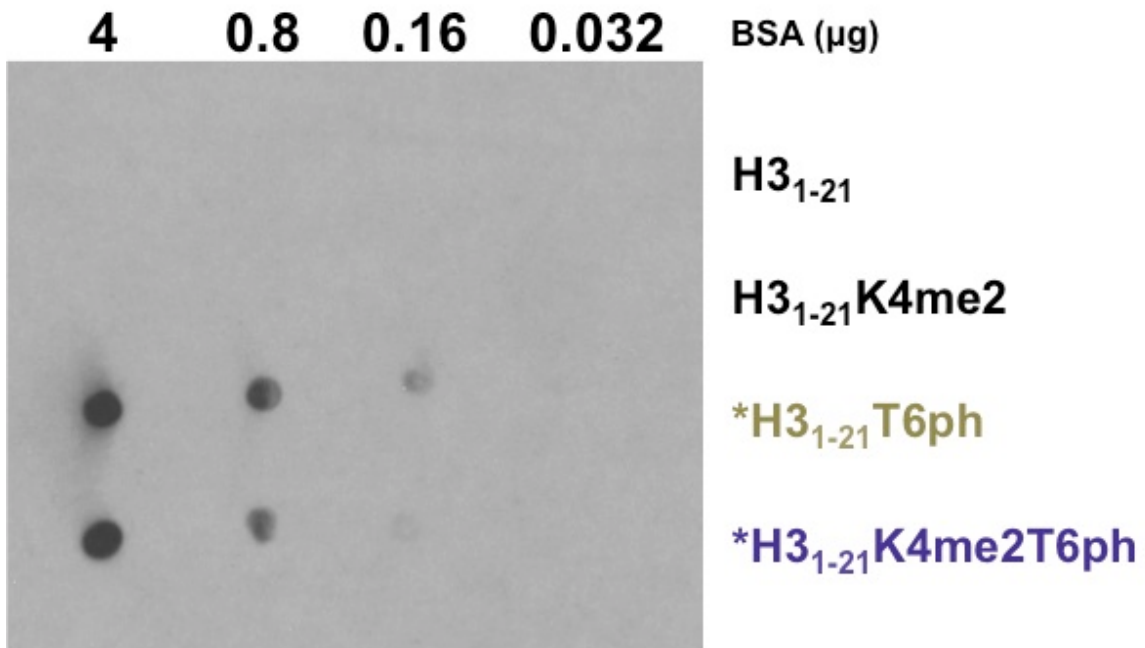
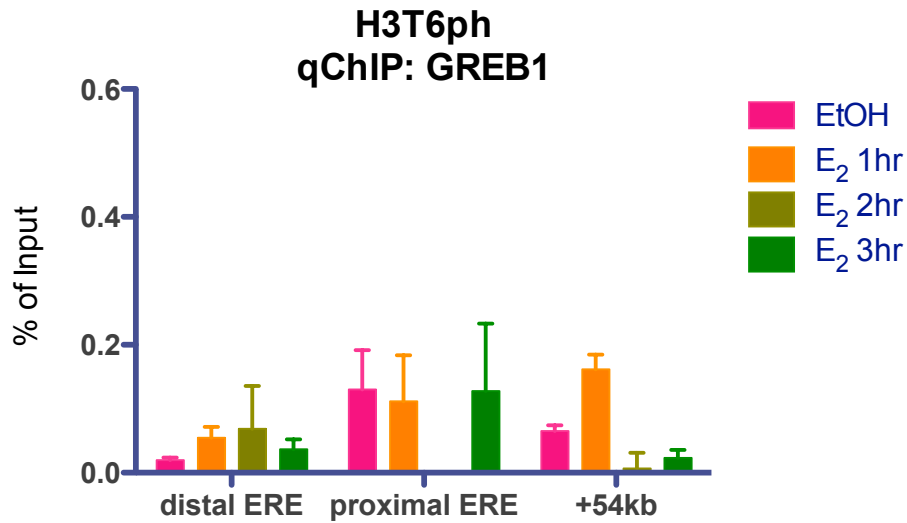


Figure 2-43 (A-B). Changes of H3T6 phosphorylation upon estrogen treatment. qChIP analyses of H3T6ph occupancy on *GREB1* EREs in the indicated time course of 10nM estrogen (E₂) normalized with (A) input or (H3). Average numbers from triplicates. Error bars = SEM.

A



B

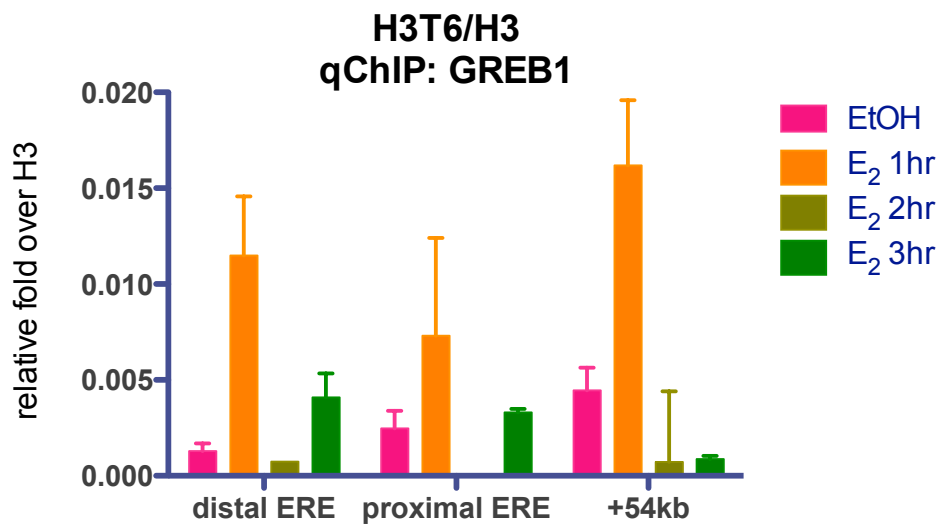
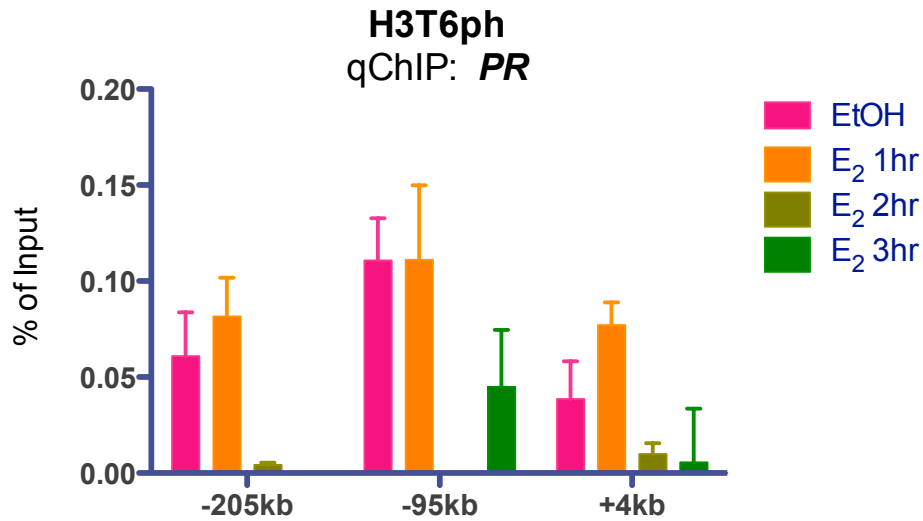


Figure 2-43 (C-D). Changes of H3T6 phosphorylation upon estrogen treatment. qChIP analyses of H3T6ph occupancy on *PR* EREs in the indicated time course of 10nM estrogen (E_2) normalized with (A) input or (H3). Average numbers from triplicates. Error bars = SEM.

C



D

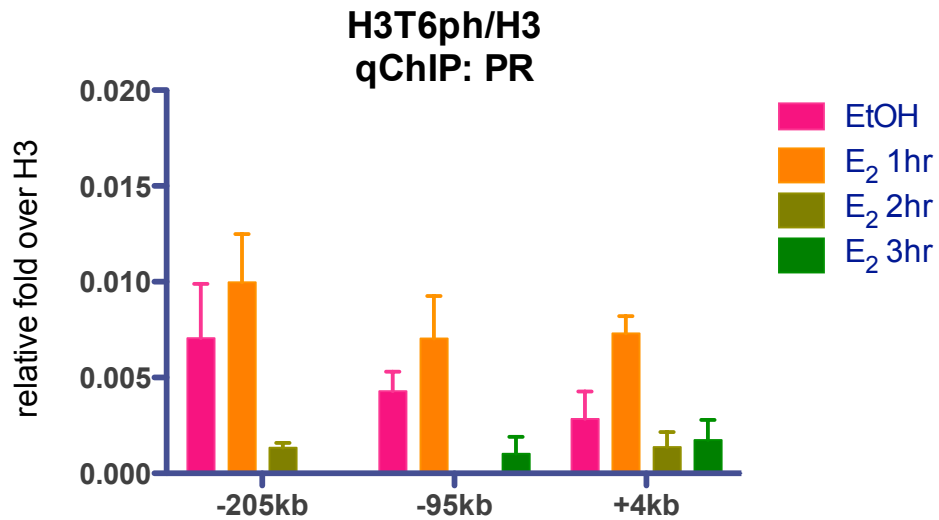
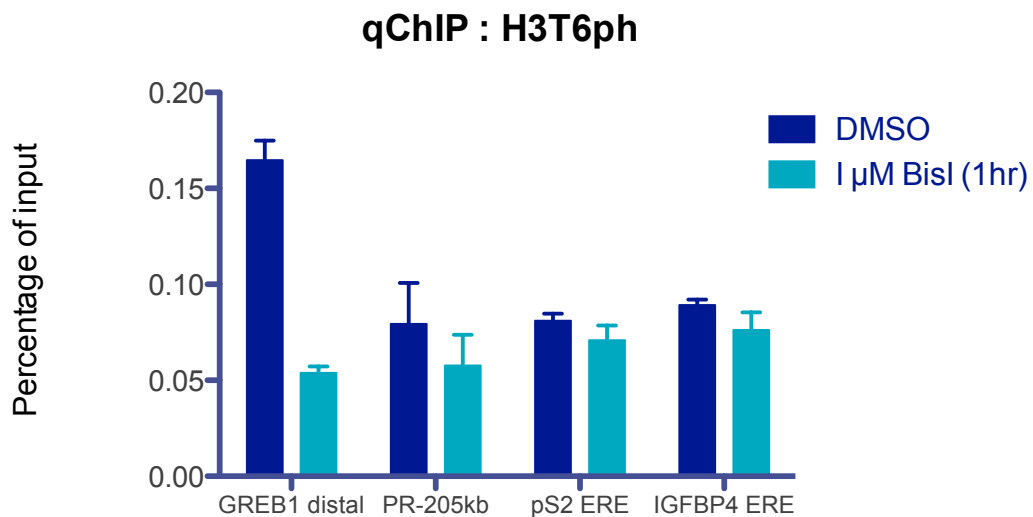


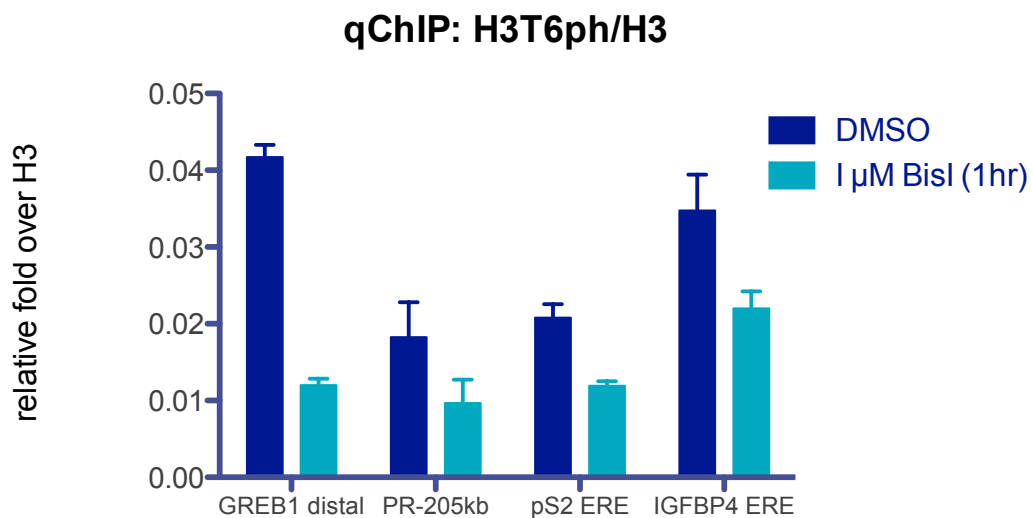
Figure 2-44. Inhibition of H3T6-specific protein kinase C (PKC) by BisI leads to dephosphorylation of H3T6 at *GREB1*, *PR*, *pS2* and *IGFBP4* EREs.

qChIPs normalized by (A) percent of input or (B) relative fold over H3 for H3T6ph occupancy in vehicle (DMSO)-treated or 1 μ M bis-indolylmaleimide I (BisI) for 1 hour at *GREB1*, *PR*, *pS2* and *IGFBP4* EREs. Average numbers from duplicates. Error bars = SEM.

A



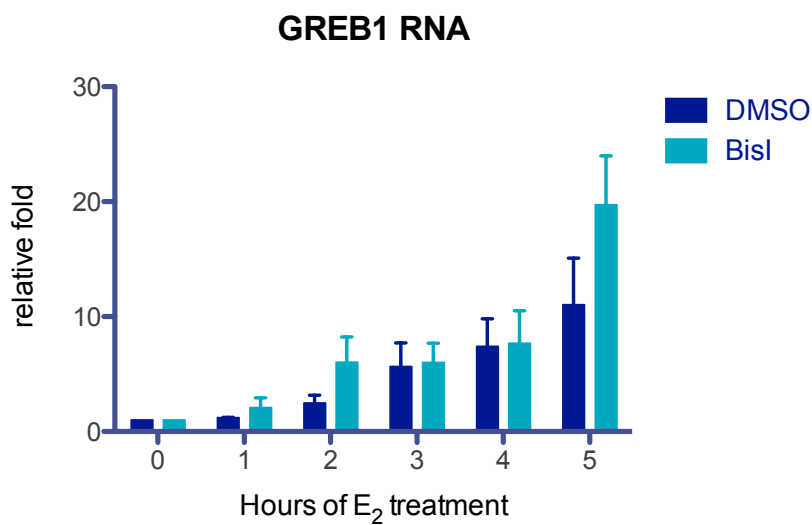
B



Dephosphorylation of H3T6 at *GREB1* and *PR* EREs occurs between 1 hr and 2 hr after E₂ treatment (Figure 2-43). Constantly, BisI up-regulates *GREB1* and *PR* expression at $t = 1$ hr and $t = 2$ hr (Figure 2-45 A-B). For *pS2* gene, the up-regulation occurs later at $t = 5$ hr (Figure 2-45C), whereas the activation of *IGFBP4* is not affected at all (Figure 2-45D). These observations demonstrated that H3T6ph might potentially regulate ER α -mediated transcription in a subset of target genes.

Figure 2-45 (A-B). Effects of BisI on ER α target gene induction. qPCR analyses of estrogen-induced activation of (A) *GREB1*, (B) *PR*, (C) *pS2*, and (D) *IGFBP4* in vehicle (DMSO)- or bis-indolylmaleimide I (BisI)-treated cells. Treatment of 1 μ M BisI for one hour in addition to the indicated treatment time of 10nM estrogen. RNA levels are normalized to *GAPDH*; vehicle-treated MCF7 is set as one. Average numbers from duplicates. Error bars = SEM.

A



B

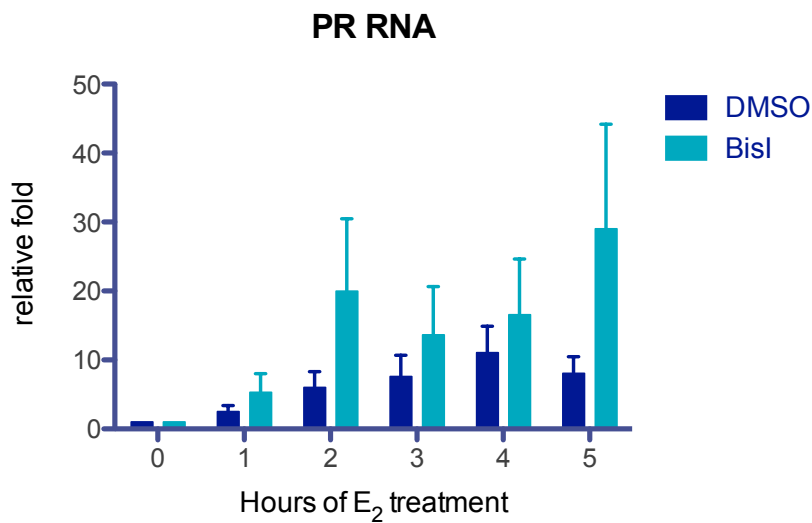
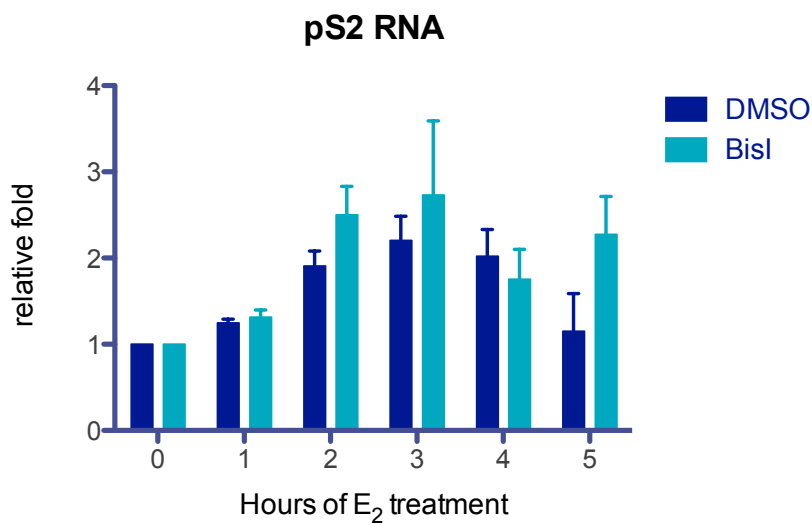
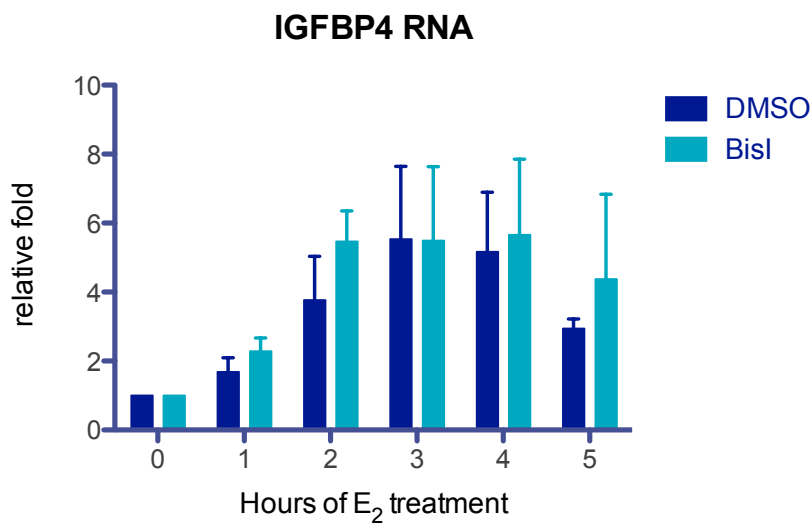


Figure 2-45 (C-D). Effects of BisI on ER α target gene induction. qPCR analyses of estrogen-induced activation of (A) *GREB1*, (B) *PR*, (C) *pS2*, and (D) *IGFBP4* in vehicle (DMSO)- or bis-indolylmaleimide I (BisI)-treated cells. Treatment of 1 μ M BisI for one hour in addition to the indicated treatment time of 10nM estrogen. RNA levels are normalized to *GAPDH*; vehicle-treated MCF7 is set as one. Average numbers from duplicates. Error bars = SEM.

C



D



2.4. FUTURE DIRECTIONS AND PRELIMINARY RESULTS

2.4.1. Does depletion of LSD1 also exert time-specific effect?

This study established a detailed recruitment profile of ER α and several co-activators, as well as dynamic H3K4me occupancy on EREs, which is useful when functional assays are designed to determine the efficiency of an epigenetic drug. For example, on *GREB1* ERE, dramatic inhibitory effect of TCP for is observed for TRIM24 and ER α recruitment when cells have been treated with estrogen for 180min (Figure 2-32 A and B), because LSD1 recruitment peaks at $t = 180$ min (Figure 2-17). However, at $t = 300$ min, when LSD1 is disengaged from the chromatin and H3K4me2 accumulates (Figure 2-17), preliminary results showed that the addition of TCP further increases the level of H3K4me2 on *GREB1* EREs (Figure 2-34C). However, engagement of TRIM24 (Figure 2-35A) and ER α (Figure 2-35B) only slightly decreases. For future studies, the profile can be expanded by depleting LSD1 (using siRNA or shRNA construct) and perform ChIP assays over a detailed time course. These findings will provide a comprehensive analysis when the designing functional assays in future investigation of LSD1 inhibitors.

2.4.2. Does TRIM24 and LSD1 physically interact and when?

My results demonstrated that TRIM24 and LSD1 are co-recruited at specific time points, but at other time, LSD1 recruitment precedes TRIM24. Intriguingly, unpublished mass spectrometry data from our lab revealed a possible interaction between TRIM24 and LSD1 in several cell lines, suggesting

that these two proteins may physically interact with each other at a given time course. Preliminary data suggested that at $t = 0$ and $t = 180\text{min}$, endogenous TRIM24 and LSD1 are not immunoprecipitated together in the whole cell lysates (data not shown). However, further studies should address whether their interaction is present only at specific time course of estrogen. Another question is whether the interaction only happens on the chromatin. Re-ChIP assays at specific E_2 induction time points (tested in the kinetic ChIP experiments) will be an excellent approach to address this.

2.4.3. Role of H3T6 phosphorylation in regulating estrogen response?

My findings suggested that H3T6 phosphorylation possibly play a critical role in mediating estrogen response. One important observation is that H3T6ph shows dynamic and gene-specific changes at EREs at specific time points in MCF7 cells. Essentially, pulldown assays showed that H3T6 phosphorylation abolishes the interaction between TRIM24 and histone H3 peptide, while demethylation assays by others showed that H3T6ph inhibits LSD1-mediated demethylation of H3K4me2 [31]. These observations suggested that H3T6 phosphorylation is probably upstream of LSD1 and TRIM24 in regulating the chromatin for efficient and timely estrogen response. Constant with the findings by Metzger et al. in prostate cancer cells LNCaP [31], I observed phosphorylation of H3T6 at *GREB1* EREs and promoter at $t = 1\text{hr}$. However, both dephosphorylation of H3T6 is observed at *GREB1* and *PR* between 1hr to 2hr of hormone induction. Responses at these time points were not reported in previous

study by Metzger et al. Future studies should establish the kinetic profile of H3T6ph over a time course and compare it with H3K4me2 occupancy, as well as recruitments of LSD1, ER α and TRIM24. Using kinase inhibitors or PKC knockdown, detailed ChIP analyses should be performed to determine how phosphorylation of H3T6 affects H3K4me2 demethylation and recruitment of TRIM24.

2.5. DISCUSSIONS

2.5.1. Immediate E₂-induced changes of chromatin structure at enhancers

ER α is known to regulate gene expression patterns through facilitation of the transcription machinery as well as a plethora of co-regulators. Epigenetic regulation represents an essential mechanism that determines the accessibility of DNA through changes of the surrounding chromatin structure. In this thesis, I showed that estrogen stimulation immediately triggers an open form of chromatin, enriched with H3K23ac and H3K27ac on the ERE sites. These immediate changes on the chromatin is consistent with the previously termed “transcriptionally unproductive cycle” of ER α , marked by chromatin remodeler, HATs and HMTs [73].

In contrast to the previously reported cyclical pattern of total H3 methylation [73], in this study I have demonstrated a dynamic H3K4 methylation profile. Intriguingly, I consistently observed immediate estrogen-induced gain of H3K4me3 on several of the ERE sites examined, which contrasts with the

commonly accepted view that H3K4me3 is often associated with transcription start sites of actively transcribed genes [34,142,143] but not with enhancer regions [73,144]. However, other reports have also suggested H3K4me3 enrichment at enhancer regions [34,142,143,145,146]. My experimental results strongly suggest that monomethylation, dimethylation, and trimethylation of H3K4 are present at specific time points upon estrogen stimulation at estrogen-responsive enhancer regions. I also demonstrated that H3K4me3 loss is concurrent with H3K4me2 gain, which shortly precedes H3K4me1 enrichment (Figures 2-20, 2-22, and 2-24). Therefore, my results suggest that estrogen immediately induces H3K4me3 methylation, and then H3K4me3 is enzymatically demethylated to H3K4me1/2 at the ERE sites examined. However, it remains to be determined which H3K4 methyltransferase(s) mediate H3K4me3 methylation and whether other H3K4 demethylases are also involved.

2.5.2. Cyclical recruitment of LSD1 and concurrent changes in H3K4me

Here I demonstrated that LSD1 and TRIM24 co-regulate transcriptional activation of a subset of ER α target gene in a time-dependent manner. I also showed that LSD1 and TRIM24 are cyclically recruited to EREs, constantly with previous findings of other ER α co-regulators [73]. For the ERE sites examined here, LSD1 has a recruitment cycle of 90min and the first recruitment of LSD1 always coincides with ER α and TRIM24. LSD1 binding is negatively correlated with H3K4me2 level during each cycle. Importantly, LSD1 binding precedes TRIM24 at the time points studied here. When LSD1 is enzymatically inhibited by

TCP, H3K4me2 is re-methylated and TRIM24 binding is impaired, suggesting that demethylated chromatin mediated by LSD1 is essential for subsequent recruitment of TRIM24. My results established the mechanism of how LSD1 regulates TRIM24-mediated functions through H3K4me2 demethylation, and further confirmed our previous findings that TRIM24 specifically recognizes unmethylated-H3K4, and global binding of TRIM24 preferentially concentrates in genomic regions depleted of H3K4me2 [57].

2.5.3. TRIM24 binding not always concurrent with H3K4me2 demethylation

TRIM24 is recruited to the chromatin, along with ER α , as early as $t = 15$ min, during which H3K4me3 is at the highest. Previous isothermal titration calorimetry (ITC) analyses suggested that the presence of tri-methylated H3K4 completely abolished TRIM24 interaction with H3 [57]. Note, however, that TRIM24 PHD-Bromo can still bind to H3K4me3K23ac [57], suggesting that in certain cellular contexts, recognition of H3K23ac by TRIM24-Bromo can allow TRIM24 to retain its affinity to H3 even when H3K4 is methylated. Accordingly, I also observed H3K23ac enrichment at $t = 15$ min, when TRIM24 is initially recruited to EREs. These observations point to a more complex model of histone language, in which the dual epigenetic reader TRIM24 can determine which histone mark to recognize in a context-specific manner. Intriguingly, a previous study from my lab showed that TRIM24 PHD-Bromo also binds to H3K9me1/2/3 and H3K9ac [57]. How H3K9 methylation and acetylation changes through the time course examined here remains unknown. A related question is how TRIM24 distinguishes between methylated and acetylated H3K9, or between methylated

H3K4 and H3K9, which adds to the complexity of the histone code recognized by TRIM24.

2.5.4. Inhibition of LSD1 does not affect H3K4me3 or H3K9me2

In this thesis I demonstrated the addition of TCP to estrogen-induced cells result in re-methylation of H3K4me2, but no change in H3K4me1, H3K4me3, or H3K9me3 at several EREs examined here. These observations suggested that the demethylation of H3K4me2, and possibly H3K4me1, is inhibited in the presence of TCP, while this inhibitor is not specific for H3K4me3 or H3K9me2 demethylation. This observation is constantly with previous findings that overexpression of LSD1 in MCF7 cells only lead to H3K4me2 decrease but no change in H3K9me2. Taken together, this evidence strongly suggested that in MCF7 cells, neither H3K4me3 nor H3K9me2 is a substrate for LSD1, which specifically targets H3K4me1/2 [4,16].

2.5.5. Establishment of the role of H3T6ph in ER α -regulated transcription

This work also identified a previously unknown inhibitory histone mark for TRIM24-PHD, namely, phosphorylated H3T6. Interestingly, I found that this histone mark also interferes the H3K4 recognition by RBP2-PHD, a histone demethylase involved in estrogen response. Metzger et al. also showed that H3T6ph inhibits demethylation of H3K4me1/2 by LSD1 and H3K4me2/3 by JARID1B [31]. I also showed that inhibition of H3T6 kinase up-regulated ER α -regulated gene activation in a subset of target genes. Collectively, H3T6

phosphorylation may influence a number of readers and histone demethylases to regulation transcription.

CHAPTER 3: **BIOLOGICAL SIGNIFICANCE OF TRIM24- AND LSD1-MEDIATED ER-ALPHA CO-ACTIVATION IN BREAST CANCER CELLS**

(Part of this chapter is published: *Wen-Wei Tsai, *Zhanxin Wang, Teresa T Yiu, et. al and Barton MC. 2010. Nature 468, 927–932. *Equal contribution)

3.1. INTRODUCTION

3.1.1. Epigenetics and cancers

Both genetic mutations and epigenetic misregulation contribute to tumor initiation and progression [147]. Recently, epigenetic regulation represents a promising new area for translational research due to its reversible nature. Briefly, epigenetic factors can modulate the disease states by 1) genetic mutation or aberrant expression, and/or 2) altering the gene expression profiles in cooperation with upstream cellular and environmental signals [8,148]. In order to further our understanding, the tissue-specific cancer epigenomes are being established by compiling the expression of dysregulated epigenetic regulator proteins, as well as altered global and local histone modifications [149,150]. The development of small molecule inhibitors also aims to alter the disease states (such as cancer) through manipulating the underlying epigenetic events [8,151,152]. For example, a number of HDAC (histone deacetylase) inhibitors are already in the clinic to treat cancers and other diseases [8]. On the other hand, a growing list of literatures also reported the possibility of drugging epigenetic factors, which include lysine demethylases, bromodomain-containing reader

proteins, methyl-lysine readers, and others [8]. Essentially, epigenetic inhibitors can possibly target the “undruggable” oncoproteins by altering the chromatin interactions. For example, BRD4 (bromodomain-containing protein 4) reader protein specifically recognizes acetylated lysines and modulates transcription of target genes of *MYC* (myelocytomatosis viral oncogene homolog, oncogenic transcription factor) through its chromatin interaction [153,154]. Importantly, inhibition of BRD4 is able to reduce MYC binding to its target loci as well as down-regulation of *MYC* gene transcription [155,156]. Taken together, elucidation of more in-depth knowledge of epigenetic regulatory mechanisms may contribute to the development of effective cancer therapeutics.

3.1.2. Implication of histone methylation in oncogenesis

Epigenetic factors responsible to “write”, “read”, or erase” the histone marks in response to cellular and environmental signals are important for normal cellular processes. Therefore, aberration of these regulatory proteins is often associated with the development of various cancers (summarized in Figure 3-1) [157]. For example, *MLL* (*mixed-lineage leukemia*) gene encodes H3K4-specific methyltransferases [158,159] and is frequently rearranged in acute myeloid (AML) or lymphoid leukemias [160,161]. The most common *MLL* rearrangement form, *MLL-PTD* [161,162], retains the C-terminal H3K4me- catalytic domain [160] and in the mouse it has been shown to cause aberrant up-regulation of H3K4 methylation at the *HOXA* loci [163,164]. Apart from epigenetic “writers”, “readers” such as PHD-finger-containing *JARID1A*, also fuses with *NUP98* (*nucleoporin 98*)

in leukemias [165]. Intriguingly, mutation of single amino acid in JARID1A-PHD responsible for H3K4me_{2/3} recognition is critical for oncogenic potential in leukemias [166]. Moreover, demethylases such as LSD1 (to be further discussed below) and Jumonji-family proteins have also been implicated in cancers. For example, JARID1B is overexpressed in both breast and prostate cancer [167,168]. JARID1B plays critical roles in facilitating G1/S [167] and mitotic spindle checkpoints [169]. JARID1B also represses metallothionein genes and tumor suppressor genes such as *BRCA1* and *caelin1* by demethylating H3K4me_{2/3} [167,169]. Taken together, epigenetic regulators have functional significance in oncogenesis and are worth for further investigation.

Figure 3-1. H3K4 methylation is tightly associated with cancer development. Reprinted by permission from Macmillan Publishers Ltd: *Nat Rev Cancer* **10** (2010) 457-469, copyright (2010) [157].

Category	Gene ID	Deregulation in human cancer
<i>H3K4me</i>		
Writer	<i>MLL</i>	Rearrangement of <i>MLL</i> commonly found in myeloid and lymphoblastic leukaemia
	<i>MLL2</i>	Somatic mutation of <i>MLL2</i> found in renal cell carcinoma
Reader	<i>ING1, ING2, ING3, ING4 and ING5</i>	Loss-of-function mutations of putative tumour suppressor genes <i>ING1–5</i> , including somatic mutation, allelic loss, downregulation of expression and aberrant cytoplasmic sequestration, associate with various solid tumors. A subset of <i>ING2</i> somatic mutations interferes with binding to H3K4me3 specifically
	<i>PHF23</i>	Owing to chromosomal translocation, the H3K4me3-binding PHD finger of <i>PHF23</i> is fused to <i>NUP98</i> in myeloid leukaemia. It has been shown that H3K4me3 binding is crucial for leukaemogenesis induced by <i>NUP98–PHF23</i> oncoproteins
	<i>PYGO2</i>	<i>PYGO2</i> , a component of the β -catenin signalling pathway, is crucial for self-renewal of mammary progenitor cells. <i>Pygo</i> levels are high in malignant breast tumours and low in non-malignant breast cells
Eraser	<i>LSD1</i>	<i>LSD1</i> , a component of NuRD–Mi-2 repressive complexes, demethylates H3K4me2/1 and suppresses the invasiveness and metastasis of breast cancer cells. <i>LSD1</i> is downregulated in breast carcinoma tissues
	<i>JARID1A</i>	Similar to <i>PHF23</i> , the PHD finger of <i>JARID1A</i> is fused to <i>NUP98</i> in a subset of myeloid leukaemia, forming an oncoprotein <i>NUP98–JARID1A</i> . H3K4me3 binding by the <i>JARID1A</i> PHD finger is crucial for leukaemogenesis
	<i>JARID1B</i>	Overexpression of <i>JARID1B</i> was found in advanced breast and prostate cancers
	<i>JARID1C</i>	Recurrent inactivating mutation of <i>JARID1C</i> was detected in around 3% of renal carcinoma
	<i>JHDM1B*</i>	Upregulation of <i>JHDM1B</i> or a related gene <i>JHDM1A</i> is commonly found in retrovirus-induced rat T cell lymphomas

3.1.3. Aberrant expression of TRIM24 is correlated with tumorigenesis

Previous studies have suggested a functional role of TRIM24 in cancers. For example, TRIM24 has been shown to be an oncogenic fusion partner via chromosomal translocation in acute promyelocytic leukemia [169], papillary thyroid carcinomas [170], myeloproliferative syndrome (EMS) [60,171] and liver cancer [60,172]. Particularly, TRIM24 PHD-Bromo domain is fused to the tyrosine kinase domain in EMS. In this fuse protein, TRIM24 PHD-Bromo facilitates the dimerization and constitutive activation of FGFR1, resulting in cellular transformation [171]. However, it is still unclear whether TRIM24-FGFR1 confers tumor formation.

In addition, our lab has reported that TRIM24 is a negative regulator of p53 and knockdown of TRIM24 by small interfering RNAs (siRNAs) induces apoptosis, which can be rescued by the depletion of p53. Indeed, TRIM24 depletion in human breast cancers causes p53-dependent apoptosis [173]. In addition, TRIM24 is also a co-activator of ER α [57], indicating that aberrant expression of TRIM24 may promote tumorigenesis through disruption in p53-mediated tumor suppression and over-activation of ER α -regulated cellular processes.

Moreover, our lab published a cohort study of breast cancer patients and revealed that high levels of TRIM24 protein are tightly associated with poor survival [57], which has been further confirmed by another recent publication [174], which suggested that aberrant over-expression of TRIM24 can be used as a prognostic factor in breast tumorigenesis. In fact, TRIM24 is highly expressed

in several breast cancer cell lines, as revealed by Western blot analysis (performed by Dr. Khandan Keyomarsi's Laboratory, data not shown). Taken together, these observations raised the question of whether TRIM24 contributes to the early stages of tumorigenesis in breast cancer.

3.1.4. Possible roles of TRIM24 in breast cancer transformation and cell cycle regulation

Unpublished data from our laboratory revealed that TRIM24 protein expression progressively increases as human mammary epithelial cells (HMECs) transform from nonmalignant to hyperplastic, and then to invasive, metastatic phenotype (data not shown), suggesting that TRIM24 may function as a pivotal driver of mammary tumorigenesis. Interestingly, studies compiled in Oncomine Database (URL: <http://www.oncomine.org>) revealed that high levels of TRIM24 RNA levels are even more prominent in high-grade ER α -positive breast carcinomas, suggesting that TRIM24 may also promote mammary tumorigenesis partially through ER α -regulated functions.

In addition, TRIM24 may also be involved in cell cycle regulation. I obtained cell cycle-synchronized RNA lysates from Dr. Khandan Keyomarsi's Laboratory and performed qPCR analysis on TRIM24 expression. I found that TRIM24 expression (Figure 3-3) and its binding to ER α target genes *GREB1* and *pS2* (Figure 3-4) are highly enriched during G2/M phase. Moreover, bioinformatics analysis performed by Kadir Atdemir in our lab also suggested that TRIM24 binds to approximate 300 genes in the category of cell cycle (Figure 3-

2). Preliminary data by our group also suggest that TRIM24 plays a critical role in G2/M transition in cultured breast cancer cells (data not shown), implying that TRIM24 may tightly control cycle cell progression.

3.1.5. Roles of LSD1 in tumorigenesis

LSD1 is over-expressed in various human cancers, including breast, prostate, colorectal, gastric, lung, bladder cancer, neuroblastoma, chondrosarcoma, Ewing's sarcoma, osteosarcoma, rhabdomyosarcoma and others [31,175,176,177,178,179,180,181]. Many reports have supported the role of LSD1 in driving cell proliferation due to its ability to demethylate histones and non-histone proteins. One example is the tumor suppressor p53, which interacts with LSD1. LSD1 demethylates p53, represses p53-mediated transcription and inhibits apoptosis [177]. LSD1 also physically interacts with and demethylate MYPT1, a known RB regulator [182]. LSD1-mediated demethylation of MYPT targets MPT1 for proteosomal degradation, increases phosphorylated (activated) RB1 and E2F activity in cancer cells [182]. On the other hand, LSD1 localizes to centrosomes and spindle poles during metaphase and telophase of the cell cycle [183]. LSD1 also positively regulates BUBR1 (Bub-1 related kinase) and MAD2 (mitotic arrest deficient 2-like protein) expression [183]. Take together, LSD1 play an essential role in chromosomal segregation during mitosis possibly through transcription regulation of BUBR1 and MAD2 [183]. Moreover, LSD1 plays critical roles in EMT (epithelial-mesenchymal transition) by upregulating E-cadherin and EMT-driven cell migration [184,185]. Notably, oncoprotein MYC

binds and recruits LSD1 to the chromatin, while knockdown of LSD1 inhibits transcription of MYC target genes and leads to H3K4me2 demethylation on these gene loci [186]. In a mouse model mimicking human AML, LSD1 is essential for blocking differentiation and inducing proliferation of immature blast cells [187]. LSD1 co-localizes with genes bound by *MLL* fusion MLL-AF9 and correlates with decreased H3K4me2 at these gene loci. Notably, pharmacologic inhibition of LSD1 enzymatic activity phenocopies LSD1 knockdown *in vitro* and *in vivo*. These observations suggested that LSD1 may be selectively targeted in MLL leukemia and other cancers.

Figure 3-2. Global TRIM24 target genes upon E₂ treatment. Genes within 10kb of TRIM24 binding were assessed by Kadir Atdemir using Ingenuity Pathway Analysis (IPA, <http://ingenuity.com>) and the following categories were enriched: transcription, metabolic process, biosynthetic process, cell cycle, kinase activity, signal transduction, development, and chromosome organization.

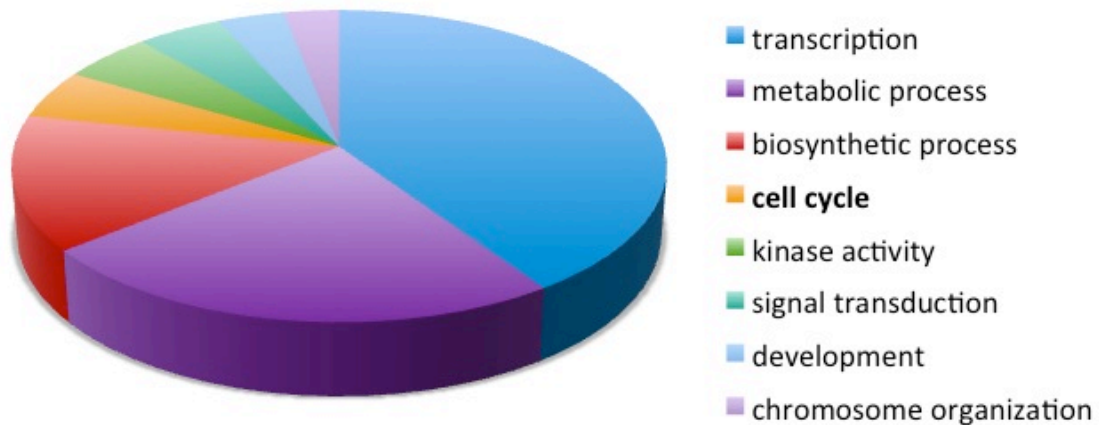


Figure 3-3. TRIM24 expression is highly enriched in E₂-treated cells during G₂/M transition. Cell cycle-synchronized RNA lysates obtained from Dr. Keyomarsi's laboratory were used to make cDNA and perform qPCR to assess TRIM24 expression through cell cycle. The corresponding cell cycle phases were marked under the time after Levostatin release. RNA levels are normalized to *GAPDH*; vehicle-treated MCF7 is set as one. Average numbers from triplicates. Error bars = SEM.

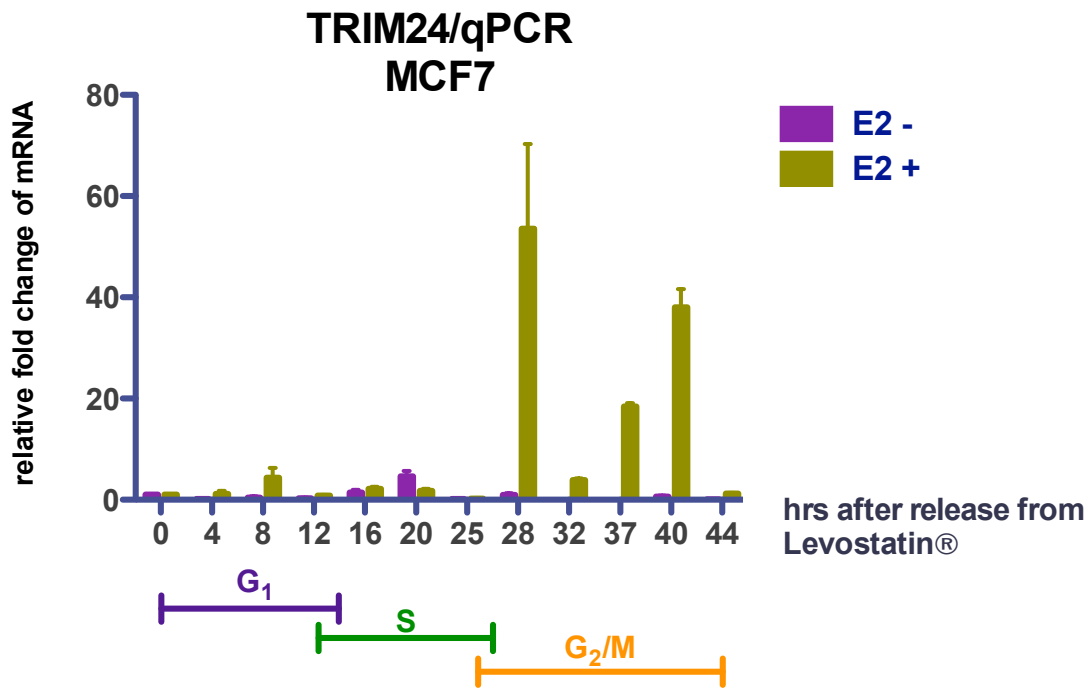


Figure 3-4A. TRIM24 binding to ER α target genes during cell cycle. Synchronized cell lysates obtained from Dr. Keyomarsi's laboratory were used to perform ChIP experiments. Binding of TRIM24 on (A) *GREB1* distal ERE and (B) *pS2* ERE were quantified by qPCR analyses. The corresponding cell cycle phases were marked under the time after Levostatin release. Average numbers from duplicates. Error bars = SEM.

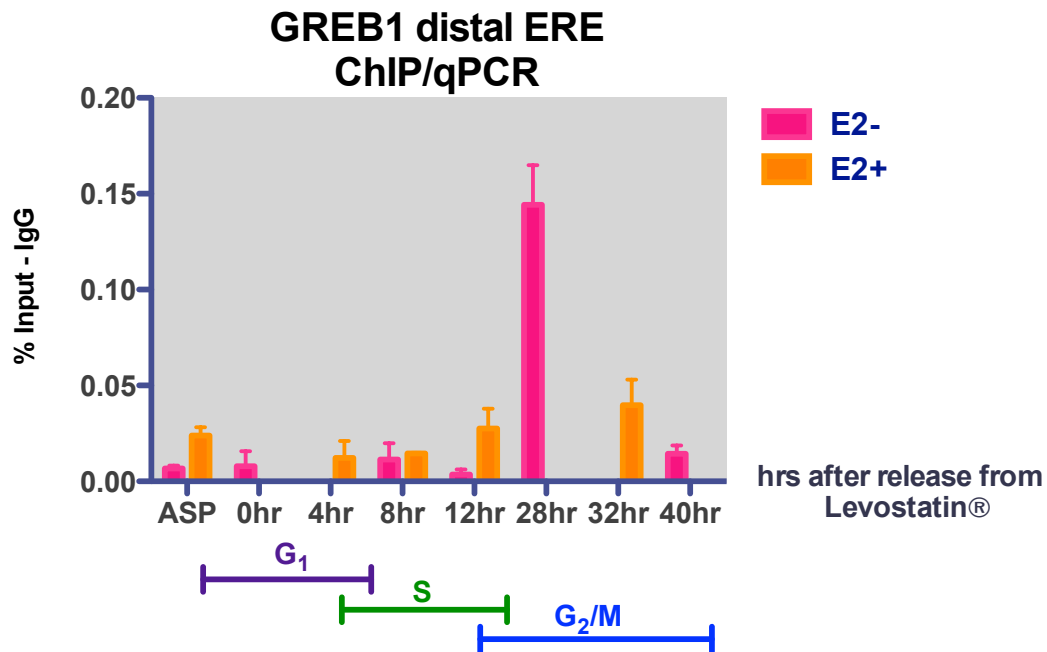
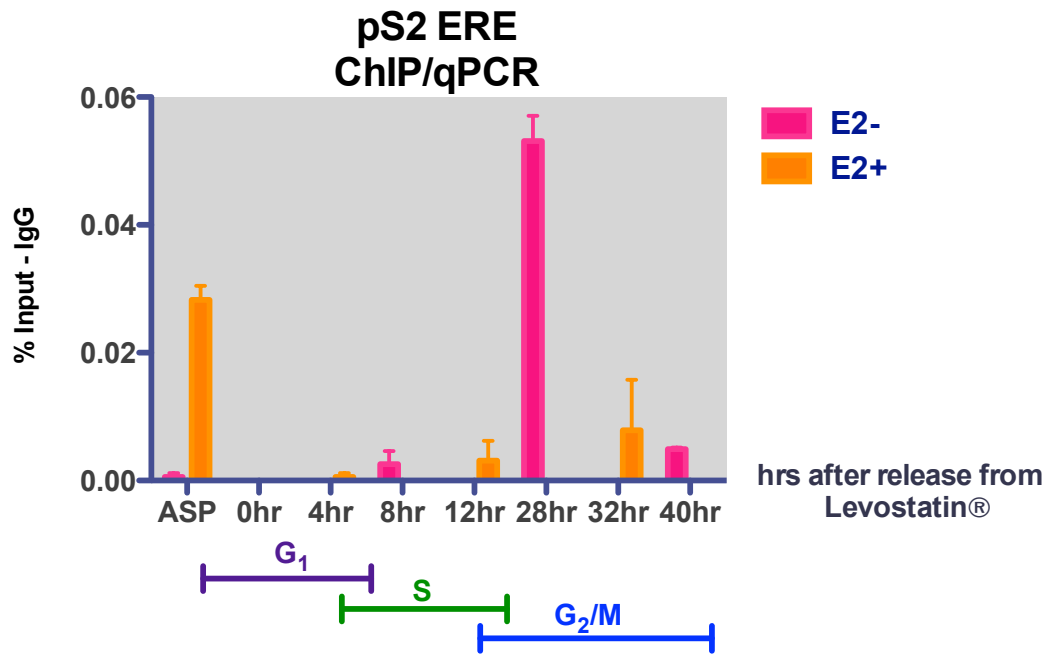


Figure 3-4B. TRIM24 binding to ER α target genes during cell cycle. Synchronized cell lysates obtained from Dr. Keyomarsi's laboratory were used to perform ChIP experiments. Binding of TRIM24 on (A) *GREB1* distal ERE and (B) *pS2* ERE were quantified by qPCR analyses. The corresponding cell cycle phases were marked under the time after Levostatin release. Average numbers from duplicates. Error bars = SEM.



3.1.6. Hypothesis: Function of TRIM24 for the survival and proliferation of breast cancer cells is dependent on the enzymatic activity of LSD1

Several lines of published and preliminary evidence imply that TRIM24 may regulate mammary tumorigenesis by controlling ER α -mediated transcriptional activation of cancer-promoting genes and regulating cell cycle progression. Similarly, LSD1 is also overexpressed in breast cancer and drives cellular proliferation through several mechanisms. Chapter 2 established the interplay between LSD1 and TRIM24 in chromatin regulation, therefore, I **hypothesize** that *function of TRIM24 for the survival and proliferation of breast cancer cells is dependent on the enzymatic activity of LSD1*. To test the hypothesis, I have formulated the following specific aims and tested them using clonogenic assays in cultured cells:

- Confirm the growth inhibitory effects of 4-hydroxy-tamoxifen (4-OHT) in wildtype cells (MCF7 parental cells)
- Determine whether TRIM24 depletion leads to reduced survival and proliferation, and whether 4-OHT (Tamoxifen) exerts additive inhibition
- Determine whether inhibition of LSD1 by TCP exerts a dose-dependent reduction in survival and proliferation in MCF7 cells
- Determine whether TRIM24 depletion has additive effects to Tamoxifen- and TCP-mediated reduction in colony formation

In summary, the results presented in this chapter suggested that 4-OHT or TRIM24 depletion alone effectively reduced the formation of colony, indicating that the ability of MCF7 cells to survive and proliferate during the indicated time course of culture is impaired. Moreover, combination of TRIM24 depletion and 4-OHT and/or TCP treatment results in highly additive effects in the survival and proliferation of MCF7 cells.

3.2. MATERIALS AND METHODS

3.2.1. Clonogenic assay

Clonogenic assays performed in parental wildtype MCF7 cells where 500 cells are seeded in DMEM medium supplemented with 10% FBS and 1% Pen/Strep solution in 60mm² tissue culture dishes for 14 days, in the presence of the indicated treatment.

For Tetracyclin-inducible shTRIM24 and shControl MCF cells, 1000 cells are seeded. In these cells, in addition to the indicated treatment, 500ng of Tetracyclin (Tet) are added for shRNA induction. Medium is replaced every three days with fresh Tetracycline (Tet), estrogen (E₂), Tranylcypramine (TCP), and/or 4-hydroxy-Tamoxifen (4-OHT). After 14 days in culture, colonies are fixed and stained with 1X crystal violet dissolved in ethanol. Colonies of ≥ 50 cells are counted. Experiments performed in at least three biological replicates.

3.2.2. Statistical analysis

GraphPad Prism software 5.0 is utilized to calculate the averaged value and error bars (based on standard error of mean, SEM) of independent experiments in biological triplicates. The two-tailed paired student *t* test p-value is used to calculate the statistical significant when comparing the differences between two indicated groups. *P*-values of less than 0.05 are considered statistically significant.

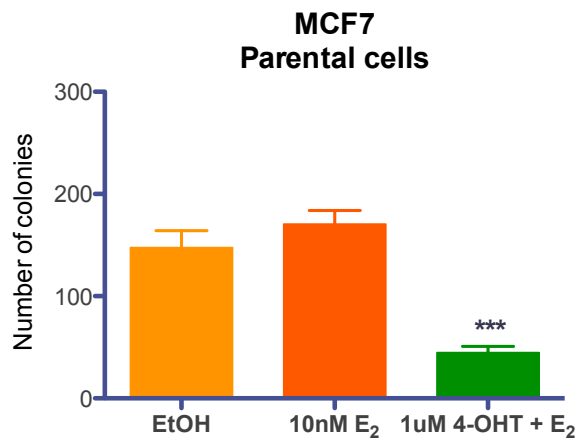
3.3. RESULTS

3.3.1. Activated ER α is required for the survival and proliferation of MCF7

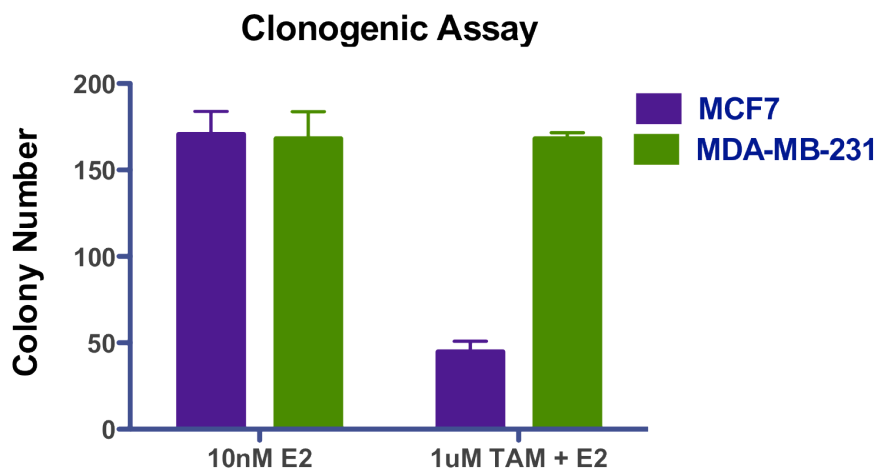
In order to determine whether estrogen signaling contributes to the survival and proliferation of breast cancer cells, I performed clonogenic assays and determined the effect of ER α -mediated transcription on the survival and proliferation of MCF7 breast cancer cells. Because MCF7 cells fail to continue growing for 14 days in phenol red-free medium supplemented with charcoal-stripped serum (data not shown), these cells are cultured in medium containing phenol-red, which is estrogenic. Possibly because of the abundance of estrogen in the medium, the addition of 17 β -estradiol (10nM E₂, Figure 3-5A) does not show significant increase in colony formation. Therefore, I grow the cells in the presence of 17 β -estradiol alone (E₂) or in addition to 4-hydroxy-tamoxifen (1 μ M 4-OHT + E₂, Figure 3-5A), an antagonist of ER α [188]. The number of colonies formed from these treated cells after 14 days are compared to vehicle control (EtOH, Figure 3-5A). Colonies formed from 4-OHT treatment (Figure 3-5A) leads to significantly reduction in the number after 14 days, when compared to E₂-treated cells (Figure 3-5A, p-value<0.0001). In contrast, tamoxifen treatment does not affect colony formation in MDA-MB-231 cells (Figure 3-5B), which lacks endogenous ER α expression. These observations confirmed the inhibitory effect of tamoxifen in MCF7 cells and set up the growth condition for the following clonogenic experiments.

Figure 3-5: 4-hydroxy-tamoxifen (4-OHT)-induced reduction of colony formation in MCF7 but not MDA-MB-231 cells. (A) Parental MCF7 (wildtype) cells or (B) MDA-MB-231 cells were allowed to grow for 14 days in the presence of the indicated treatment: vehicle control (ethanol, EtOH), 10nM of 17 β -estradiol (10nM E₂), or 1 μ M 4-OHT plus E₂. Colonies after 14 days were stained with crystal violet. Average numbers from six independent experiments. Error bars = SEM (Student *t* test, ***p-value<0.001, compared to EtOH control).

A



B



3.3.2. Depletion of TRIM24 affects survival and proliferation of MCF7

The addition of tamoxifen not only down-regulates estrogen-induced activation of ER α target genes *GREB1* and *PR* (Figure 3-6). In TRIM24-depleted cells (Figure 3-6), the inhibitory effect by tamoxifen is additive to shTRIM24-mediated reduction on target gene induction. To test whether TRIM24 expression is critical for cell survival and proliferation, MCF7 cells engineered with Tetracycline (Tet)-inducible shRNA targeting TRIM24 (Tet-shTRIM24) or shRNA control (Tet-shControl) are utilized to perform clonogenic assays (representative images presented in Figure 3-7). These cells were generated by Chunlei Jin in our lab. In the absence of Tet induction, shRNA is not activated and there is no difference in colonies formed in shControl and shTRIM24 (10nM E₂, Figure 3-8A). Addition of Also, 4-OHT treatment leads to significant decline in number of colonies in both shControl and shTRIM24 cells (1 μ M 4-OHT + E₂, Figure 3-8A). These observations suggest that in the absence of Tet induction, both of these cell lines behave similarly to wild-type MCF7 parental cells (Fig. 3-5). Most importantly, the Tet-inducible construct is not leaky and does not cause any differences in shControl and shTRIM24 before Tet-induction.

When shRNA construct is activated by Tet treatment, depletion of TRIM24 significantly triggers the inhibition of cell proliferation and survival, when compared to Tet-shControl (Figure 3-8B, p-value<0.05), suggesting that depletion of TRIM24 leads to a significant reduction in the survival and proliferation of MCF7 cells. Notably, addition of ER α inhibitor 4-OHT reduced the numbers of colonies in both shControl and shTRIM24 MCF7 cells, to nearly

comparable levels (Figure 3-8B, p-value<0.001). Taken together, reduced survival and proliferation mediated by loss of TRIM24 may be compensated by ER α inhibition.

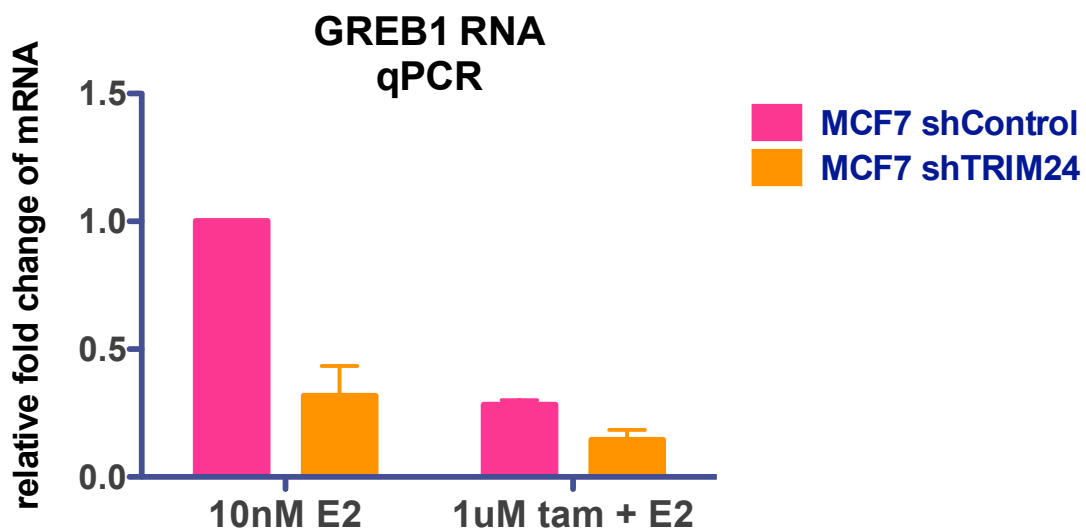
3.3.3. Inhibition of LSD1 by TCP affects survival and proliferation of MCF7

In the absence of Tet-induction, shControl and shTRIM24 cells respond similarly to increasing dosage of tranylcypromine (TCP). Significant reduction in colonies is observed in the presence of 30 μ M or 100 μ M TCP in both shControl and shTRIM24 cells (Figure 3-8A, p value<0.01). This observation again confirms that without Tet treatment, both cell lines respond similarly to TCP treatment.

When shRNA construct is activated by the addition of Tet, we saw limited effect of TCP on the formation of colonies by shControl MCF7 cells, which responded significantly only to high doses of TCP (100 μ M). In contrast, in combination with loss of TRIM24 in shTRIM24 MCF7 cells, colony formation was significantly affected by inhibition of LSD1 enzymatic activity by 10 μ M TCP (Figure 3-8B, p value<0.001). These observations suggest that treatment with TCP further reduces the survival and proliferation in MCF7 cells depleted of TRIM24.

Figure 3-6. Depletion of TRIM24 has additive effect in Tamoxifen-inhibited ER α target gene activation. Gene expression of estrogen-induced (A) GREB1 and (B) PR is inhibited by the addition of ER α inhibitor, 4-hydroxy-Tamoxifen, and the gene induction is progressively down-regulated in TRIM24 depleted MCF7 cells (shTRIM24). RNA levels are normalized to *GAPDH*; E₂-only MCF7 is set as one. Averaged results from triplicates. Error bars = SEM.

A



B

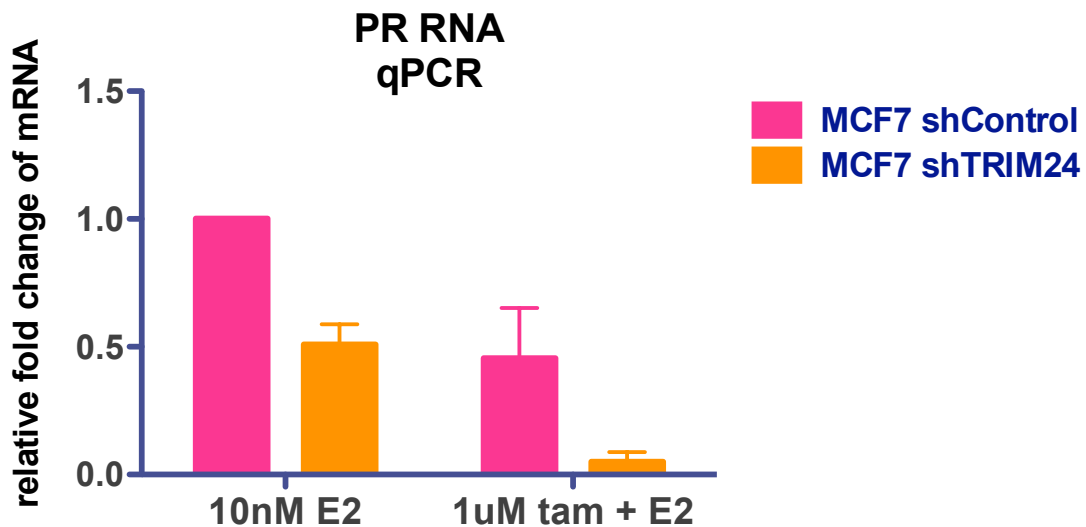


Figure 3-7. Representative images of Tet-treated colonies in the presence of the indicated treatment. Tranylpramine (TCP): 0 μ M, 2 μ M, 10 μ M, 30 μ M, and 100 μ M in shControl or shTRIM24 cells treated with or without 4-hydroxy-Tamxifen (4-OHT)

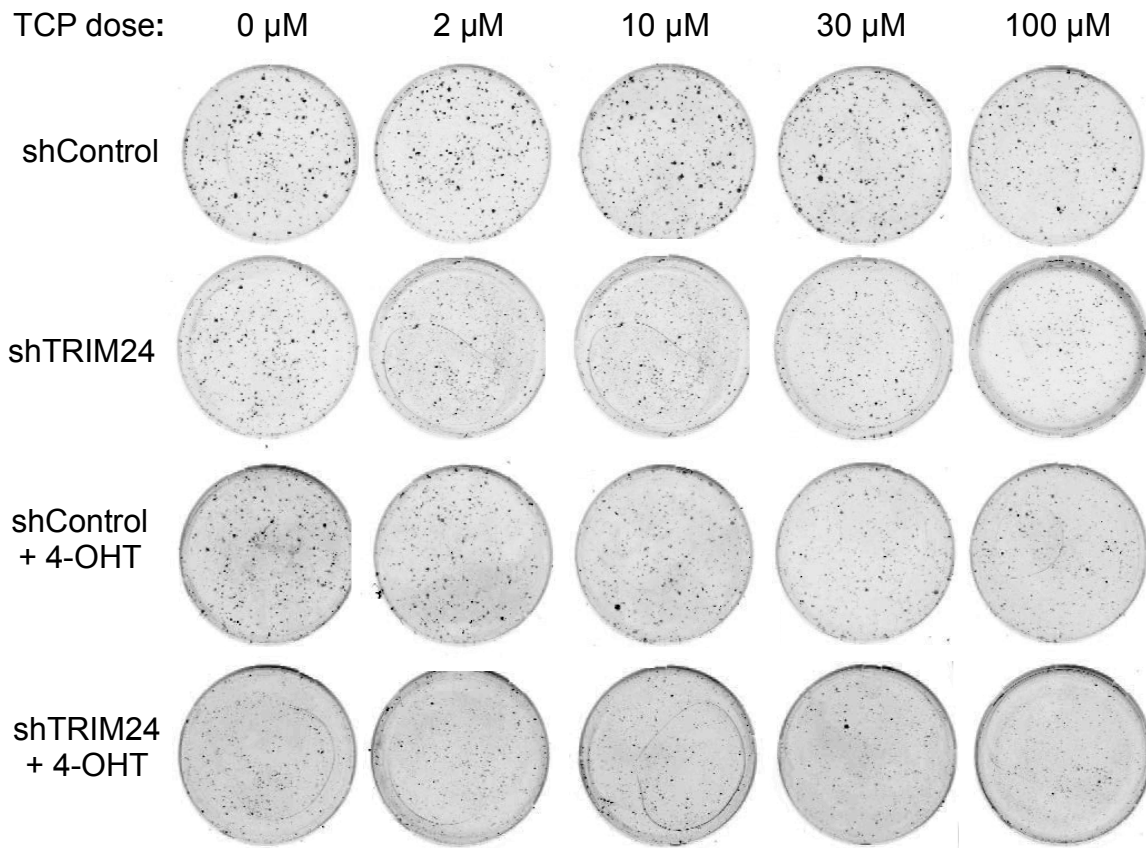


Figure 3-8A: Depletion of TRIM24 expression leads inhibit the survival of MCF7 breast cancer cells, and is highly additive to 4-hydroxy-tamoxifen (4-OHT)-induced survival inhibition. MCF7 shControl and shTRIM24 were used to perform clonogenic assays in the presence of 10nM E₂ or 1μM 4-OHT + E₂, (A) without or (B) with Tetracyclin (Tet). Average from triplicates. Error bars = SEM (Student *t* test: *p-value<0.05; **p-value<0.01; ***p-value<0.001).

A

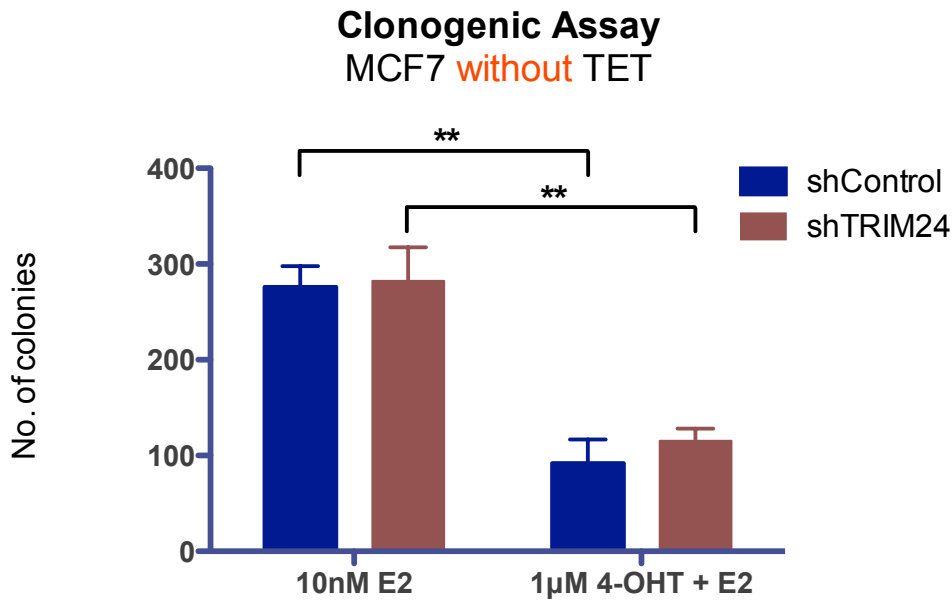
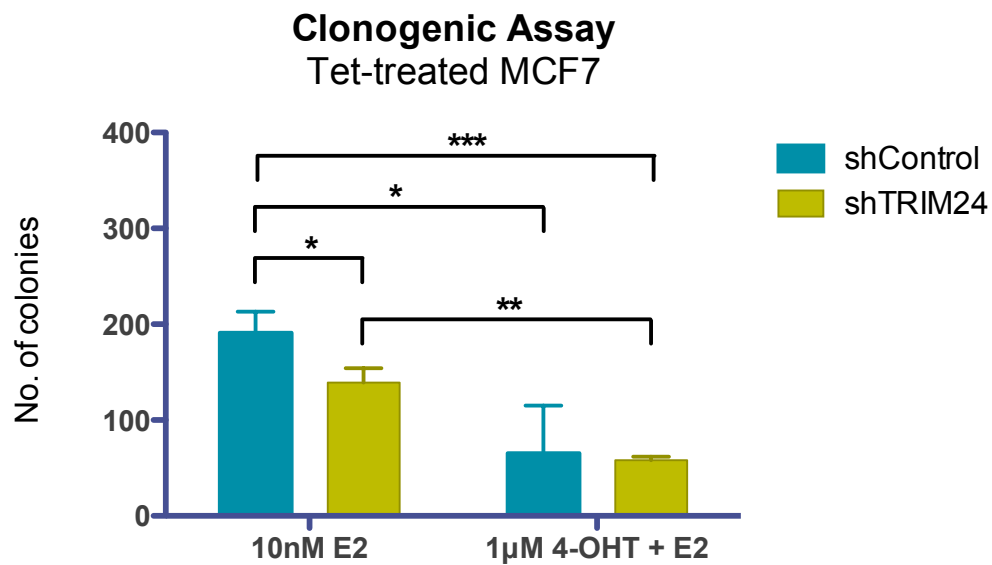


Figure 3-8B: Depletion of TRIM24 expression leads inhibit the survival of MCF7 breast cancer cells, and is highly additive to 4-hydroxy-tamoxifen (4-OHT)-induced survival inhibition. MCF7 shControl and shTRIM24 were used to perform clonogenic assays in the presence of 10nM E₂ or 1μM 4-OHT + E₂, (A) without or (B) with Tetracyclin (Tet). Average from triplicates. Error bars = SEM (Student *t* test: *p-value<0.05; **p-value<0.01; ***p-value<0.001).

B



3.3.4. Knockdown of TRIM24 is highly additive to TCP- and 4-OHT-induced inhibition in colony formation

In the absence of Tet induction, treatment with 4-OHT lowered the baseline of colony formation by shControl MCF7 cells, regardless of TCP dosage (Figure 3-10A). On the other hand, addition of 4-OHT in Tet-induced shControl cells does not affect their response to TCP (Figure 3-10B). Similarly, treatment with 4-OHT lowers the baseline clonogenicity in shTRIM24 MCF7 cells, in which I saw even further loss in clonogenicity by 10 μ M TCP. Notably, in combination with 10 μ M TCP and 4-OHT, loss of TRIM24 in shTRIM24 MCF7 leads to further reduction in colony number. Taken together, LSD1 and TRIM24 function additively to regulate survival and proliferation of MCF7 cells, but the underlying mechanism is not solely dependent on ER α activation.

Figure 3-9A: Decreased TRIM24 expression sensitizes MCF7 cells to lower dosage of TCP-mediated reduction in colonies. Response of MCF7 shControl and shTRIM24 cells (before Tet-treatment) to increasing dosage of Tranylcypromine (TCP) in the (A) absence or (B) presence of TET. Average numbers of colonies formed after 14 days from triplicate experiments. Error bars = SEM (Student *t* test: *p-value<0.05; **p-value<0.01).

A

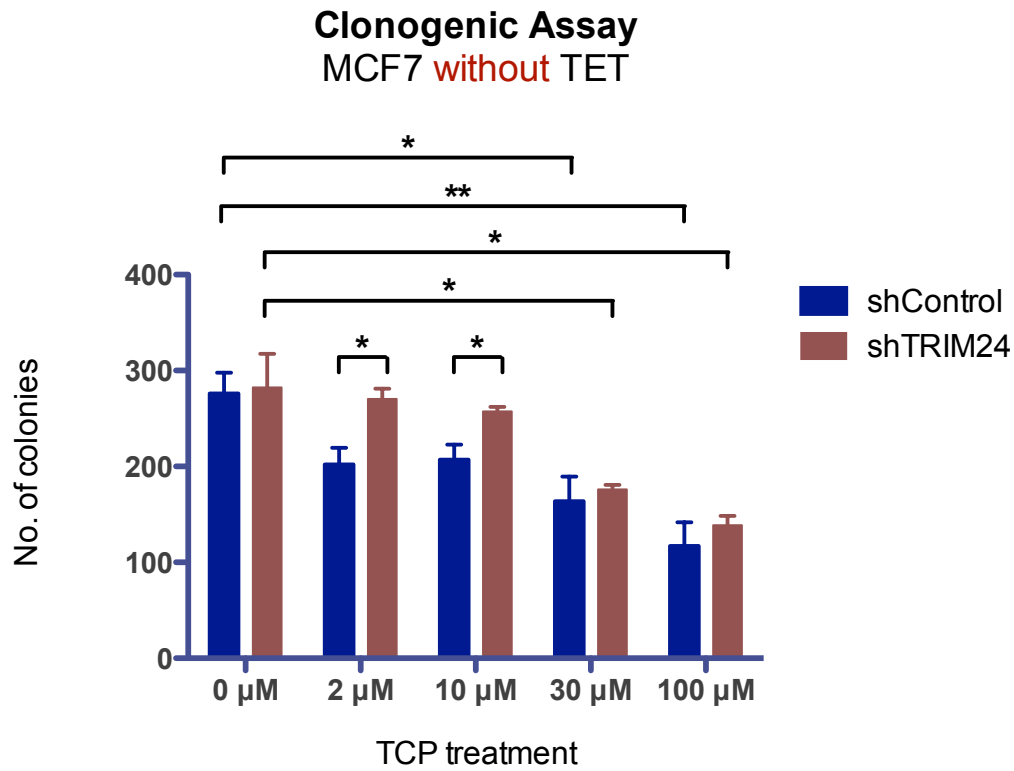


Figure 3-9B: Decreased TRIM24 expression sensitizes MCF7 cells to lower dosage of TCP-mediated reduction in colonies. Response of Tet-induced MCF7 shControl and shTRIM24 cells to increasing dosage of Tranylcyproline (TCP) in the (A) absence or (B) presence of TET. Average numbers of colonies formed after 14 days from triplicate experiments. Error bars = SEM (Student *t* test: *p-value<0.05; **p-value<0.01; ***p-value<0.001).

B

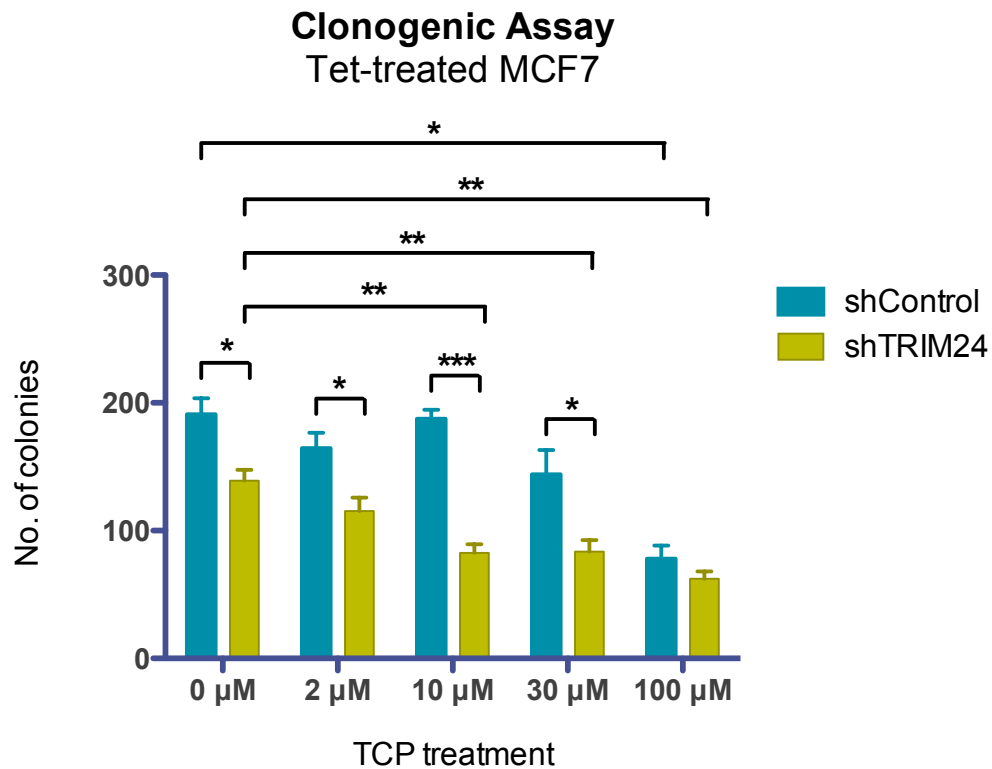


Figure 3-10A: Knockdown of TRIM24 is highly additive to TCP- and 4-OHT-induced inhibition in colony formation. Response of MCF7 shControl and shTRIM24 cells (before Tet-treatment) to increasing dosage of Tranylcyproline (TCP) with or without 4-OHT in the (A) absence or (B) presence of TET. Average numbers of colonies formed after 14 days from triplicate experiments. Error bars = SEM (Student *t* test: *p-value<0.05; **p-value<0.01).

A

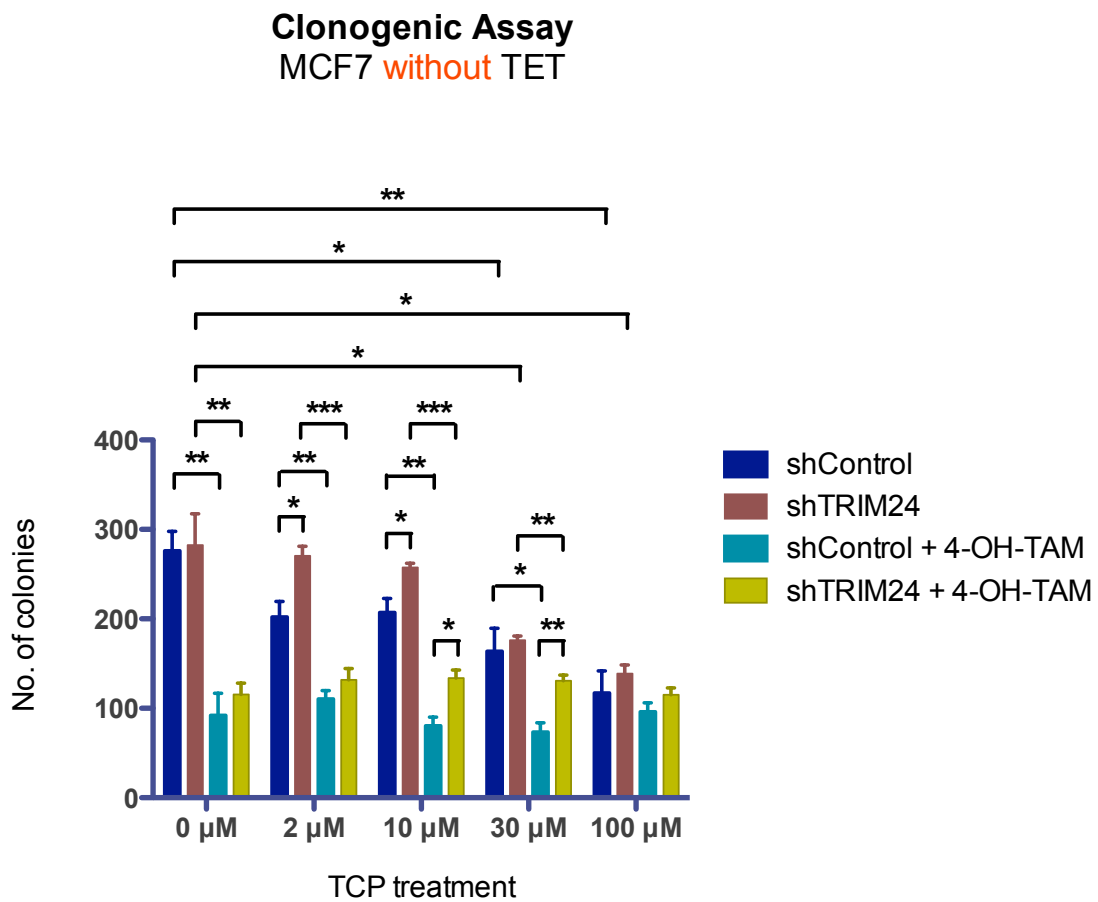
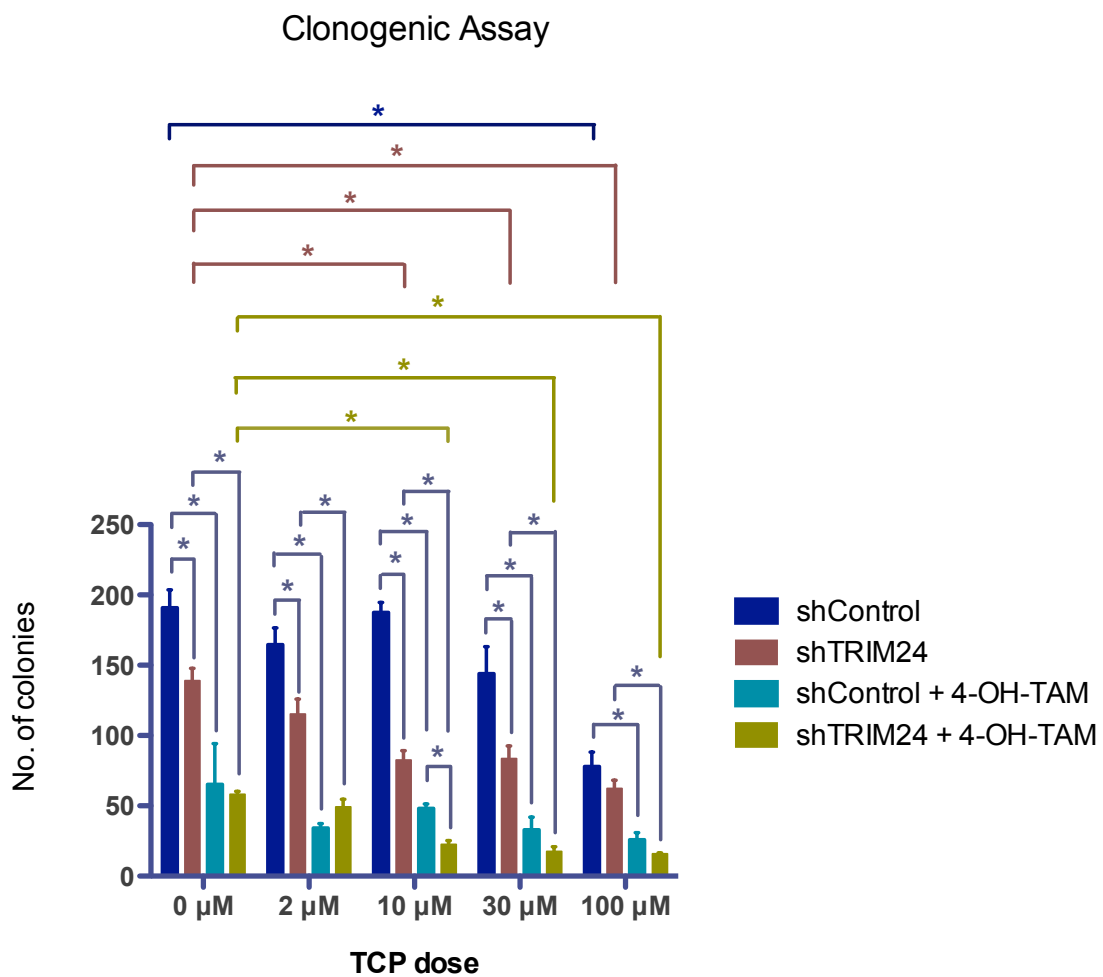


Figure 3-10B: Knockdown of TRIM24 is highly additive to TCP- and 4-OHT-induced inhibition in colony formation. Response of Tet-induced MCF7 shControl and shTRIM24 cells to increasing dosage of Tranylcypromine (TCP), with or without 4-OHT in the (A) absence or (B) presence of TET. Average numbers of colonies formed after 14 days from triplicate experiments. Error bars = SEM (Student *t* test: *p-value<0.05; **p-value<0.01; ***p-value<0.001).

B



3.4. DISCUSSIONS AND FUTURE DIRECTIONS

3.4.1. TRIM24 affects breast cancer cell survival and proliferation

In this thesis I demonstrated that TRIM24 expression is enriched and strongly binds to ER α target genes during G2/M phase of the cell cycle. I have also shown that depletion of TRIM24 reduces the survival and proliferation of MCF7 cells, as revealed by clonogenic assays. TRIM24 depletion also leads to additive effect of 4-OHT. Consistently, breast cancer patients with high level of TRIM24 are associated with poor prognosis and reduced survival [57,174], suggesting that TRIM24 plays essential roles in breast tumorigenesis.

3.4.2 Correlation of TCP effectiveness and TRIM24 expression?

I demonstrated in Chapter 2 how histone recognition by TRIM24 is affected by LSD1-mediated histone demethylation. Here, I demonstrated that MCF7 cells respond to TCP-induced inhibition of survival and proliferation in a dose-dependent manner when TRIM24 is depleted. Thus TRIM24 co-regulates specific genes that are critical for breast cancer-derived cells to respond to estrogen, and effects of LSD1 depletion or inhibition on estrogen response are primary mediated through TRIM24. Moreover, LSD1 and TRIM24 also interact with genes associated with breast cancer in an estrogen-independent manner [57,174,179], suggesting their involvement in estrogen-independent regulation of genes by mechanisms that remain to be determined.

Therefore, my results suggested that TRIM24 levels may be critical for the responsiveness to TCP in the cells. Future studies should investigate several breast cancer cell lines with various TRIM24 expression levels, and determine if TCP response is different in these cells. Knockdown or overexpression of TRIM24 will be an excellent tool to address whether differences in TCP responsiveness are directly related to TRIM24 expression. In addition, the potent LSD1 inhibitors (studied in Chapter 2) can also be tested in these experiments.

3.4.3. HDAC inhibitors and TRIM24 knockdown?

Hyperacetylated nucleosomes are known to prevent LSD1-mediated demethylation, indicating that deacetylation of nucleosomes by HDACs may cooperate with LSD1-mediated demethylation. Accordingly, the HDAC inhibitor Trichostatin A (TSA) leads to de-repression of LSD1 target genes. These observations suggest that combined treatment of HDAC and LSD1 inhibitors may serve as a potential therapeutics targeting breast cancer cells that do not respond to conventional therapeutics [189]. Notably, TRIM24-Bromo domain preferentially recognizes acetylated lysines, in addition to unmethylated H3K4 [57], leading to the questions of how TRIM24-depleted cells respond to HDAC inhibitors (when histones are hyperacetylated) and whether LSD1 inhibitors retain their additive effect to HDAC inhibitors when TRIM24 is knocked down.

3.4.5. Biological functions of LSD1 and TRIM24 *in vivo*?

Although the studies presented here are performed in human tumor-derived MCF cells, they provide important knowledge for further investigation in the mouse models. Based on the molecular studies of TRIM24 and its correlation in breast cancer patients, TRIM24 likely functions as an oncoprotein. Surprisingly, TRIM24 null mice develop hepatocellular carcinoma [68,69]. Note, however, that preliminary data from my lab suggested that absence of TRIM24 in the mouse model leads to aberrations in chromosomal segregation and many other cell cycle defects as well as metabolic dysfunctions in the liver, which may explain why these animals are more susceptible to tumorigenesis. TRIM24-transgenic and -knockout mice are now available in my lab and are under intensive investigation. Domain-specific TRIM24-transgenic will also be an excellent tool to dissect biological functions of each domain, especially PHD and bromodomains, which mediate chromatin interaction.

Similarly, despite the LSD1 overexpression in many cancers and its functions in driving cell proliferation, LSD1 inhibits breast cancer cell invasion and angiogenesis when ER α is not expressed [190,191]. These observations raise the question of whether LSD1 plays contradictory roles in tumorigenesis and metastasis. LSD1 knockout mice are also available in my lab through a collaborative project. These mouse models serve as a useful tool to determine how LSD1 contributes to breast cancer development and metastases, and determine how the collaborative roles of TRIM24 and LSD1 in chromatin regulation translate into biological functions *in vivo*.

Chapter 4: CONCLUSION

The histone code hypothesis proposes that single or combinatorial post-translation modifications of histones can be recognized by specific reader modules to amplify a cascade of downstream responses. Histone PTMs modulate chromatin structure and thus control DNA accessibility for estrogen-induced ER α binding. In fact, estrogen induces cyclical and sequential binding of ER α , the transcription machinery and co-regulators. H3K4-specific methyltransferases and demethylases have been shown to regulate ER α -mediated transcription activation, suggesting that this step-wise process likely involves histone methylation/demethylation to allow the recruitment of ER α and co-activator complexes. However, a comprehensive analysis and kinetic profile of H3K4 methylation is lacking. How demethylation of H3K4 by LSD1 and recognition by TRIM24 becomes the main focus of this thesis.

In first part, I demonstrated that TRIM24 and LSD1 expression allows for timely induction of ER α target gene activation induced by estrogen. TRIM24 is essential for mediating induced *GREB1* transcription at lower levels of estrogen. Importantly, re-induction of TRIM24-WT but not PHD-mutant is able to rescue TRIM24 functions in depleted cells. Importantly, estrogen triggers immediate gain of H3K23ac and H3K27ac on EREs, accompanied with demethylation of H3K4me3 to H3K4me2, and then to H3K4me1. I also showed that LSD1 and TRIM24 are cyclically recruited upon estrogen stimulation over a time course. LSD1 binding is inversely correlated with gain of H3K4me2 during each cycle. Importantly, at later cycle of LSD1, recruitment of LSD1 precedes that of TRIM24.

When LSD1 enzymatic activity is inhibited by TCP, estrogen-induced cells exhibit re-methylation of H3K4me2 as well as impaired TRIM24 and ER α binding, but no change in H3K4me1, H3K4me3, or H3K9me3. I also studied the effects of several LSD1 inhibitors in down-regulating ER α target gene activation and increasing total H3K4me2 levels. Notably, I have established a potential role of H3T6 phosphorylation in ER α regulation. Because H3T6ph inhibits demethylation of H3K4me1/2 by LSD1, as well as recognition of H3K4me0 by BHC80 and AIRE, I demonstrated here that this histone mark interferes TRIM24 and RBP2 from recognizing H3K4me0. I also showed that dephosphorylation of H3T6 is essential for estrogen-induced transcription activation of *GREB1* and *PR*, which likely influences a number of readers and histone demethylases to mediate transcription regulation.

In the second part, I furthered my study of LSD1 and TRIM24 into the cooperative biological functions. I demonstrated that TRIM24 is highly enriched and binds to *GREB1* and *PR* during G2/M transition of the cell cycle. Consistent with previous findings that poor survival of breast cancer patients associate with high TRIM24 level, I showed that MCF7 cells respond significantly affected by inhibition of LSD1 enzymatic activity by TCP when TRIM24 is depleted. Treatment with 4-OHT further reduces the survival and proliferation in shTRIM24 MCF7 cells treated with TCP. Taken together, LSD1 and TRIM24 function additively to regulate survival and proliferation of MCF7s, but the underlying mechanism is not solely dependent on ER α activation. My findings also suggested that TRIM24 level may determine responsiveness to LSD1 inhibitors.

Collectively, this dissertation demonstrated that function of TRIM24 is dependent on at least two histone modifications, unmethylated H3K4me2 and dephosphorylated H3T6. I also revealed the dynamic H3K4 methylation profile upon estrogen treatment, suggesting that several other H3K4-specific writers, readers, and erasers may be involved in mediating estrogen response. This work also emphasizes a highly time-dependent binding of LSD1 and TRIM24 to EREs upon estrogen. Importantly, inhibition of LSD1 and depletion of TRIM24 also have additive effects in inhibiting survival and proliferation in MCF7 cells. Taken together, this work supported the “histone code” hypothesis and provided important knowledge in how histone PTMs translate into gene transcription through a reader (TRIM24) and an eraser (LSD1). This project established the fundamental framework for future investigation of the roles of LSD1 and TRIM24 in the mouse models.

REFERENCES

- [1] K. Luger, A.W. Mader, R.K. Richmond, D.F. Sargent, T.J. Richmond, Crystal structure of the nucleosome core particle at 2.8 Å resolution, *Nature* 389 (1997) 251-260.
- [2] R.E. Kingston, G.J. Narlikar, ATP-dependent remodeling and acetylation as regulators of chromatin fluidity, *Genes Dev* 13 (1999) 2339-2352.
- [3] M. Vignali, A.H. Hassan, K.E. Neely, J.L. Workman, ATP-dependent chromatin-remodeling complexes, *Mol Cell Biol* 20 (2000) 1899-1910.
- [4] J. Wu, M. Grunstein, 25 years after the nucleosome model: chromatin modifications, *Trends Biochem Sci* 25 (2000) 619-623.
- [5] T. Jenuwein, C.D. Allis, Translating the histone code, *Science* 293 (2001) 1074-1080.
- [6] E.I. Campos, D. Reinberg, Histones: annotating chromatin, *Annu Rev Genet* 43 (2009) 559-599.
- [7] T. Kouzarides, Chromatin modifications and their function, *Cell* 128 (2007) 693-705.
- [8] C.H. Arrowsmith, C. Bountra, P.V. Fish, K. Lee, M. Schapira, Epigenetic protein families: a new frontier for drug discovery, *Nat Rev Drug Discov* 11 (2012) 384-400.
- [9] M. Grunstein, Histone acetylation in chromatin structure and transcription, *Nature* 389 (1997) 349-352.

- [10] T.R. Hebbes, A.W. Thorne, C. Crane-Robinson, A direct link between core histone acetylation and transcriptionally active chromatin, *EMBO J* 7 (1988) 1395-1402.
- [11] D.Y. Lee, J.J. Hayes, D. Pruss, A.P. Wolffe, A positive role for histone acetylation in transcription factor access to nucleosomal DNA, *Cell* 72 (1993) 73-84.
- [12] J.D. Anderson, P.T. Lowary, J. Widom, Effects of histone acetylation on the equilibrium accessibility of nucleosomal DNA target sites, *J Mol Biol* 307 (2001) 977-985.
- [13] G.F. Sewack, T.W. Ellis, U. Hansen, Binding of TATA binding protein to a naturally positioned nucleosome is facilitated by histone acetylation, *Mol Cell Biol* 21 (2001) 1404-1415.
- [14] C. Tse, T. Sera, A.P. Wolffe, J.C. Hansen, Disruption of higher-order folding by core histone acetylation dramatically enhances transcription of nucleosomal arrays by RNA polymerase III, *Mol Cell Biol* 18 (1998) 4629-4638.
- [15] B.D. Strahl, C.D. Allis, The language of covalent histone modifications, *Nature* 403 (2000) 41-45.
- [16] S.L. Berger, An embarrassment of niches: the many covalent modifications of histones in transcriptional regulation, *Oncogene* 20 (2001) 3007-3013.
- [17] Y. Zhang, D. Reinberg, Transcription regulation by histone methylation: interplay between different covalent modifications of the core histone tails, *Genes Dev* 15 (2001) 2343-2360.

- [18] S.Y. Roth, J.M. Denu, C.D. Allis, Histone acetyltransferases, *Annu Rev Biochem* 70 (2001) 81-120.
- [19] R. Margueron, P. Trojer, D. Reinberg, The key to development: interpreting the histone code?, *Curr Opin Genet Dev* 15 (2005) 163-176.
- [20] L. Zhang, E.E. Eugeni, M.R. Parthun, M.A. Freitas, Identification of novel histone post-translational modifications by peptide mass fingerprinting, *Chromosoma* 112 (2003) 77-86.
- [21] K. Zhang, J.S. Siino, P.R. Jones, P.M. Yau, E.M. Bradbury, A mass spectrometric "Western blot" to evaluate the correlations between histone methylation and histone acetylation, *Proteomics* 4 (2004) 3765-3775.
- [22] A.J. Bannister, T. Kouzarides, Histone methylation: recognizing the methyl mark, *Methods Enzymol* 376 (2004) 269-288.
- [23] M. Albert, K. Helin, Histone methyltransferases in cancer, *Semin Cell Dev Biol* 21 (2010) 209-220.
- [24] P.M. Dehe, V. Geli, The multiple faces of Set1, *Biochem Cell Biol* 84 (2006) 536-548.
- [25] S. Kato, A. Yokoyama, R. Fujiki, Nuclear receptor coregulators merge transcriptional coregulation with epigenetic regulation, *Trends Biochem Sci* 36 (2011) 272-281.
- [26] T. Banerjee, D. Chakravarti, A peek into the complex realm of histone phosphorylation, *Mol Cell Biol* 31 (2011) 4858-4873.

- [27] S.J. Nowak, V.G. Corces, Phosphorylation of histone H3: a balancing act between chromosome condensation and transcriptional activation, *Trends Genet* 20 (2004) 214-220.
- [28] S.S. Oliver, J.M. Denu, Dynamic interplay between histone H3 modifications and protein interpreters: emerging evidence for a "histone language", *ChemBiochem* 12 (2011) 299-307.
- [29] A.L. Garske, S.S. Oliver, E.K. Wagner, C.A. Musselman, G. LeRoy, B.A. Garcia, T.G. Kutateladze, J.M. Denu, Combinatorial profiling of chromatin binding modules reveals multisite discrimination, *Nat Chem Biol* 6 (2010) 283-290.
- [30] K. van Dijk, K.E. Marley, B.R. Jeong, J. Xu, J. Hesson, R.L. Cerny, J.H. Waterborg, H. Cerutti, Monomethyl histone H3 lysine 4 as an epigenetic mark for silenced euchromatin in *Chlamydomonas*, *Plant Cell* 17 (2005) 2439-2453.
- [31] E. Metzger, A. Imhof, D. Patel, P. Kahl, K. Hoffmeyer, N. Friedrichs, J.M. Muller, H. Greschik, J. Kirfel, S. Ji, N. Kunowska, C. Beisenherz-Huss, T. Gunther, R. Buettner, R. Schule, Phosphorylation of histone H3T6 by PKC β (I) controls demethylation at histone H3K4, *Nature* 464 (2010) 792-796.
- [32] E. Metzger, N. Yin, M. Wissmann, N. Kunowska, K. Fischer, N. Friedrichs, D. Patnaik, J.M. Higgins, N. Potier, K.H. Scheidtmann, R. Buettner, R. Schule, Phosphorylation of histone H3 at threonine 11 establishes a novel

- chromatin mark for transcriptional regulation, *Nat Cell Biol* 10 (2008) 53-60.
- [33] Y. Shi, J.R. Whetstine, Dynamic regulation of histone lysine methylation by demethylases, *Mol Cell* 25 (2007) 1-14.
- [34] H. Santos-Rosa, R. Schneider, A.J. Bannister, J. Sherriff, B.E. Bernstein, N.C. Emre, S.L. Schreiber, J. Mellor, T. Kouzarides, Active genes are trimethylated at K4 of histone H3, *Nature* 419 (2002) 407-411.
- [35] X. Shi, T. Hong, K.L. Walter, M. Ewalt, E. Michishita, T. Hung, D. Carney, P. Pena, F. Lan, M.R. Kaadige, N. Lacoste, C. Cayrou, F. Davrazou, A. Saha, B.R. Cairns, D.E. Ayer, T.G. Kutateladze, Y. Shi, J. Cote, K.F. Chua, O. Gozani, ING2 PHD domain links histone H3 lysine 4 methylation to active gene repression, *Nature* 442 (2006) 96-99.
- [36] S.D. Taverna, H. Li, A.J. Ruthenburg, C.D. Allis, D.J. Patel, How chromatin-binding modules interpret histone modifications: lessons from professional pocket pickers, *Nat Struct Mol Biol* 14 (2007) 1025-1040.
- [37] M. Yun, J. Wu, J.L. Workman, B. Li, Readers of histone modifications, *Cell Res* 21 (2011) 564-578.
- [38] F. Chignola, M. Gaetani, A. Rebane, T. Org, L. Mollica, C. Zucchelli, A. Spitaleri, V. Mannella, P. Peterson, G. Musco, The solution structure of the first PHD finger of autoimmune regulator in complex with non-modified histone H3 tail reveals the antagonistic role of H3R2 methylation, *Nucleic Acids Res* 37 (2009) 2951-2961.

- [39] F. Lan, R.E. Collins, R. De Cegli, R. Alpatov, J.R. Horton, X. Shi, O. Gozani, X. Cheng, Y. Shi, Recognition of unmethylated histone H3 lysine 4 links BHC80 to LSD1-mediated gene repression, *Nature* 448 (2007) 718-722.
- [40] F. Martino, S. Kueng, P. Robinson, M. Tsai-Pflugfelder, F. van Leeuwen, M. Ziegler, F. Cubizolles, M.M. Cockell, D. Rhodes, S.M. Gasser, Reconstitution of yeast silent chromatin: multiple contact sites and O-AADPR binding load SIR complexes onto nucleosomes in vitro, *Mol Cell* 33 (2009) 323-334.
- [41] W. Walter, D. Clynes, Y. Tang, R. Marmorstein, J. Mellor, S.L. Berger, 14-3-3 interaction with histone H3 involves a dual modification pattern of phosphoacetylation, *Mol Cell Biol* 28 (2008) 2840-2849.
- [42] S.K. Ooi, C. Qiu, E. Bernstein, K. Li, D. Jia, Z. Yang, H. Erdjument-Bromage, P. Tempst, S.P. Lin, C.D. Allis, X. Cheng, T.H. Bestor, DNMT3L connects unmethylated lysine 4 of histone H3 to de novo methylation of DNA, *Nature* 448 (2007) 714-717.
- [43] J. Otani, T. Nankumo, K. Arita, S. Inamoto, M. Ariyoshi, M. Shirakawa, Structural basis for recognition of H3K4 methylation status by the DNA methyltransferase 3A ATRX-DNMT3-DNMT3L domain, *EMBO Rep* 10 (2009) 1235-1241.
- [44] J. Kim, J. Daniel, A. Espejo, A. Lake, M. Krishna, L. Xia, Y. Zhang, M.T. Bedford, Tudor, MBT and chromo domains gauge the degree of lysine methylation, *EMBO Rep* 7 (2006) 397-403.

- [45] A. Kirmizis, H. Santos-Rosa, C.J. Penkett, M.A. Singer, R.D. Green, T. Kouzarides, Distinct transcriptional outputs associated with mono- and dimethylated histone H3 arginine 2, *Nat Struct Mol Biol* 16 (2009) 449-451.
- [46] Y. Tsukada, J. Fang, H. Erdjument-Bromage, M.E. Warren, C.H. Borchers, P. Tempst, Y. Zhang, Histone demethylation by a family of JmjC domain-containing proteins, *Nature* 439 (2006) 811-816.
- [47] H. Li, S. Ilin, W. Wang, E.M. Duncan, J. Wysocka, C.D. Allis, D.J. Patel, Molecular basis for site-specific read-out of histone H3K4me3 by the BPTF PHD finger of NURF, *Nature* 442 (2006) 91-95.
- [48] H. van Ingen, F.M. van Schaik, H. Wienk, J. Ballering, H. Rehmann, A.C. Dechesne, J.A. Kruijzer, R.M. Liskamp, H.T. Timmers, R. Boelens, Structural insight into the recognition of the H3K4me3 mark by the TFIID subunit TAF3, *Structure* 16 (2008) 1245-1256.
- [49] H. Wen, J. Li, T. Song, M. Lu, P.Y. Kan, M.G. Lee, B. Sha, X. Shi, Recognition of histone H3K4 trimethylation by the plant homeodomain of PHF2 modulates histone demethylation, *J Biol Chem* 285 (2010) 9322-9326.
- [50] A. Palacios, I.G. Munoz, D. Pantoja-Uceda, M.J. Marcaida, D. Torres, J.M. Martin-Garcia, I. Luque, G. Montoya, F.J. Blanco, Molecular basis of histone H3K4me3 recognition by ING4, *J Biol Chem* 283 (2008) 15956-15964.

- [51] S.D. Taverna, S. Ilin, R.S. Rogers, J.C. Tanny, H. Lavender, H. Li, L. Baker, J. Boyle, L.P. Blair, B.T. Chait, D.J. Patel, J.D. Aitchison, A.J. Tackett, C.D. Allis, Yng1 PHD finger binding to H3 trimethylated at K4 promotes NuA3 HAT activity at K14 of H3 and transcription at a subset of targeted ORFs, *Mol Cell* 24 (2006) 785-796.
- [52] C. Loenarz, W. Ge, M.L. Coleman, N.R. Rose, C.D. Cooper, R.J. Klose, P.J. Ratcliffe, C.J. Schofield, PHF8, a gene associated with cleft lip/palate and mental retardation, encodes for an Nepsilon-dimethyl lysine demethylase, *Hum Mol Genet* 19 (2010) 217-222.
- [53] Z. Chen, J. Zang, J. Kappler, X. Hong, F. Crawford, Q. Wang, F. Lan, C. Jiang, J. Whetstone, S. Dai, K. Hansen, Y. Shi, G. Zhang, Structural basis of the recognition of a methylated histone tail by JMJD2A, *Proc Natl Acad Sci U S A* 104 (2007) 10818-10823.
- [54] C. Bian, C. Xu, J. Ruan, K.K. Lee, T.L. Burke, W. Tempel, D. Barsyte, J. Li, M. Wu, B.O. Zhou, B.E. Fleharty, A. Paulson, A. Allali-Hassani, J.Q. Zhou, G. Mer, P.A. Grant, J.L. Workman, J. Zang, J. Min, Sgf29 binds histone H3K4me2/3 and is required for SAGA complex recruitment and histone H3 acetylation, *EMBO J* 30 (2011) 2829-2842.
- [55] V. Hoppmann, T. Thorstensen, P.E. Kristiansen, S.V. Veiseth, M.A. Rahman, K. Finne, R.B. Aalen, R. Aasland, The CW domain, a new histone recognition module in chromatin proteins, *EMBO J* 30 (2011) 1939-1952.

- [56] S.L. Berger, The complex language of chromatin regulation during transcription, *Nature* 447 (2007) 407-412.
- [57] W.W. Tsai, Z. Wang, T.T. Yiu, K.C. Akdemir, W. Xia, S. Winter, C.Y. Tsai, X. Shi, D. Schwarzer, W. Plunkett, B. Aronow, O. Gozani, W. Fischle, M.C. Hung, D.J. Patel, M.C. Barton, TRIM24 links a non-canonical histone signature to breast cancer, *Nature* 468 (2010) 927-932.
- [58] G. Meroni, G. Diez-Roux, TRIM/RBCC, a novel class of 'single protein RING finger' E3 ubiquitin ligases, *Bioessays* 27 (2005) 1147-1157.
- [59] A. Reymond, G. Meroni, A. Fantozzi, G. Merla, S. Cairo, L. Luzi, D. Riganelli, E. Zanaria, S. Messali, S. Cainarca, A. Guffanti, S. Minucci, P.G. Pelicci, A. Ballabio, The tripartite motif family identifies cell compartments, *EMBO J* 20 (2001) 2140-2151.
- [60] B. Le Douarin, A.L. Nielsen, J.M. Garnier, H. Ichinose, F. Jeanmougin, R. Losson, P. Chambon, A possible involvement of TIF1 alpha and TIF1 beta in the epigenetic control of transcription by nuclear receptors, *EMBO J* 15 (1996) 6701-6715.
- [61] B. Le Douarin, C. Zechel, J.M. Garnier, Y. Lutz, L. Tora, P. Pierrat, D. Heery, H. Gronemeyer, P. Chambon, R. Losson, The N-terminal part of TIF1, a putative mediator of the ligand-dependent activation function (AF-2) of nuclear receptors, is fused to B-raf in the oncogenic protein T18, *EMBO J* 14 (1995) 2020-2033.
- [62] E. vom Baur, C. Zechel, D. Heery, M.J. Heine, J.M. Garnier, V. Vivat, B. Le Douarin, H. Gronemeyer, P. Chambon, R. Losson, Differential ligand-

- dependent interactions between the AF-2 activating domain of nuclear receptors and the putative transcriptional intermediary factors mSUG1 and TIF1, *EMBO J* 15 (1996) 110-124.
- [63] S. Thenot, C. Henriquet, H. Rochefort, V. Cavailles, Differential interaction of nuclear receptors with the putative human transcriptional coactivator hTIF1, *J Biol Chem* 272 (1997) 12062-12068.
- [64] S. Thenot, S. Bonnet, A. Boulahtouf, E. Margeat, C.A. Royer, J.L. Borgna, V. Cavailles, Effect of ligand and DNA binding on the interaction between human transcription intermediary factor 1alpha and estrogen receptors, *Mol Endocrinol* 13 (1999) 2137-2150.
- [65] C. Teyssier, C.Y. Ou, K. Khetchoumian, R. Losson, M.R. Stallcup, Transcriptional intermediary factor 1alpha mediates physical interaction and functional synergy between the coactivator-associated arginine methyltransferase 1 and glucocorticoid receptor-interacting protein 1 nuclear receptor coactivators, *Mol Endocrinol* 20 (2006) 1276-1286.
- [66] E. Remboutsika, K. Yamamoto, M. Harbers, M. Schmutz, The bromodomain mediates transcriptional intermediary factor 1alpha -nucleosome interactions, *J Biol Chem* 277 (2002) 50318-50325.
- [67] N. Mosammaparast, Y. Shi, Reversal of histone methylation: biochemical and molecular mechanisms of histone demethylases, *Annu Rev Biochem* 79 (2010) 155-179.

- [68] K. Khetchoumian, M. Teletin, J. Tisserand, B. Herquel, K. Ouararhni, R. Losson, Trim24 (Tif1 alpha): an essential 'brake' for retinoic acid-induced transcription to prevent liver cancer, *Cell Cycle* 7 (2008) 3647-3652.
- [69] K. Khetchoumian, M. Teletin, J. Tisserand, M. Mark, B. Herquel, M. Ignat, J. Zucman-Rossi, F. Cammas, T. Lerouge, C. Thibault, D. Metzger, P. Chambon, R. Losson, Loss of Trim24 (Tif1alpha) gene function confers oncogenic activity to retinoic acid receptor alpha, *Nat Genet* 39 (2007) 1500-1506.
- [70] M. Ignat, M. Teletin, J. Tisserand, K. Khetchoumian, C. Dennefeld, P. Chambon, R. Losson, M. Mark, Arterial calcifications and increased expression of vitamin D receptor targets in mice lacking TIF1alpha, *Proc Natl Acad Sci U S A* 105 (2008) 2598-2603.
- [71] J. Tisserand, K. Khetchoumian, C. Thibault, D. Dembele, P. Chambon, R. Losson, Tripartite motif 24 (Trim24/Tif1alpha) tumor suppressor protein is a novel negative regulator of interferon (IFN)/signal transducers and activators of transcription (STAT) signaling pathway acting through retinoic acid receptor alpha (Raralpha) inhibition, *J Biol Chem* 286 (2011) 33369-33379.
- [72] Y. Shi, F. Lan, C. Matson, P. Mulligan, J.R. Whetstine, P.A. Cole, R.A. Casero, Y. Shi, Histone demethylation mediated by the nuclear amine oxidase homolog LSD1, *Cell* 119 (2004) 941-953.
- [73] R. Metivier, G. Penot, M.R. Hubner, G. Reid, H. Brand, M. Kos, F. Gannon, Estrogen receptor-alpha directs ordered, cyclical, and combinatorial

- recruitment of cofactors on a natural target promoter, *Cell* 115 (2003) 751-763.
- [74] R. Beckstead, J.A. Ortiz, C. Sanchez, S.N. Prokopenko, P. Chambon, R. Losson, H.J. Bellen, Bonus, a *Drosophila* homolog of TIF1 proteins, interacts with nuclear receptors and can inhibit betaFTZ-F1-dependent transcription, *Mol Cell* 7 (2001) 753-765.
- [75] M.G. Rosenfeld, V.V. Lunyak, C.K. Glass, Sensors and signals: a coactivator/corepressor/epigenetic code for integrating signal-dependent programs of transcriptional response, *Genes Dev* 20 (2006) 1405-1428.
- [76] M. Kikuchi, F. Okumura, T. Tsukiyama, M. Watanabe, N. Miyajima, J. Tanaka, M. Imamura, S. Hatakeyama, TRIM24 mediates ligand-dependent activation of androgen receptor and is repressed by a bromodomain-containing protein, BRD7, in prostate cancer cells, *Biochim Biophys Acta* 1793 (2009) 1828-1836.
- [77] E. Remboutsika, Y. Lutz, A. Gansmuller, J.L. Vonesch, R. Losson, P. Chambon, The putative nuclear receptor mediator TIF1alpha is tightly associated with euchromatin, *J Cell Sci* 112 (Pt 11) (1999) 1671-1683.
- [78] M.E. Torres-Padilla, M. Zernicka-Goetz, Role of TIF1alpha as a modulator of embryonic transcription in the mouse zygote, *J Cell Biol* 174 (2006) 329-338.
- [79] P. Stavropoulos, G. Blobel, A. Hoelz, Crystal structure and mechanism of human lysine-specific demethylase-1, *Nat Struct Mol Biol* 13 (2006) 626-632.

- [80] F. Forneris, C. Binda, M.A. Vanoni, A. Mattevi, E. Battaglioli, Histone demethylation catalysed by LSD1 is a flavin-dependent oxidative process, *FEBS Lett* 579 (2005) 2203-2207.
- [81] Y.J. Shi, C. Matson, F. Lan, S. Iwase, T. Baba, Y. Shi, Regulation of LSD1 histone demethylase activity by its associated factors, *Mol Cell* 19 (2005) 857-864.
- [82] M.G. Lee, C. Wynder, N. Cooch, R. Shiekhattar, An essential role for CoREST in nucleosomal histone 3 lysine 4 demethylation, *Nature* 437 (2005) 432-435.
- [83] A. Yokoyama, S. Takezawa, R. Schule, H. Kitagawa, S. Kato, Transrepressive function of TLX requires the histone demethylase LSD1, *Mol Cell Biol* 28 (2008) 3995-4003.
- [84] S.W. Lee, Y.S. Cho, J.M. Na, U.H. Park, M. Kang, E.J. Kim, S.J. Um, ASXL1 represses retinoic acid receptor-mediated transcription through associating with HP1 and LSD1, *J Biol Chem* 285 (2010) 18-29.
- [85] M. Godmann, V. Auger, V. Ferraroni-Aguiar, A. Di Sauro, C. Sette, R. Behr, S. Kimmins, Dynamic regulation of histone H3 methylation at lysine 4 in mammalian spermatogenesis, *Biol Reprod* 77 (2007) 754-764.
- [86] J. Wang, K. Scully, X. Zhu, L. Cai, J. Zhang, G.G. Prefontaine, A. Krones, K.A. Ohgi, P. Zhu, I. Garcia-Bassets, F. Liu, H. Taylor, J. Lozach, F.L. Jayes, K.S. Korach, C.K. Glass, X.D. Fu, M.G. Rosenfeld, Opposing LSD1 complexes function in developmental gene activation and repression programmes, *Nature* 446 (2007) 882-887.

- [87] J. Wang, S. Hevi, J.K. Kurash, H. Lei, F. Gay, J. Bajko, H. Su, W. Sun, H. Chang, G. Xu, F. Gaudet, E. Li, T. Chen, The lysine demethylase LSD1 (KDM1) is required for maintenance of global DNA methylation, *Nat Genet* 41 (2009) 125-129.
- [88] E.G. Clements, H.P. Mohammad, B.R. Leadem, H. Easwaran, Y. Cai, L. Van Neste, S.B. Baylin, DNMT1 modulates gene expression without its catalytic activity partially through its interactions with histone-modifying enzymes, *Nucleic Acids Res* 40 (2012) 4334-4346.
- [89] S. Saleque, J. Kim, H.M. Rooke, S.H. Orkin, Epigenetic regulation of hematopoietic differentiation by Gfi-1 and Gfi-1b is mediated by the cofactors CoREST and LSD1, *Mol Cell* 27 (2007) 562-572.
- [90] S.T. Su, H.Y. Ying, Y.K. Chiu, F.R. Lin, M.Y. Chen, K.I. Lin, Involvement of histone demethylase LSD1 in Blimp-1-mediated gene repression during plasma cell differentiation, *Mol Cell Biol* 29 (2009) 1421-1431.
- [91] A. Adamo, B. Sese, S. Boue, J. Castano, I. Paramonov, M.J. Barrero, J.C. Izpisua Belmonte, LSD1 regulates the balance between self-renewal and differentiation in human embryonic stem cells, *Nat Cell Biol* 13 (2011) 652-659.
- [92] J. Wang, F. Lu, Q. Ren, H. Sun, Z. Xu, R. Lan, Y. Liu, D. Ward, J. Quan, T. Ye, H. Zhang, Novel histone demethylase LSD1 inhibitors selectively target cancer cells with pluripotent stem cell properties, *Cancer Res* 71 (2011) 7238-7249.

- [93] J.E. Dallman, J. Allopenna, A. Bassett, A. Travers, G. Mandel, A conserved role but different partners for the transcriptional corepressor CoREST in fly and mammalian nervous system formation, *J Neurosci* 24 (2004) 7186-7193.
- [94] P. Mulligan, F. Yang, L. Di Stefano, J.Y. Ji, J. Ouyang, J.L. Nishikawa, D. Toiber, M. Kulkarni, Q. Wang, S.H. Najafi-Shoushtari, R. Mostoslavsky, S.P. Gygi, G. Gill, N.J. Dyson, A.M. Naar, A SIRT1-LSD1 corepressor complex regulates Notch target gene expression and development, *Mol Cell* 42 (2011) 689-699.
- [95] S. Sommer, S.A. Fuqua, Estrogen receptor and breast cancer, *Semin Cancer Biol* 11 (2001) 339-352.
- [96] S. Nilsson, S. Makela, E. Treuter, M. Tujague, J. Thomsen, G. Andersson, E. Enmark, K. Pettersson, M. Warner, J.A. Gustafsson, Mechanisms of estrogen action, *Physiol Rev* 81 (2001) 1535-1565.
- [97] J.F. Couse, K.S. Korach, Estrogen receptor null mice: what have we learned and where will they lead us?, *Endocr Rev* 20 (1999) 358-417.
- [98] A.M. Brzozowski, A.C. Pike, Z. Dauter, R.E. Hubbard, T. Bonn, O. Engstrom, L. Ohman, G.L. Greene, J.A. Gustafsson, M. Carlquist, Molecular basis of agonism and antagonism in the oestrogen receptor, *Nature* 389 (1997) 753-758.
- [99] B.J. Cheskis, J.G. Greger, S. Nagpal, L.P. Freedman, Signaling by estrogens, *J Cell Physiol* 213 (2007) 610-617.

- [100] N. Hah, C.G. Danko, L. Core, J.J. Waterfall, A. Siepel, J.T. Lis, W.L. Kraus, A rapid, extensive, and transient transcriptional response to estrogen signaling in breast cancer cells, *Cell* 145 (2011) 622-634.
- [101] J.S. Carroll, C.A. Meyer, J. Song, W. Li, T.R. Geistlinger, J. Eeckhoutte, A.S. Brodsky, E.K. Keeton, K.C. Fertuck, G.F. Hall, Q. Wang, S. Bekiranov, V. Sementchenko, E.A. Fox, P.A. Silver, T.R. Gingeras, X.S. Liu, M. Brown, Genome-wide analysis of estrogen receptor binding sites, *Nat Genet* 38 (2006) 1289-1297.
- [102] C.M. Klinge, Estrogen receptor interaction with co-activators and co-repressors, *Steroids* 65 (2000) 227-251.
- [103] N.J. McKenna, B.W. O'Malley, Combinatorial control of gene expression by nuclear receptors and coregulators, *Cell* 108 (2002) 465-474.
- [104] A.J. Berk, Activation of RNA polymerase II transcription, *Curr Opin Cell Biol* 11 (1999) 330-335.
- [105] G. Orphanides, T. Lagrange, D. Reinberg, The general transcription factors of RNA polymerase II, *Genes Dev* 10 (1996) 2657-2683.
- [106] S. Ogbourne, T.M. Antalis, Transcriptional control and the role of silencers in transcriptional regulation in eukaryotes, *Biochem J* 331 (Pt 1) (1998) 1-14.
- [107] B.M. Emerson, Specificity of gene regulation, *Cell* 109 (2002) 267-270.
- [108] S. Malik, R.G. Roeder, Transcriptional regulation through Mediator-like coactivators in yeast and metazoan cells, *Trends Biochem Sci* 25 (2000) 277-283.

- [109] J.A. Davis, Y. Takagi, R.D. Kornberg, F.A. Asturias, Structure of the yeast RNA polymerase II holoenzyme: Mediator conformation and polymerase interaction, *Mol Cell* 10 (2002) 409-415.
- [110] N.A. Woychik, M. Hampsey, The RNA polymerase II machinery: structure illuminates function, *Cell* 108 (2002) 453-463.
- [111] G. Otero, J. Fellows, Y. Li, T. de Bizemont, A.M. Dirac, C.M. Gustafsson, H. Erdjument-Bromage, P. Tempst, J.Q. Svejstrup, Elongator, a multisubunit component of a novel RNA polymerase II holoenzyme for transcriptional elongation, *Mol Cell* 3 (1999) 109-118.
- [112] M. Sabbah, K.I. Kang, L. Tora, G. Redeuilh, Oestrogen receptor facilitates the formation of preinitiation complex assembly: involvement of the general transcription factor TFIIB, *Biochem J* 336 (Pt 3) (1998) 639-646.
- [113] S.Y. Wu, M.C. Thomas, S.Y. Hou, V. Likhite, C.M. Chiang, Isolation of mouse TFIID and functional characterization of TBP and TFIID in mediating estrogen receptor and chromatin transcription, *J Biol Chem* 274 (1999) 23480-23490.
- [114] G.J. Narlikar, H.Y. Fan, R.E. Kingston, Cooperation between complexes that regulate chromatin structure and transcription, *Cell* 108 (2002) 475-487.
- [115] M.P. Cosma, Ordered recruitment: gene-specific mechanism of transcription activation, *Mol Cell* 10 (2002) 227-236.

- [116] J.W. Lee, Y.C. Lee, S.Y. Na, D.J. Jung, S.K. Lee, Transcriptional coregulators of the nuclear receptor superfamily: coactivators and corepressors, *Cell Mol Life Sci* 58 (2001) 289-297.
- [117] S.L. Berger, Histone modifications in transcriptional regulation, *Curr Opin Genet Dev* 12 (2002) 142-148.
- [118] R. Kurokawa, D. Kalafus, M.H. Ogliaastro, C. Kioussi, L. Xu, J. Torchia, M.G. Rosenfeld, C.K. Glass, Differential use of CREB binding protein-coactivator complexes, *Science* 279 (1998) 700-703.
- [119] J. Yanagisawa, H. Kitagawa, M. Yanagida, O. Wada, S. Ogawa, M. Nakagomi, H. Oishi, Y. Yamamoto, H. Nagasawa, S.B. McMahon, M.D. Cole, L. Tora, N. Takahashi, S. Kato, Nuclear receptor function requires a TFIIIC-type histone acetyl transferase complex, *Mol Cell* 9 (2002) 553-562.
- [120] T. Heinzel, R.M. Lavinsky, T.M. Mullen, M. Soderstrom, C.D. Laherty, J. Torchia, W.M. Yang, G. Brard, S.D. Ngo, J.R. Davie, E. Seto, R.N. Eisenman, D.W. Rose, C.K. Glass, M.G. Rosenfeld, A complex containing N-CoR, mSin3 and histone deacetylase mediates transcriptional repression, *Nature* 387 (1997) 43-48.
- [121] L. Nagy, H.Y. Kao, D. Chakravarti, R.J. Lin, C.A. Hassig, D.E. Ayer, S.L. Schreiber, R.M. Evans, Nuclear receptor repression mediated by a complex containing SMRT, mSin3A, and histone deacetylase, *Cell* 89 (1997) 373-380.
- [122] T. Suganuma, J.L. Workman, Crosstalk among Histone Modifications, *Cell* 135 (2008) 604-607.

- [123] R.J. Klose, Y. Zhang, Regulation of histone methylation by demethylimination and demethylation, *Nat Rev Mol Cell Biol* 8 (2007) 307-318.
- [124] I. Garcia-Bassets, Y.S. Kwon, F. Telese, G.G. Prefontaine, K.R. Hutt, C.S. Cheng, B.G. Ju, K.A. Ohgi, J. Wang, L. Escoubet-Lozach, D.W. Rose, C.K. Glass, X.D. Fu, M.G. Rosenfeld, Histone methylation-dependent mechanisms impose ligand dependency for gene activation by nuclear receptors, *Cell* 128 (2007) 505-518.
- [125] T. Ito, M. Bulger, M.J. Pazin, R. Kobayashi, J.T. Kadonaga, ACF, an ISWI-containing and ATP-utilizing chromatin assembly and remodeling factor, *Cell* 90 (1997) 145-155.
- [126] S.R. Kassabov, B. Zhang, J. Persinger, B. Bartholomew, SWI/SNF unwraps, slides, and rewraps the nucleosome, *Mol Cell* 11 (2003) 391-403.
- [127] A. Saha, J. Wittmeyer, B.R. Cairns, Chromatin remodelling: the industrial revolution of DNA around histones, *Nat Rev Mol Cell Biol* 7 (2006) 437-447.
- [128] T. Ito, M.E. Levenstein, D.V. Fyodorov, A.K. Kutach, R. Kobayashi, J.T. Kadonaga, ACF consists of two subunits, Acf1 and ISWI, that function cooperatively in the ATP-dependent catalysis of chromatin assembly, *Genes Dev* 13 (1999) 1529-1539.
- [129] Y. Zhang, G. LeRoy, H.P. Seelig, W.S. Lane, D. Reinberg, The dermatomyositis-specific autoantigen Mi2 is a component of a complex

- containing histone deacetylase and nucleosome remodeling activities, *Cell* 95 (1998) 279-289.
- [130] B. Belandia, R.L. Orford, H.C. Hurst, M.G. Parker, Targeting of SWI/SNF chromatin remodelling complexes to estrogen-responsive genes, *EMBO J* 21 (2002) 4094-4103.
- [131] L. De Koning, A. Corpet, J.E. Haber, G. Almouzni, Histone chaperones: an escort network regulating histone traffic, *Nat Struct Mol Biol* 14 (2007) 997-1007.
- [132] S. Sawatsubashi, T. Murata, J. Lim, R. Fujiki, S. Ito, E. Suzuki, M. Tanabe, Y. Zhao, S. Kimura, S. Fujiyama, T. Ueda, D. Umetsu, T. Ito, K. Takeyama, S. Kato, A histone chaperone, DEK, transcriptionally coactivates a nuclear receptor, *Genes Dev* 24 (2010) 159-170.
- [133] G. Reid, M.R. Hubner, R. Metivier, H. Brand, S. Denger, D. Manu, J. Beaudouin, J. Ellenberg, F. Gannon, Cyclic, proteasome-mediated turnover of unliganded and liganded ERalpha on responsive promoters is an integral feature of estrogen signaling, *Mol Cell* 11 (2003) 695-707.
- [134] E. Metzger, M. Wissmann, N. Yin, J.M. Muller, R. Schneider, A.H. Peters, T. Gunther, R. Buettner, R. Schule, LSD1 demethylates repressive histone marks to promote androgen-receptor-dependent transcription, *Nature* 437 (2005) 436-439.
- [135] M. Lupien, J. Eeckhoute, C.A. Meyer, Q. Wang, Y. Zhang, W. Li, J.S. Carroll, X.S. Liu, M. Brown, FoxA1 translates epigenetic signatures into enhancer-driven lineage-specific transcription, *Cell* 132 (2008) 958-970.

- [136] B. Perillo, M.N. Ombra, A. Bertoni, C. Cuzzo, S. Sacchetti, A. Sasso, L. Chiariotti, A. Malorni, C. Abbondanza, E.V. Avvedimento, DNA oxidation as triggered by H3K9me2 demethylation drives estrogen-induced gene expression, *Science* 319 (2008) 202-206.
- [137] M. Wissmann, N. Yin, J.M. Muller, H. Greschik, B.D. Fodor, T. Jenuwein, C. Vogler, R. Schneider, T. Gunther, R. Buettner, E. Metzger, R. Schule, Cooperative demethylation by JMJD2C and LSD1 promotes androgen receptor-dependent gene expression, *Nat Cell Biol* 9 (2007) 347-353.
- [138] F. Lan, A.C. Nottke, Y. Shi, Mechanisms involved in the regulation of histone lysine demethylases, *Curr Opin Cell Biol* 20 (2008) 316-325.
- [139] J. Wysocka, T.A. Milne, C.D. Allis, Taking LSD 1 to a new high, *Cell* 122 (2005) 654-658.
- [140] M.G. Lee, C. Wynder, D.M. Schmidt, D.G. McCafferty, R. Shiekhhattar, Histone H3 lysine 4 demethylation is a target of nonselective antidepressive medications, *Chem Biol* 13 (2006) 563-567.
- [141] S. Iwase, B. Xiang, S. Ghosh, T. Ren, P.W. Lewis, J.C. Cochrane, C.D. Allis, D.J. Picketts, D.J. Patel, H. Li, Y. Shi, ATRX ADD domain links an atypical histone methylation recognition mechanism to human mental-retardation syndrome, *Nat Struct Mol Biol* 18 (2011) 769-776.
- [142] H. Santos-Rosa, R. Schneider, B.E. Bernstein, N. Karabetsou, A. Morillon, C. Weise, S.L. Schreiber, J. Mellor, T. Kouzarides, Methylation of histone H3 K4 mediates association of the Isw1p ATPase with chromatin, *Mol Cell* 12 (2003) 1325-1332.

- [143] R. Schneider, A.J. Bannister, F.A. Myers, A.W. Thorne, C. Crane-Robinson, T. Kouzarides, Histone H3 lysine 4 methylation patterns in higher eukaryotic genes, *Nat Cell Biol* 6 (2004) 73-77.
- [144] N.D. Heintzman, R.K. Stuart, G. Hon, Y. Fu, C.W. Ching, R.D. Hawkins, L.O. Barrera, S. Van Calcar, C. Qu, K.A. Ching, W. Wang, Z. Weng, R.D. Green, G.E. Crawford, B. Ren, Distinct and predictive chromatin signatures of transcriptional promoters and enhancers in the human genome, *Nat Genet* 39 (2007) 311-318.
- [145] G.C. Hon, R.D. Hawkins, B. Ren, Predictive chromatin signatures in the mammalian genome, *Hum Mol Genet* 18 (2009) R195-201.
- [146] Y. Tian, Z. Jia, J. Wang, Z. Huang, J. Tang, Y. Zheng, Y. Tang, Q. Wang, Z. Tian, D. Yang, Y. Zhang, X. Fu, J. Song, S. Liu, J.C. van Velkinburgh, Y. Wu, B. Ni, Global mapping of H3K4me1 and H3K4me3 reveals the chromatin state-based cell type-specific gene regulation in human Treg cells, *PLoS One* 6 (2011) e27770.
- [147] G.G. Wang, C.D. Allis, P. Chi, Chromatin remodeling and cancer, Part I: Covalent histone modifications, *Trends Mol Med* 13 (2007) 363-372.
- [148] S.L. Schreiber, B.E. Bernstein, Signaling network model of chromatin, *Cell* 111 (2002) 771-778.
- [149] P.A. Jones, S.B. Baylin, The epigenomics of cancer, *Cell* 128 (2007) 683-692.

- [150] S.B. Baylin, P.A. Jones, A decade of exploring the cancer epigenome - biological and translational implications, *Nat Rev Cancer* 11 (2011) 726-734.
- [151] A. Portela, M. Esteller, Epigenetic modifications and human disease, *Nat Biotechnol* 28 (2010) 1057-1068.
- [152] T.K. Kelly, D.D. De Carvalho, P.A. Jones, Epigenetic modifications as therapeutic targets, *Nat Biotechnol* 28 (2010) 1069-1078.
- [153] J.E. Delmore, G.C. Issa, M.E. Lemieux, P.B. Rahl, J. Shi, H.M. Jacobs, E. Kastiris, T. Gilpatrick, R.M. Paranal, J. Qi, M. Chesi, A.C. Schinzel, M.R. McKeown, T.P. Heffernan, C.R. Vakoc, P.L. Bergsagel, I.M. Ghobrial, P.G. Richardson, R.A. Young, W.C. Hahn, K.C. Anderson, A.L. Kung, J.E. Bradner, C.S. Mitsiades, BET bromodomain inhibition as a therapeutic strategy to target c-Myc, *Cell* 146 (2011) 904-917.
- [154] P. Filippakopoulos, J. Qi, S. Picaud, Y. Shen, W.B. Smith, O. Fedorov, E.M. Morse, T. Keates, T.T. Hickman, I. Felletar, M. Philpott, S. Munro, M.R. McKeown, Y. Wang, A.L. Christie, N. West, M.J. Cameron, B. Schwartz, T.D. Heightman, N. La Thangue, C.A. French, O. Wiest, A.L. Kung, S. Knapp, J.E. Bradner, Selective inhibition of BET bromodomains, *Nature* 468 (2010) 1067-1073.
- [155] M.A. Dawson, R.K. Prinjha, A. Dittmann, G. Giotopoulos, M. Bantscheff, W.I. Chan, S.C. Robson, C.W. Chung, C. Hopf, M.M. Savitski, C. Huthmacher, E. Gudgin, D. Lugo, S. Beinke, T.D. Chapman, E.J. Roberts, P.E. Soden, K.R. Auger, O. Mirguet, K. Doehner, R. Delwel, A.K. Burnett,

- P. Jeffrey, G. Drewes, K. Lee, B.J. Huntly, T. Kouzarides, Inhibition of BET recruitment to chromatin as an effective treatment for MLL-fusion leukaemia, *Nature* 478 (2011) 529-533.
- [156] J. Zuber, J. Shi, E. Wang, A.R. Rappaport, H. Herrmann, E.A. Sison, D. Magoon, J. Qi, K. Blatt, M. Wunderlich, M.J. Taylor, C. Johns, A. Chicas, J.C. Mulloy, S.C. Kogan, P. Brown, P. Valent, J.E. Bradner, S.W. Lowe, C.R. Vakoc, RNAi screen identifies Brd4 as a therapeutic target in acute myeloid leukaemia, *Nature* 478 (2011) 524-528.
- [157] P. Chi, C.D. Allis, G.G. Wang, Covalent histone modifications--miswritten, misinterpreted and mis-erased in human cancers, *Nat Rev Cancer* 10 (2010) 457-469.
- [158] T.A. Milne, S.D. Briggs, H.W. Brock, M.E. Martin, D. Gibbs, C.D. Allis, J.L. Hess, MLL targets SET domain methyltransferase activity to Hox gene promoters, *Mol Cell* 10 (2002) 1107-1117.
- [159] T. Nakamura, T. Mori, S. Tada, W. Krajewski, T. Rozovskaia, R. Wassell, G. Dubois, A. Mazo, C.M. Croce, E. Canaani, ALL-1 is a histone methyltransferase that assembles a supercomplex of proteins involved in transcriptional regulation, *Mol Cell* 10 (2002) 1119-1128.
- [160] A.V. Krivtsov, S.A. Armstrong, MLL translocations, histone modifications and leukaemia stem-cell development, *Nat Rev Cancer* 7 (2007) 823-833.
- [161] J.L. Hess, MLL: a histone methyltransferase disrupted in leukemia, *Trends Mol Med* 10 (2004) 500-507.

- [162] L.Y. Shih, D.C. Liang, J.F. Fu, J.H. Wu, P.N. Wang, T.L. Lin, P. Dunn, M.C. Kuo, T.C. Tang, T.H. Lin, C.L. Lai, Characterization of fusion partner genes in 114 patients with de novo acute myeloid leukemia and MLL rearrangement, *Leukemia* 20 (2006) 218-223.
- [163] A.M. Dorrance, S. Liu, A. Chong, B. Pulley, D. Nemer, M. Guimond, W. Yuan, D. Chang, S.P. Whitman, G. Marcucci, M.A. Caligiuri, The MLL partial tandem duplication: differential, tissue-specific activity in the presence or absence of the wild-type allele, *Blood* 112 (2008) 2508-2511.
- [164] A.M. Dorrance, S. Liu, W. Yuan, B. Becknell, K.J. Arnoczky, M. Guimond, M.P. Strout, L. Feng, T. Nakamura, L. Yu, L.J. Rush, M. Weinstein, G. Leone, L. Wu, A. Ferketich, S.P. Whitman, G. Marcucci, M.A. Caligiuri, MLL partial tandem duplication induces aberrant Hox expression in vivo via specific epigenetic alterations, *J Clin Invest* 116 (2006) 2707-2716.
- [165] S. Xu, M.A. Powers, Nuclear pore proteins and cancer, *Semin Cell Dev Biol* 20 (2009) 620-630.
- [166] G.G. Wang, J. Song, Z. Wang, H.L. Dormann, F. Casadio, H. Li, J.L. Luo, D.J. Patel, C.D. Allis, Haematopoietic malignancies caused by dysregulation of a chromatin-binding PHD finger, *Nature* 459 (2009) 847-851.
- [167] K. Yamane, K. Tateishi, R.J. Klose, J. Fang, L.A. Fabrizio, H. Erdjument-Bromage, J. Taylor-Papadimitriou, P. Tempst, Y. Zhang, PLU-1 is an H3K4 demethylase involved in transcriptional repression and breast cancer cell proliferation, *Mol Cell* 25 (2007) 801-812.

- [168] Y. Xiang, Z. Zhu, G. Han, X. Ye, B. Xu, Z. Peng, Y. Ma, Y. Yu, H. Lin, A.P. Chen, C.D. Chen, JARID1B is a histone H3 lysine 4 demethylase up-regulated in prostate cancer, *Proc Natl Acad Sci U S A* 104 (2007) 19226-19231.
- [169] A.G. Scibetta, S. Santangelo, J. Coleman, D. Hall, T. Chaplin, J. Copier, S. Catchpole, J. Burchell, J. Taylor-Papadimitriou, Functional analysis of the transcription repressor PLU-1/JARID1B, *Mol Cell Biol* 27 (2007) 7220-7235.
- [170] S. Klugbauer, H.M. Rabes, The transcription coactivator HTIF1 and a related protein are fused to the RET receptor tyrosine kinase in childhood papillary thyroid carcinomas, *Oncogene* 18 (1999) 4388-4393.
- [171] E. Belloni, M. Trubia, P. Gasparini, C. Micucci, C. Tapinassi, S. Confalonieri, P. Nuciforo, B. Martino, F. Lo-Coco, P.G. Pelicci, P.P. Di Fiore, 8p11 myeloproliferative syndrome with a novel t(7;8) translocation leading to fusion of the FGFR1 and TIF1 genes, *Genes Chromosomes Cancer* 42 (2005) 320-325.
- [172] T. Miki, T.P. Fleming, M. Crescenzi, C.J. Molloy, S.B. Blam, S.H. Reynolds, S.A. Aaronson, Development of a highly efficient expression cDNA cloning system: application to oncogene isolation, *Proc Natl Acad Sci U S A* 88 (1991) 5167-5171.
- [173] K. Allton, A.K. Jain, H.M. Herz, W.W. Tsai, S.Y. Jung, J. Qin, A. Bergmann, R.L. Johnson, M.C. Barton, Trim24 targets endogenous p53 for degradation, *Proc Natl Acad Sci U S A* 106 (2009) 11612-11616.

- [174] M. Chambon, B. Orsetti, M.L. Berthe, C. Bascoul-Mollevis, C. Rodriguez, V. Duong, M. Gleizes, S. Thenot, F. Bibeau, C. Theillet, V. Cavailles, Prognostic significance of TRIM24/TIF-1alpha gene expression in breast cancer, *Am J Pathol* 178 (2011) 1461-1469.
- [175] S. Hayami, J.D. Kelly, H.S. Cho, M. Yoshimatsu, M. Unoki, T. Tsunoda, H.I. Field, D.E. Neal, H. Yamaue, B.A. Ponder, Y. Nakamura, R. Hamamoto, Overexpression of LSD1 contributes to human carcinogenesis through chromatin regulation in various cancers, *Int J Cancer* 128 (2011) 574-586.
- [176] X. Hu, R. Ybarra, Y. Qiu, J. Bungert, S. Huang, Transcriptional regulation by TAL1: a link between epigenetic modifications and erythropoiesis, *Epigenetics* 4 (2009) 357-361.
- [177] J. Huang, R. Sengupta, A.B. Espejo, M.G. Lee, J.A. Dorsey, M. Richter, S. Opravil, R. Shiekhattar, M.T. Bedford, T. Jenuwein, S.L. Berger, p53 is regulated by the lysine demethylase LSD1, *Nature* 449 (2007) 105-108.
- [178] H. Kontaki, I. Talianidis, Lysine methylation regulates E2F1-induced cell death, *Mol Cell* 39 (2010) 152-160.
- [179] S. Lim, A. Janzer, A. Becker, A. Zimmer, R. Schule, R. Buettner, J. Kirfel, Lysine-specific demethylase 1 (LSD1) is highly expressed in ER-negative breast cancers and a biomarker predicting aggressive biology, *Carcinogenesis* 31 (2010) 512-520.
- [180] C. Magerl, J. Ellinger, T. Braunschweig, E. Kremmer, L.K. Koch, T. Holler, R. Buttner, B. Luscher, I. Gutgemann, H3K4 dimethylation in hepatocellular carcinoma is rare compared with other hepatobiliary and

- gastrointestinal carcinomas and correlates with expression of the methylase Ash2 and the demethylase LSD1, *Hum Pathol* 41 (2010) 181-189.
- [181] J.H. Schulte, S. Lim, A. Schramm, N. Friedrichs, J. Koster, R. Versteeg, I. Ora, K. Pajtler, L. Klein-Hitpass, S. Kuhfittig-Kulle, E. Metzger, R. Schule, A. Eggert, R. Buettner, J. Kirfel, Lysine-specific demethylase 1 is strongly expressed in poorly differentiated neuroblastoma: implications for therapy, *Cancer Res* 69 (2009) 2065-2071.
- [182] H.S. Cho, T. Suzuki, N. Dohmae, S. Hayami, M. Unoki, M. Yoshimatsu, G. Toyokawa, M. Takawa, T. Chen, J.K. Kurash, H.I. Field, B.A. Ponder, Y. Nakamura, R. Hamamoto, Demethylation of RB regulator MYPT1 by histone demethylase LSD1 promotes cell cycle progression in cancer cells, *Cancer Res* 71 (2011) 655-660.
- [183] S. Lv, W. Bu, H. Jiao, B. Liu, L. Zhu, H. Zhao, J. Liao, J. Li, X. Xu, LSD1 is required for chromosome segregation during mitosis, *Eur J Cell Biol* 89 (2010) 557-563.
- [184] T. Lin, A. Ponn, X. Hu, B.K. Law, J. Lu, Requirement of the histone demethylase LSD1 in Snai1-mediated transcriptional repression during epithelial-mesenchymal transition, *Oncogene* 29 (2010) 4896-4904.
- [185] O.G. McDonald, H. Wu, W. Timp, A. Doi, A.P. Feinberg, Genome-scale epigenetic reprogramming during epithelial-to-mesenchymal transition, *Nat Struct Mol Biol* 18 (2011) 867-874.

- [186] S. Amente, A. Bertoni, A. Morano, L. Lania, E.V. Avvedimento, B. Majello, LSD1-mediated demethylation of histone H3 lysine 4 triggers Myc-induced transcription, *Oncogene* 29 (2010) 3691-3702.
- [187] W.J. Harris, X. Huang, J.T. Lynch, G.J. Spencer, J.R. Hitchin, Y. Li, F. Ciceri, J.G. Blaser, B.F. Greystoke, A.M. Jordan, C.J. Miller, D.J. Ogilvie, T.C. Somerville, The histone demethylase KDM1A sustains the oncogenic potential of MLL-AF9 leukemia stem cells, *Cancer Cell* 21 (2012) 473-487.
- [188] R.L. Eckert, B.S. Katzenellenbogen, Physical properties of estrogen receptor complexes in MCF-7 human breast cancer cells. Differences with anti-estrogen and estrogen, *J Biol Chem* 257 (1982) 8840-8846.
- [189] Y. Huang, S.N. Vasilatos, L. Boric, P.G. Shaw, N.E. Davidson, Inhibitors of histone demethylation and histone deacetylation cooperate in regulating gene expression and inhibiting growth in human breast cancer cells, *Breast Cancer Res Treat* 131 (2012) 777-789.
- [190] Q. Li, L. Shi, B. Gui, W. Yu, J. Wang, D. Zhang, X. Han, Z. Yao, Y. Shang, Binding of the JmjC demethylase JARID1B to LSD1/NuRD suppresses angiogenesis and metastasis in breast cancer cells by repressing chemokine CCL14, *Cancer Res* 71 (2011) 6899-6908.
- [191] Y. Wang, H. Zhang, Y. Chen, Y. Sun, F. Yang, W. Yu, J. Liang, L. Sun, X. Yang, L. Shi, R. Li, Y. Li, Y. Zhang, Q. Li, X. Yi, Y. Shang, LSD1 is a subunit of the NuRD complex and targets the metastasis programs in breast cancer, *Cell* 138 (2009) 660-672.

VITA

Teresa Tingting Yiu was born in Hong Kong Special Administrative Region, People's Republic of China on March 15, 1983, the Daughter of Ah-Chiu Yiu and Sui-Yuk Tse. From 2004 to 2005, she was an international exchange student at Baylor University in Waco, Texas, USA. Upon completion of the exchange program, she spent the following three years at the University of Houston and graduated Summa Cum Laude with a degree of Bachelor of Science in biology in May 2008. In the subsequent September, she was admitted to the Graduate School of Biomedical Sciences at the University of Texas Health Science Center at Houston, where she pursued her Ph.D. research under the guidance of Professor Michelle Barton, at the Department of Biochemistry and Molecular Biology. In December 2012, she was awarded the degree of Doctor of Philosophy in Genes and Development.

Permanent address:

706 Stubbs Bend Drive

Richmond, Texas 77479